硒同位素理论(分馏)体系的构建与应用

朱建明

jmzhu@cugb.edu.cn

1. 中国地质大学(北京)地质过程与矿产资源国家重点实验室，北京 100083；

2. 中国科学院地球化学研究所环境地球化学国家重点实验室，贵阳 550081；

2020年第三届“非传统稳定同位素地球化学暑期学校”
西北大学（西安）

2020年8月15日

报 告 提 纲

一、硒的背景知识

二、硒同位素分析方法

三、硒同位素理论分馏体系的构建

四、硒同位素应用案例分析

一、硒的背景知识

1.1 硒的基本地化性质

pH=3~9时的理论硒形态

$SeO_4^{2-} \longleftrightarrow HSeO_3^- \quad E=1.06V$

$SeO_4^{2-} \longleftrightarrow SeO_3^{2-} \quad E=0.81V$

$HSeO_3^- \longleftrightarrow Se(s) \quad E=0.78V$

$SeO_3^{2-} \longleftrightarrow Se(s) \quad E=0.90V$

$Se(s) \longleftrightarrow HSe^- \quad E=-0.23V$

$Se(s) \longleftrightarrow H_2Se \quad E=-0.12V$

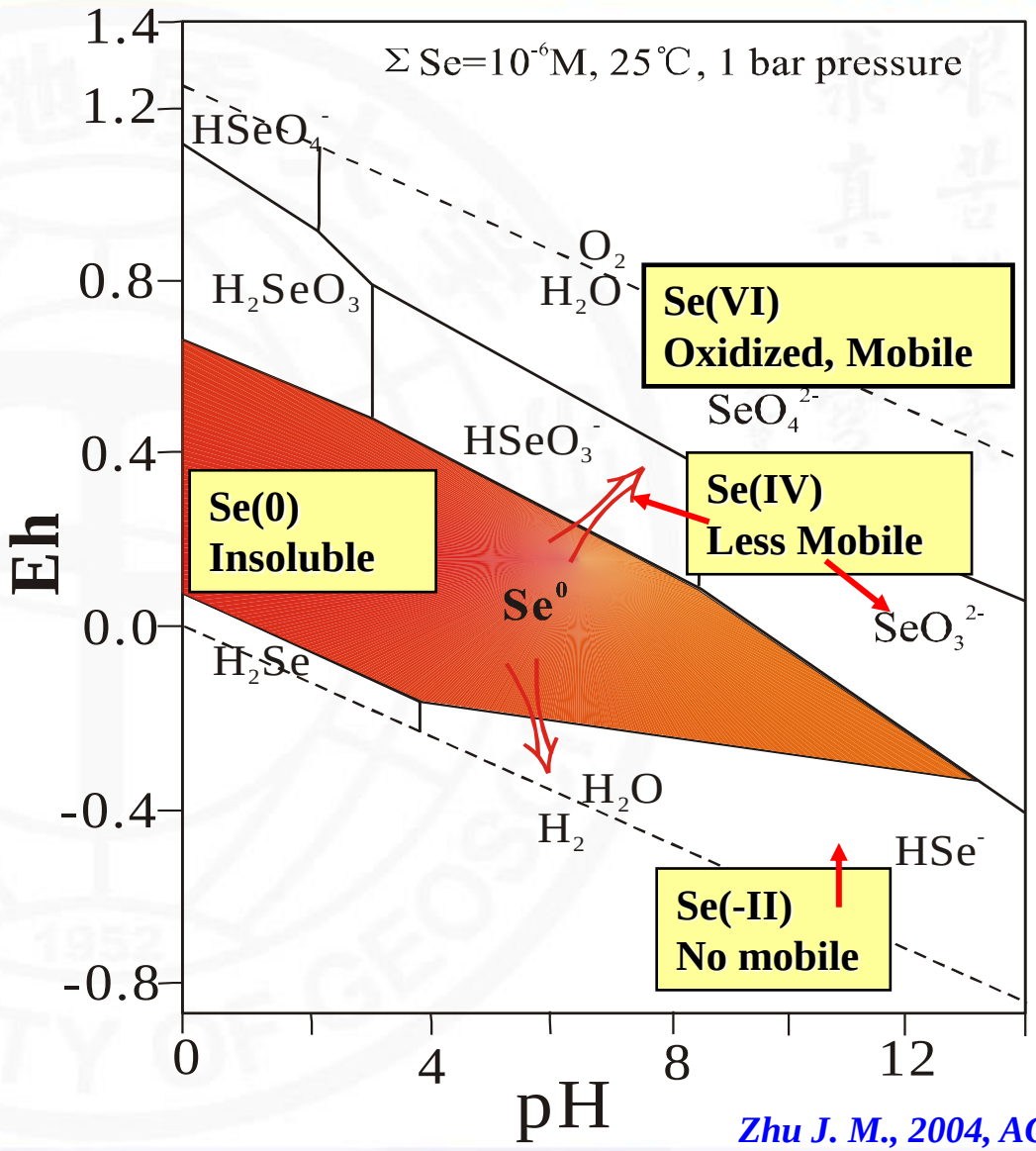

Séby, F. 2001

Zhu J. M., 2004, AG

一、硒的背景知识

硒的形态：-2, 0, +4, +6

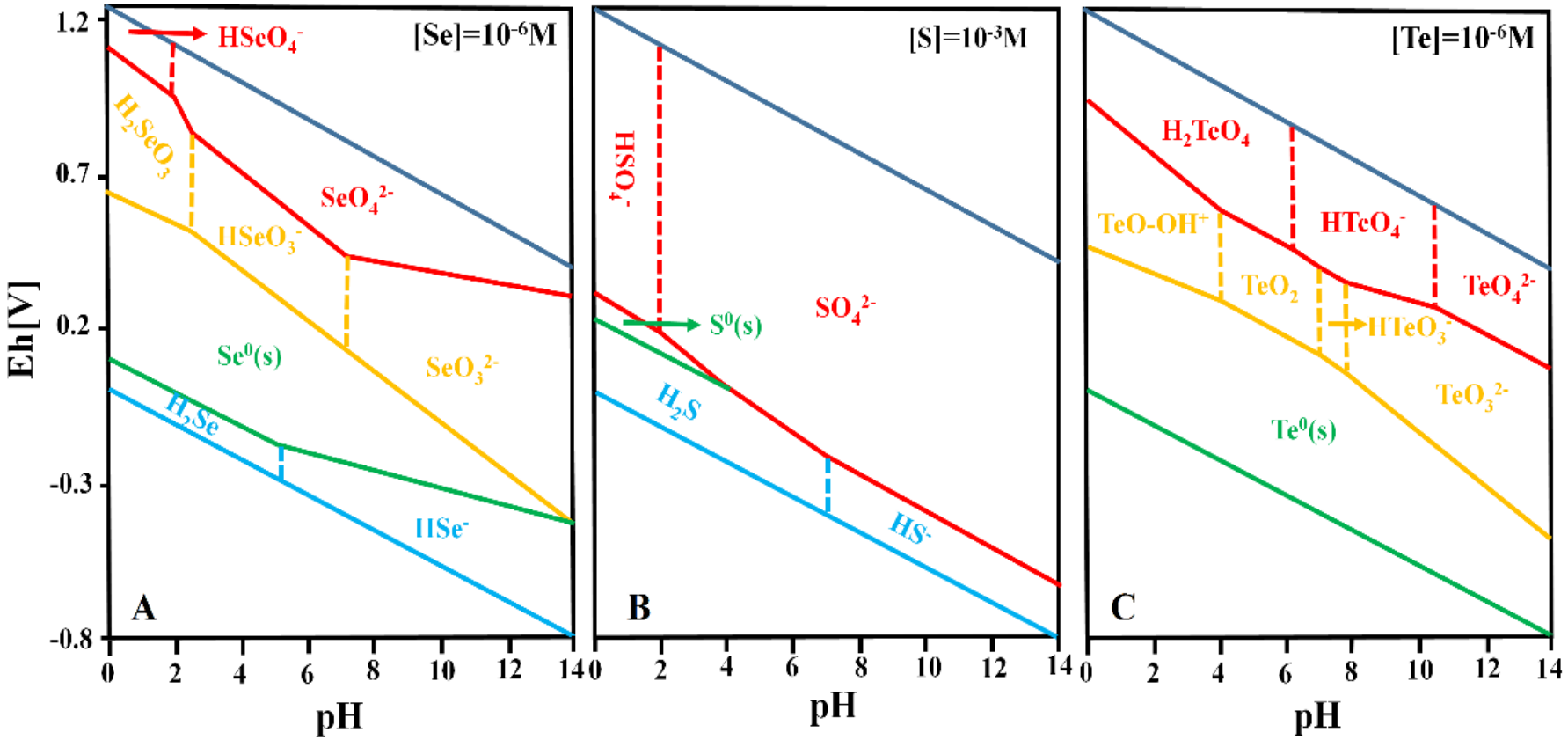

氧化环境：+4 (SeO_3^{2-}, $HSeO_3^-$, H_2SeO_3)，　+6 (SeO_4^{2-}, $HSeO_4^-$, H_2SeO_4)

还原环境：0 (Se^0), -2 (HSe^-, FeSe, Cu_2Se, $MoSe_2$ 等)

一、硒的背景知识

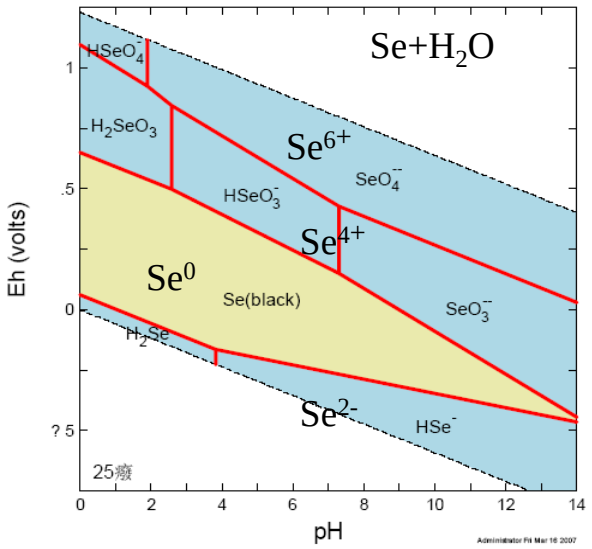

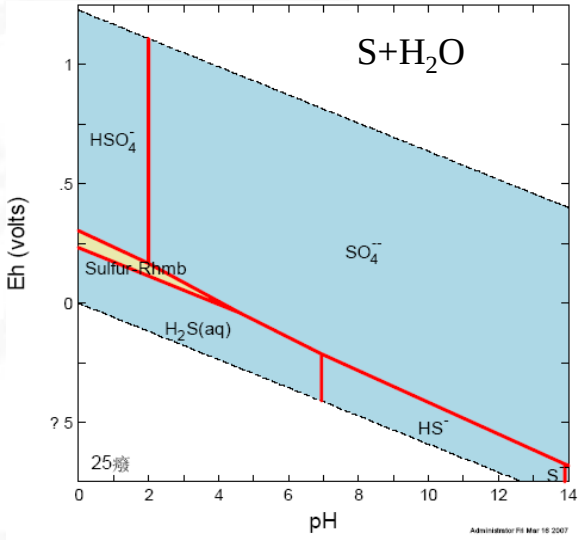

A 硒的化学性质类似硫

B 硒与硫的地化差异

C 硒是亲生物元素

D S→FeS_2;

Se→$FeSe_2$/CuSe/$CuSe_2$

稳定性
CuSe($CuSe_2$)>$FeSe_2$(FeSe)

E. 硒的有机形态
含硒蛋白(硒蛋氨酸等);
DM-Se; DMD-Se等

一、硒的背景知识

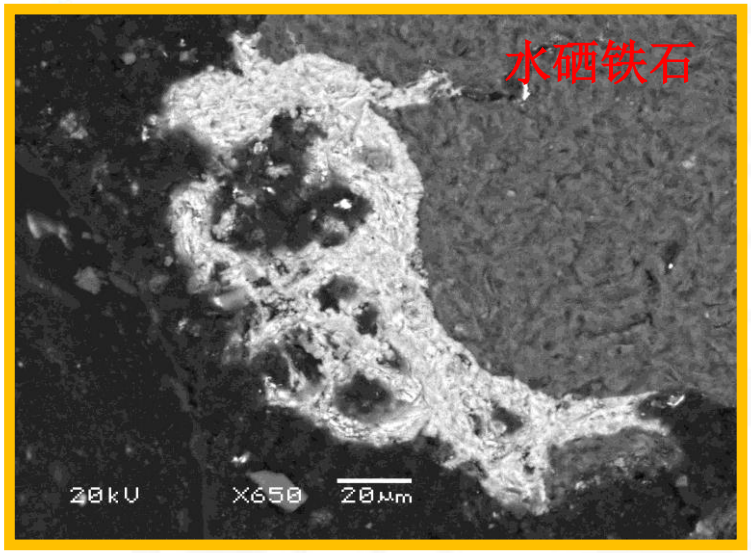

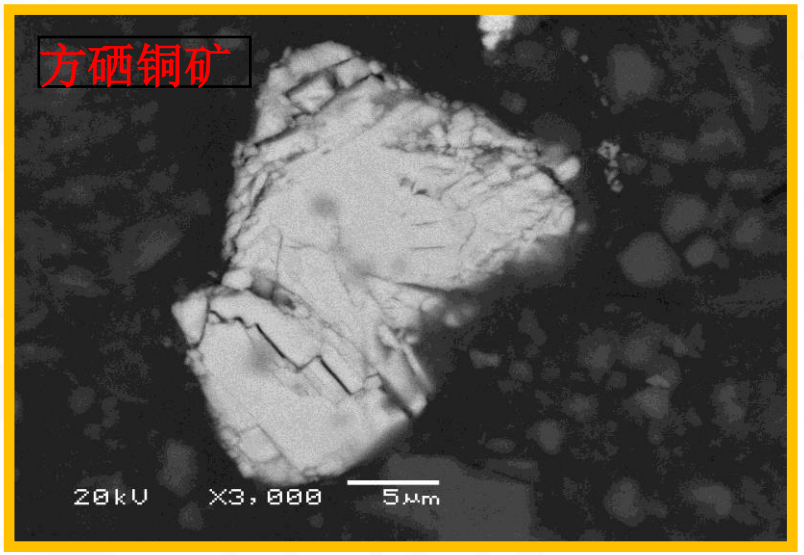

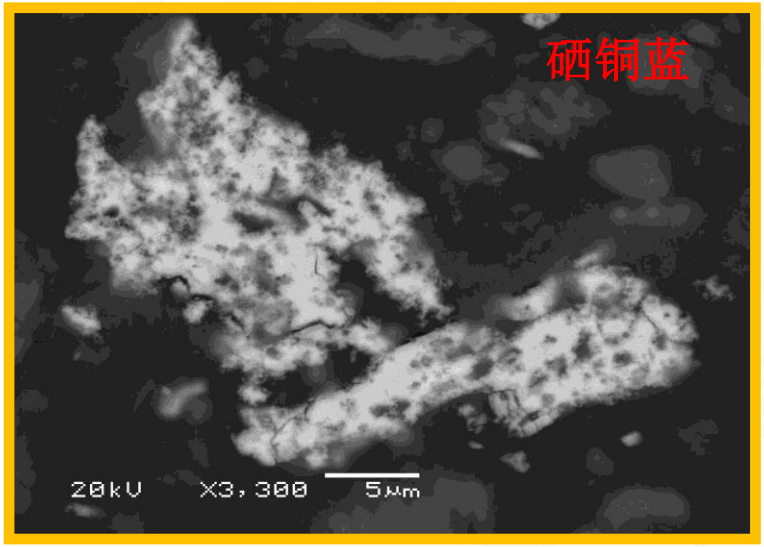

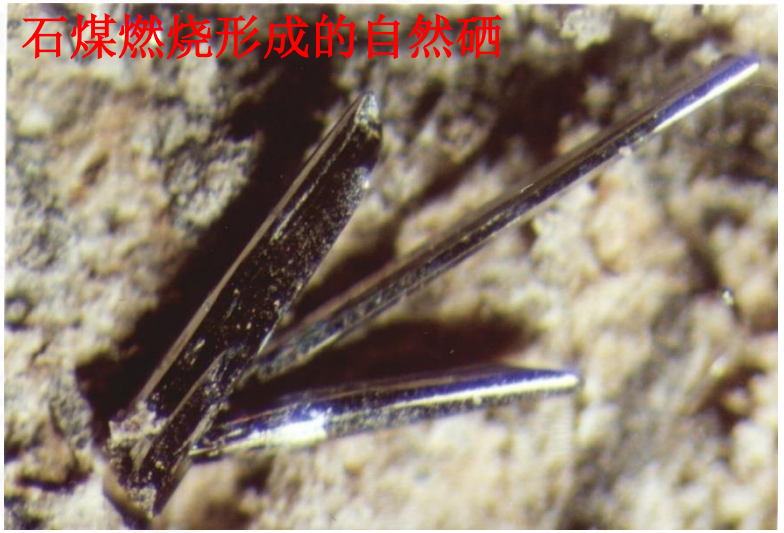

自然界发现的自然硒及其系列铁、铜硒化物。 *Zhu et al., 2012， CG*

一、硒的背景知识

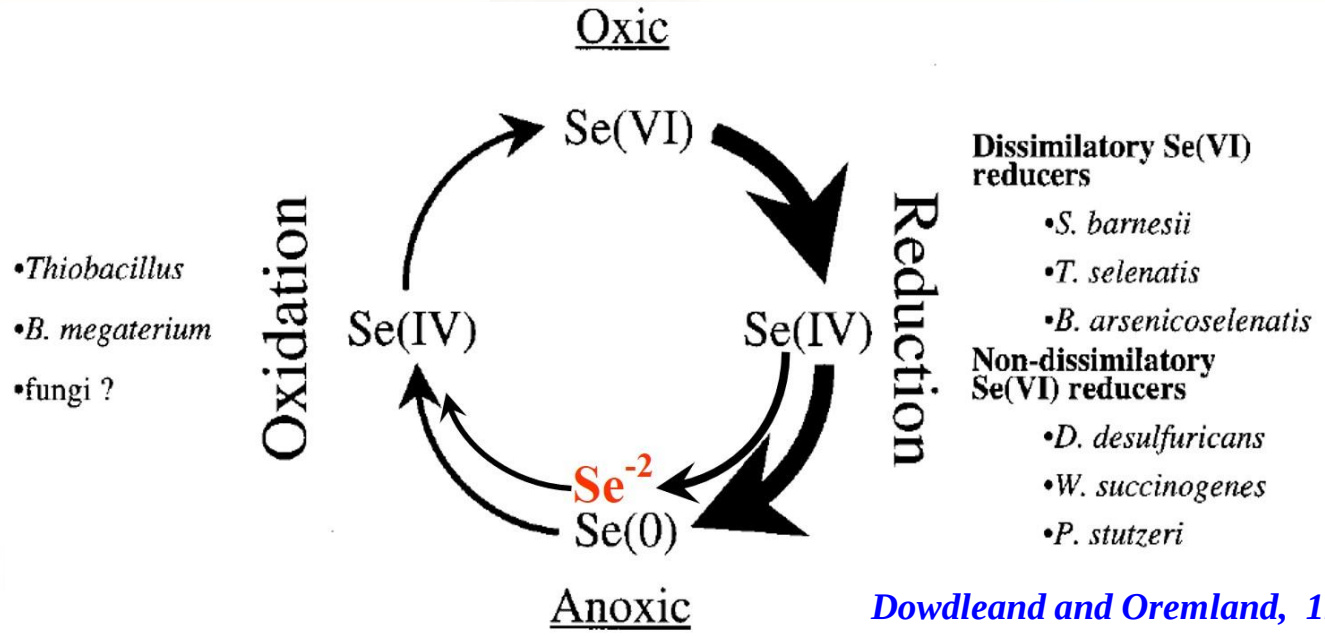

Dowdleand and Oremland, 1998, EST.

Se^{4+}的还原

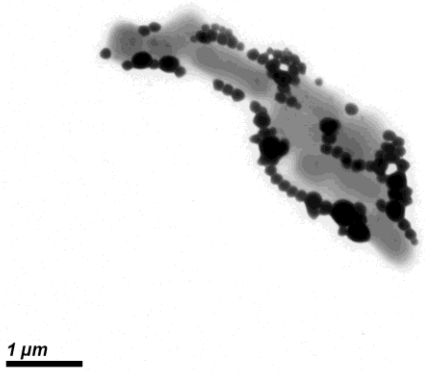

Se^{6+}的还原

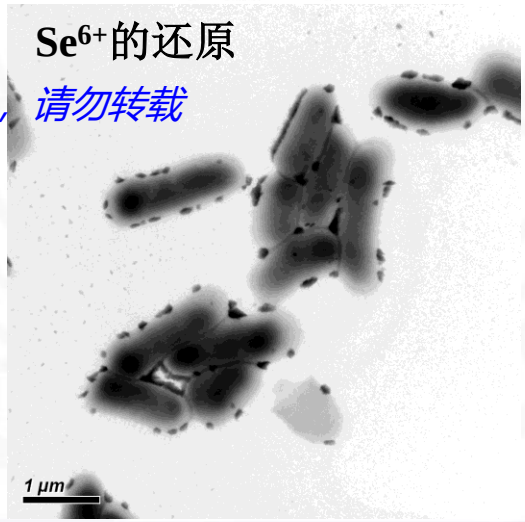

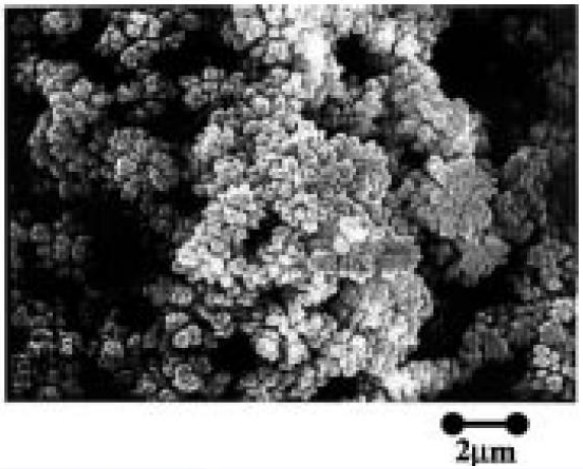

二、硒同位素的分析方法

Ge	69.92425	21.234
	71.92208	27.662
	72.92346	7.717
	73.92118	35.943
	75.92140	7.444
As	74.92160	100
Se	73.92248	0.889
	75.91921	9.366
	76.91991	7.635
	77.91773	23.772
	79.91652	49.607
	81.91671	8.731
Br	78.91834	50.686
	80.91629	49.314

同质异位素的干扰与监控

H	1.00783	99.9844
	2.01410	0.01557
O	15.99491	99.7628
	16.99913	0.0372
	17.99916	0.20004
Ar	35.96755	0.3365
	37.96273	0.0632
	39.96238	99.6003
Kr	77.92040	0.35351
	79.91638	2.28086
	81.91348	11.5830
	82.91413	11.4953
	83.91151	56.9889
	85.91061	17.2984

$^{40}Ar^{36}Ar^{+}$、$^{40}Ar^{40}Ar^{+}$、$^{75}As^{1}H$等消除

$$\delta^{82/76}Se = \left(^{82/76}Se_{sample}/^{82/76}Se_{NIST\ 3149} - 1\right) \times 10^{3}$$

二、硒同位素的分析方法

A. 杯结构

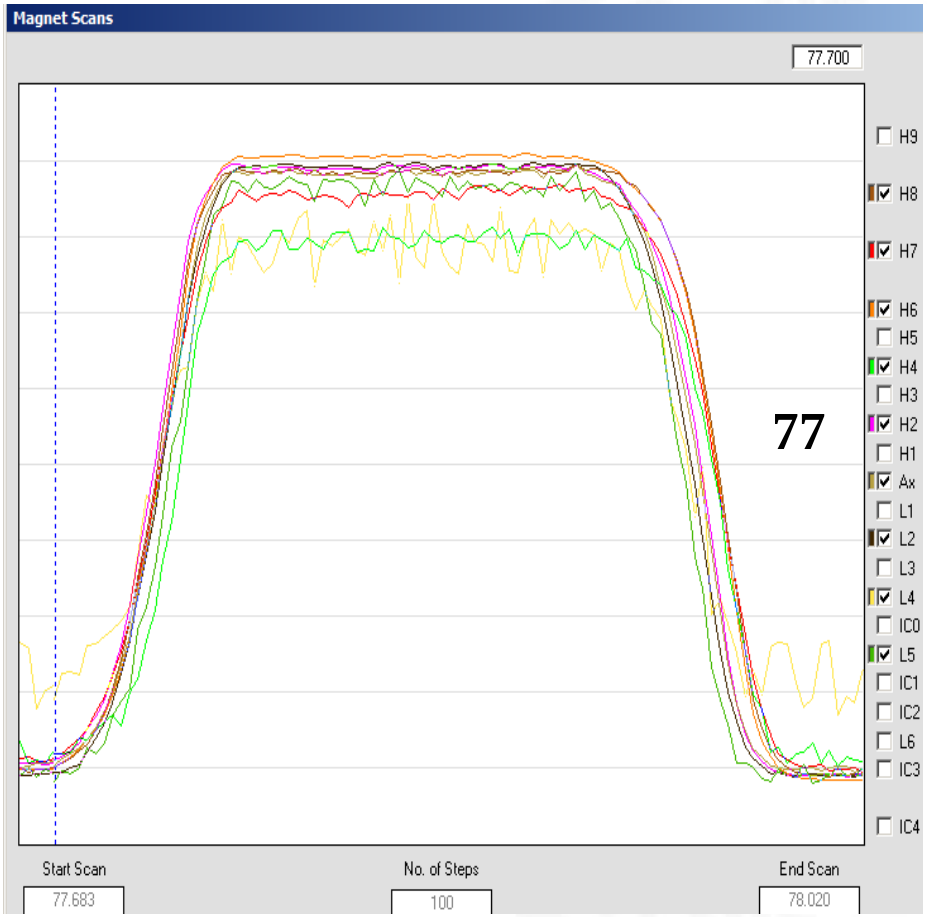

HG-Desolvation-MC-ICP-MS instrumentation operating conditions.

Component	Parameters
RF power	1050 W
Sample cone	Ni standard cone
Skimmer cone	Ni standard skimmer (H-type)
Gas flow rate (L/min)	
Cooling	16
Auxiliary	0.9–0.95
Sample	0.9–0.95
Additional (10% CH_4 in Ar)	0.03
Resolution (m/Δm)	300 (LR)
Acquisition parameters	
Number of repeats	1 block × 30 cycles
Integration times	8.32 s
Sample introduction systems	
Apex-IR temperature setting	20/4 °C
Hydride generation	
Flow rate of $NaBH_4$ and sample	0.2 mL min^{-1}
$NaBH_4$ concentration	1.0% (w/w)
Sample acidity HCl	1.0 mol L^{-1}

Cup configuration

Cup	L4	L3	L2	L1	C	H1	H2	H3	H4
Isotopes	^{73}Ge	^{74}Se	^{75}As	^{76}Se	^{77}Se	^{78}Se	^{80}Se	^{82}Se	^{83}Kr

Nu Plasma II MC

Zhu et al., unpublished

Neptune MC

Chang et al., 2017, CG

二、硒同位素的分析方法

进样系统：氢化物发生系统

硒、汞、锗、碲、锑等元素都能够形成氢化物，在适宜的酸度和还原剂条件下，它们的氢化物发生效率可以接近100%。

原理如下：

1. $NaBH_4 + 3H_2O + HCl \rightarrow H_3BO_4 + NaCl + 8H^+$

2. $Em+ + 8H+ \rightarrow EHn$ (气体) + H_2 (气体) （E代表能够发生氢化物的元素）

二、硒同位素的分析方法

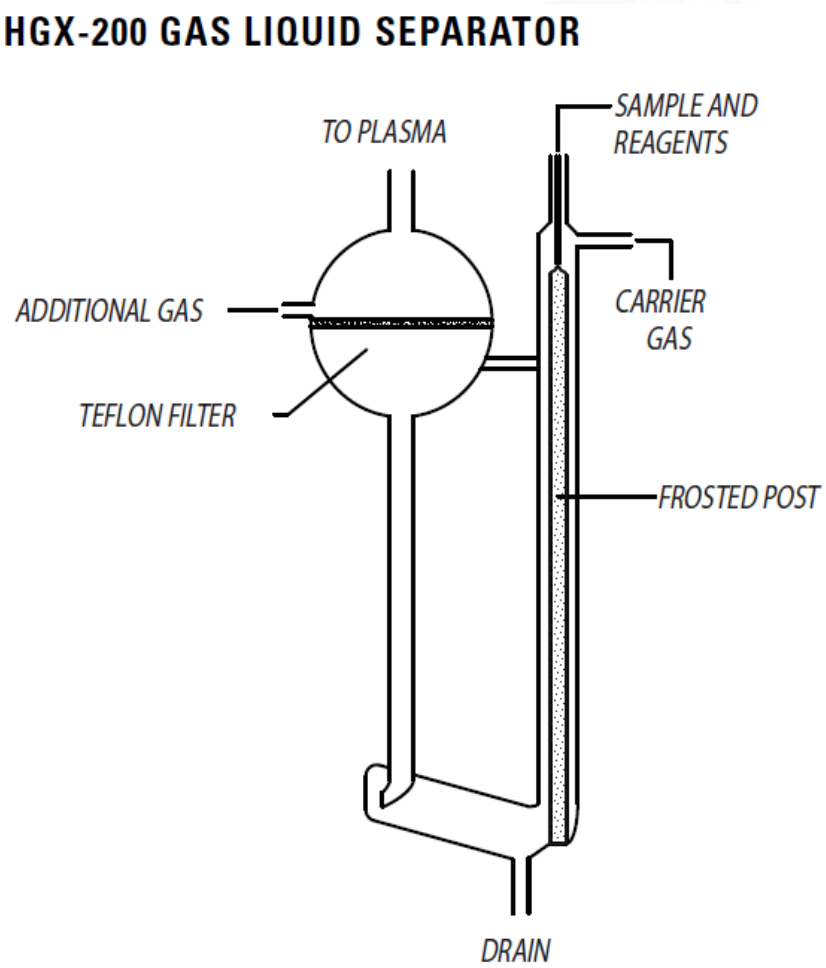

商业产品：HGX-200型氢化物发生系统(只为科研提供参考图片，无广告作用)

二、硒同位素的分析方法

进样系统

Nu Plasma II MC

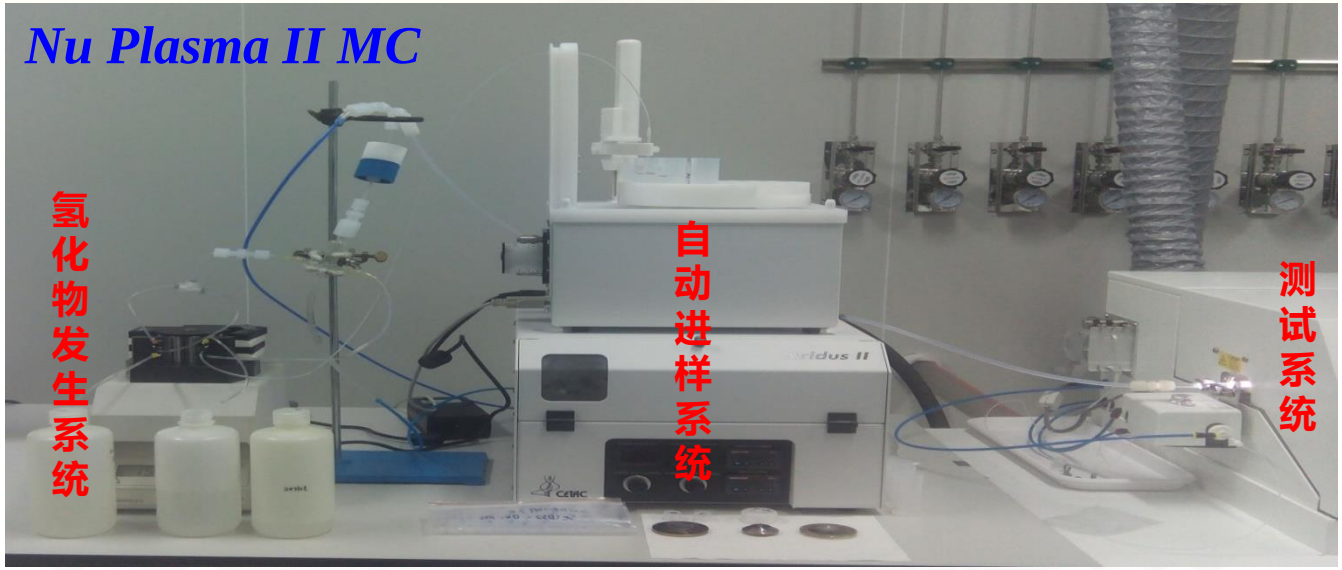

Neptune MC

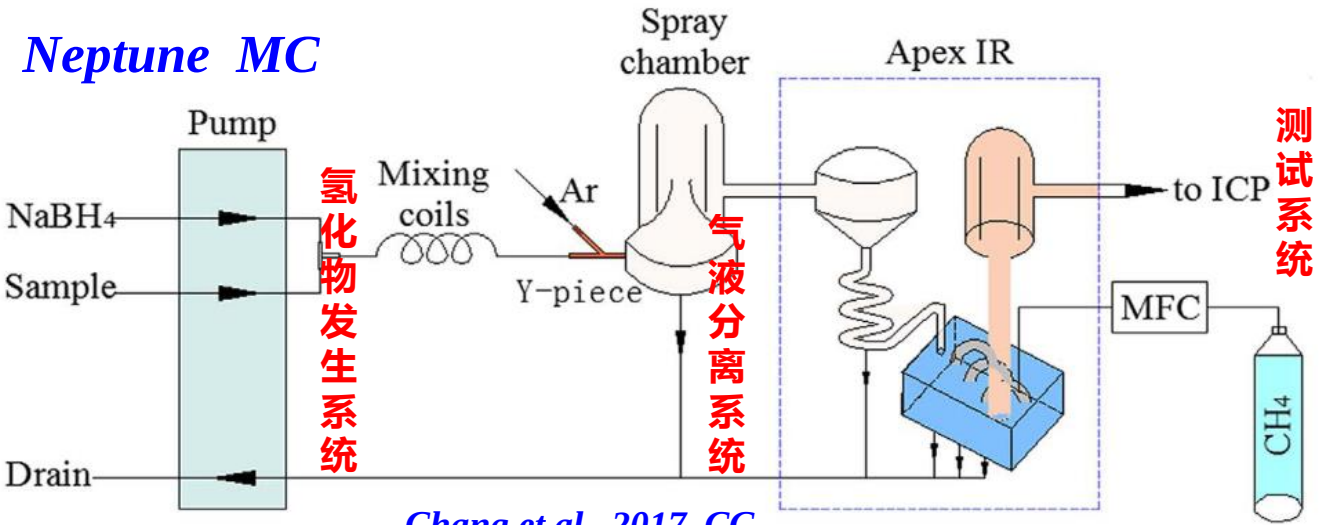

Chang et al., 2017, CG

二、硒同位素的分析方法

Table 1 Faraday collectors array for measurement of Se isotopes and the blank signals of interfering species

Collectors	L5	L4	L3	L2	Ax	H2	H4	H5	H6
Mass	74	75	76	77	78	79	80	81	82
Se isotopes	^{74}Se		^{76}Se	^{77}Se	^{78}Se		^{80}Se		^{82}Se
Isobaric interferences	$^{38}Ar^{36}Ar^{+}$ $^{74}Ge^{+}$ $^{58}Ni^{16}O^{+}$	$^{40}Ar^{35}Cl^{+}$ $^{38}Ar^{37}Cl^{+}$ $^{38}Ar^{36}ArH^{+}$ $^{75}As^{+}$ $^{74}GeH^{+}$	$^{40}Ar^{36}Ar^{+}$ $^{38}Ar^{38}Ar^{+}$ $^{76}Ge^{+}$ $^{75}AsH^{+}$ $^{60}Ni^{16}O^{+}$	$^{40}Ar^{37}Cl^{+}$ $^{40}Ar^{36}ArH^{+}$ $^{76}SeH^{+}$ $^{76}GeH^{+}$ $^{61}Ni^{16}O^{+}$	$^{40}Ar^{38}Ar^{+}$ $^{77}SeH^{+}$ $^{62}Ni^{16}O^{+}$	$^{79}Br^{+}$ $^{78}SeH^{+}$	$^{40}Ar^{40}Ar^{+}$ $^{80}Kr^{+}$ $^{79}BrH^{+}$	$^{40}Ar^{40}ArH^{+}$ ^{81}Br	$^{82}Kr^{+}$ $^{81}BrH^{+}$ $^{12}C^{35}Cl_{2}^{+}$ (?)
Blank signal (mV)	4	2	32	5	11	5	5500	140	2

硒同位素干扰来自载气Ar，基体As、Ge和SeH^{+}，$^{80}ArAr^{+}$与$^{80}Se^{+}$峰分开的分辨率至少在2万以上，目前存在困难。其背景校正方式选择On Peak Zero方式，其它校正方式如半高峰和ESA deflector均不适用。

Zhu et al.,2008, CJAC

二、硒同位素的分析方法

样品消解(Se^{4+}、Se^{6+})+稀释剂

还原法(TCF,Se形态统一)

消解：硝酸+双氧水+MQ水

必要样品：Ag 1-X8, 除 (As)

Se^{4+}: 2NHCl+KBH_4

方法特点：一定普适性，但对BIF不工作

对比方法

Se^{4+}; Ag 1-X8, 6M HCl (Fe);

Se^{4+}; Si-HS, 0.8M HCl (Ge);

Se^{6+}; 氧化, $K_2S_2O_8$

Se^{4+}: 2NHCl+KBH4

方法特点：普适性

开发方法

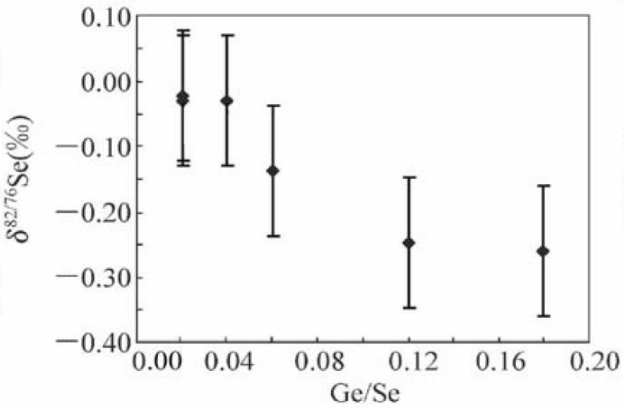

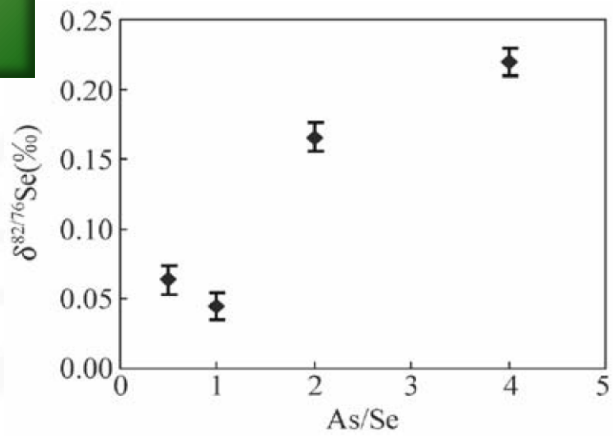

Zhu et al.,2008, CJAC

二、硒同位素的分析方法

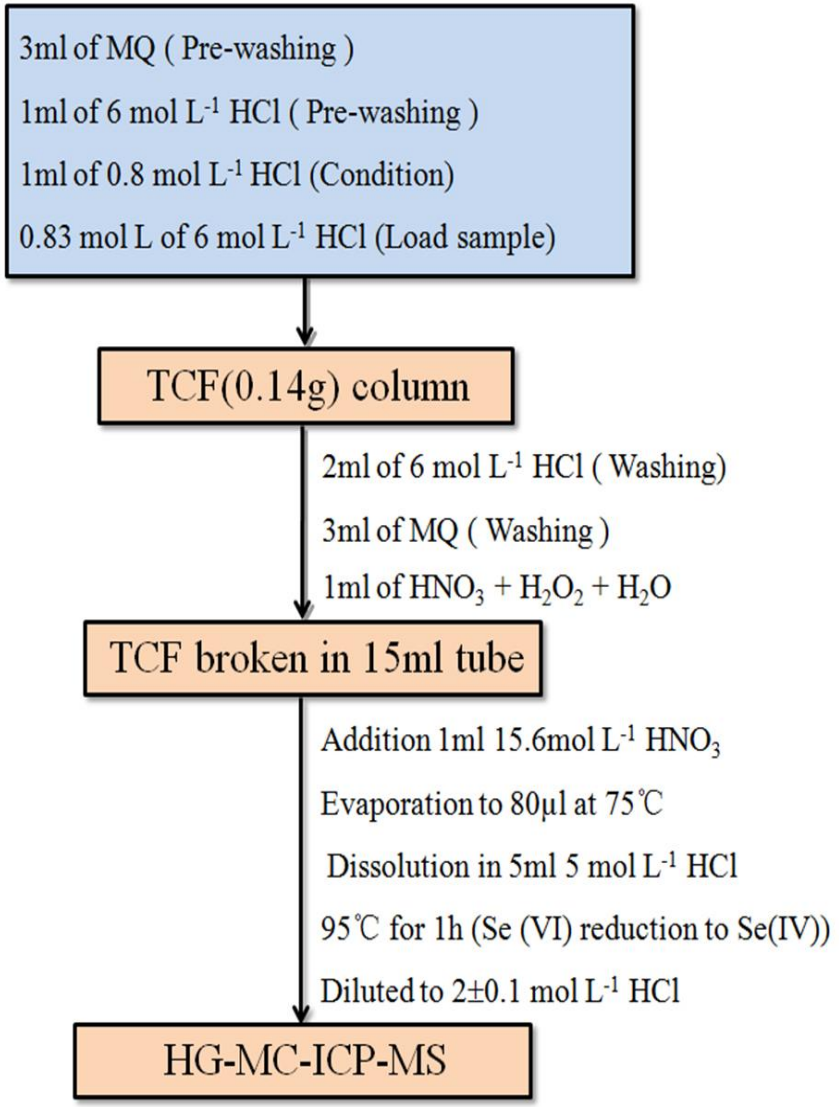

Zhu et al.,2008, CJAC

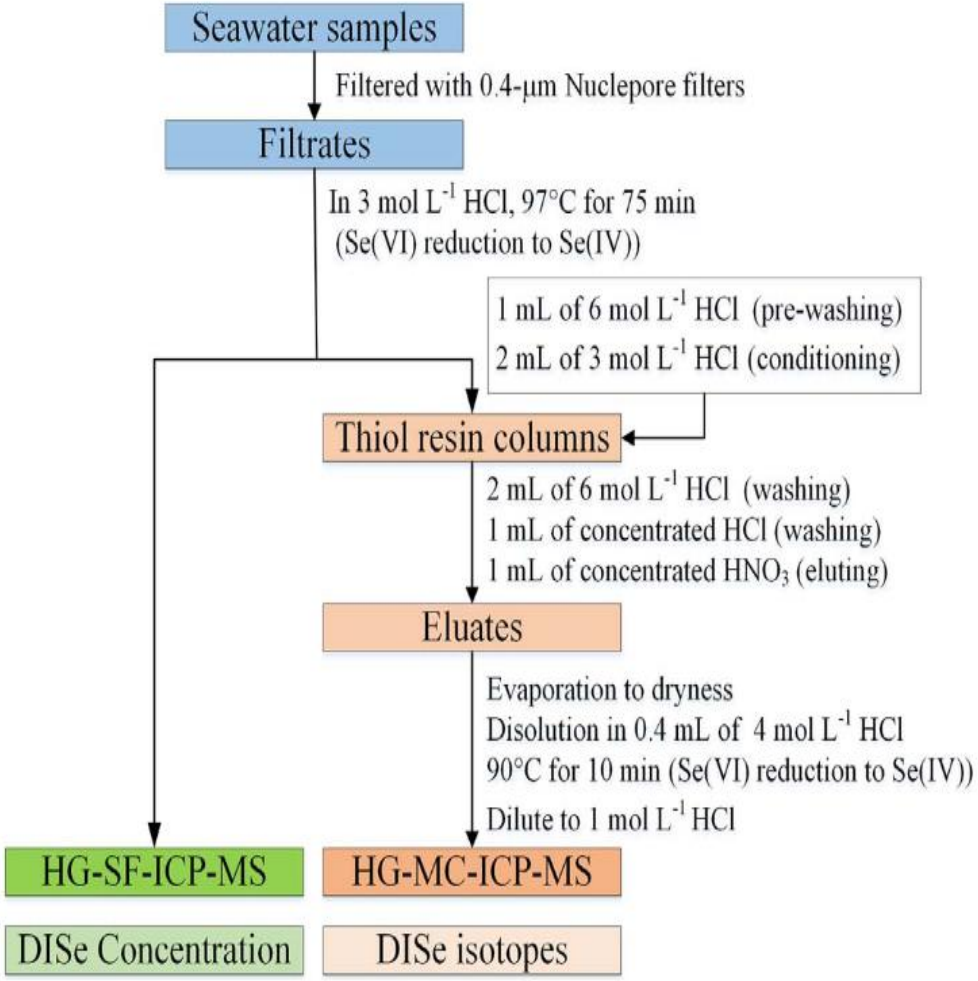

Fig. 1. Analytical procedure for determination of DISe concentration and isotopes in seawater.

Chang et al., 2017, CG

二、硒同位素的分析方法

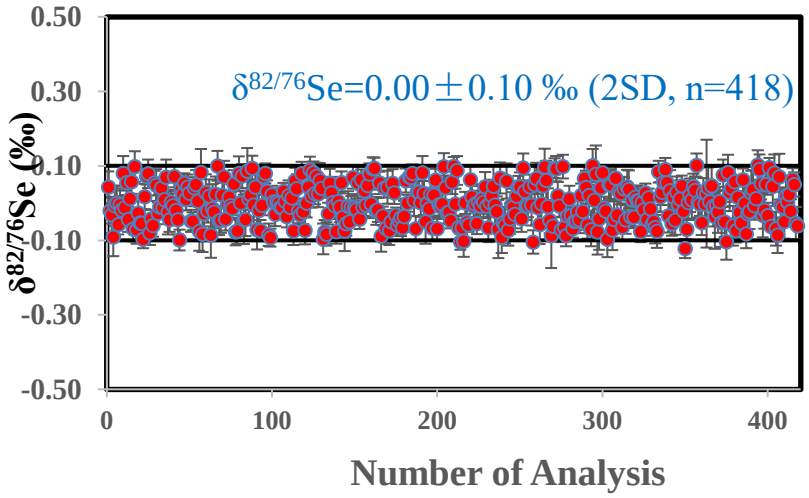

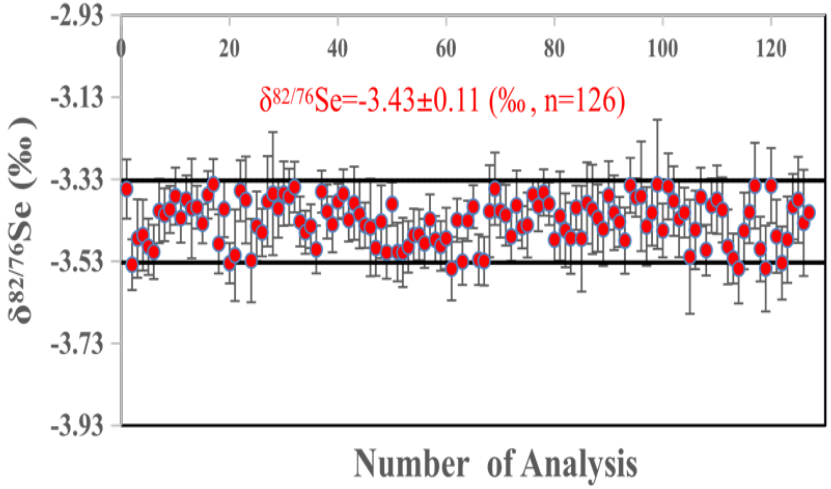

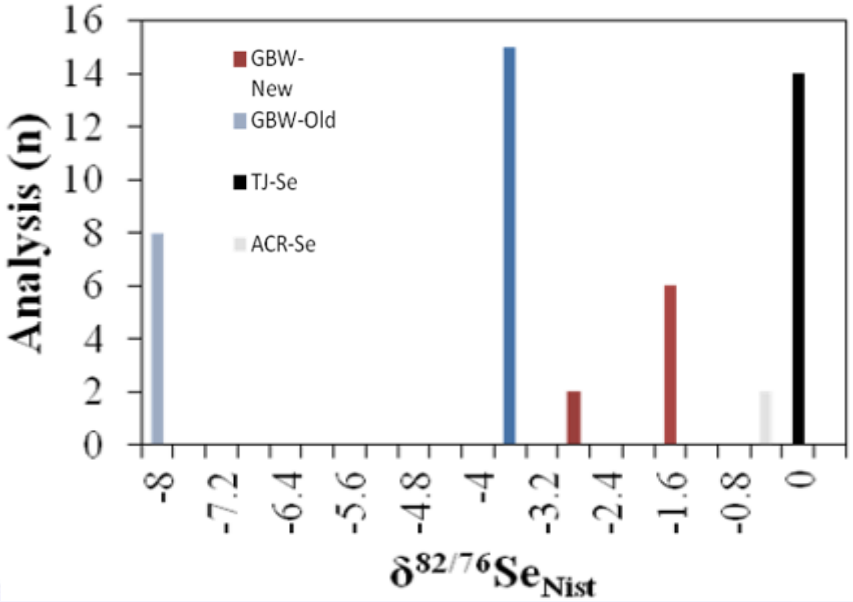

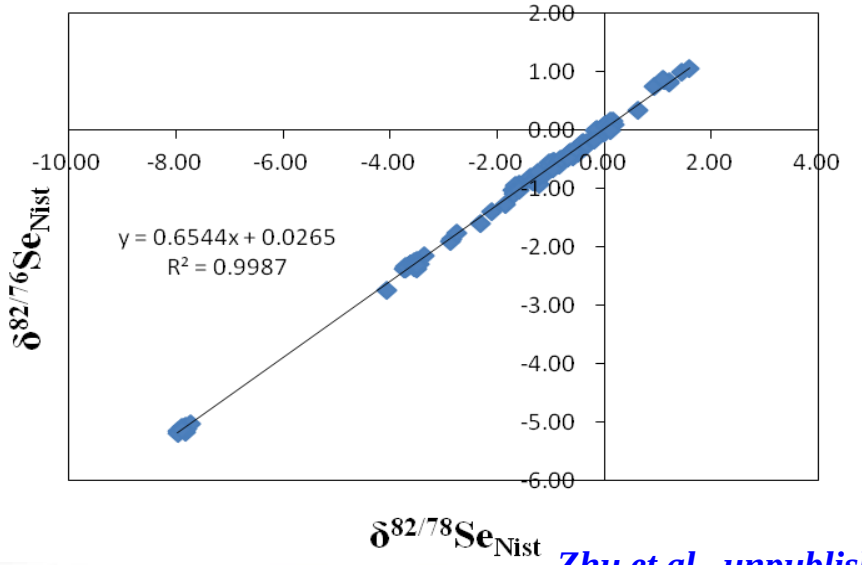

Zhu et al., unpublished

二、硒同位素的分析方法

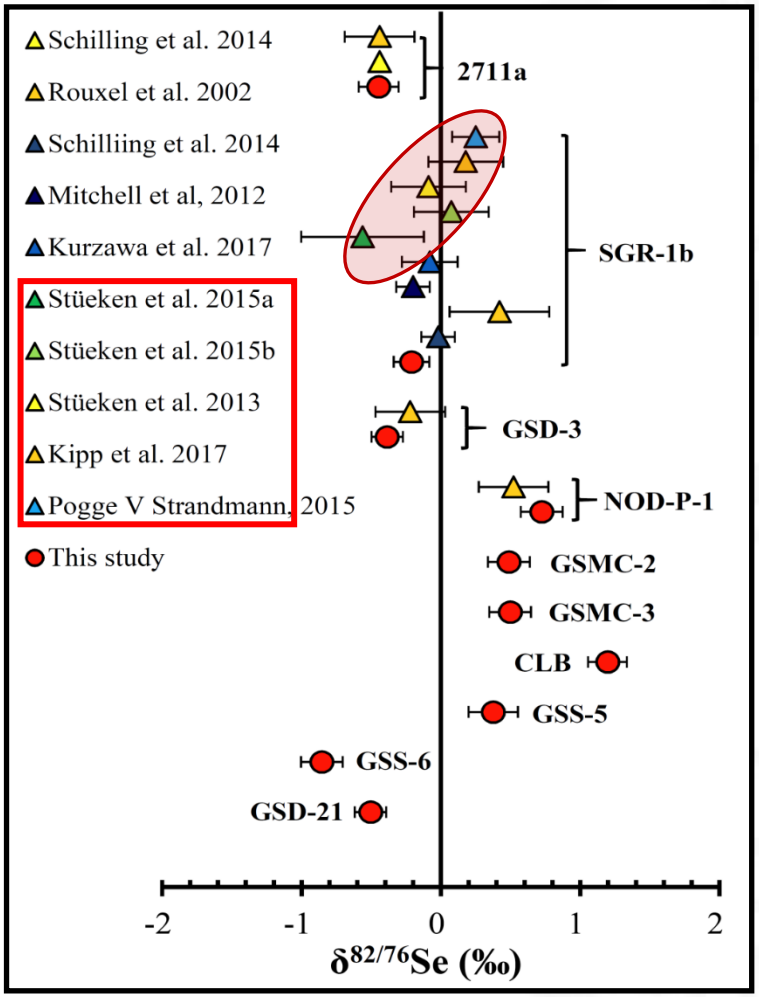

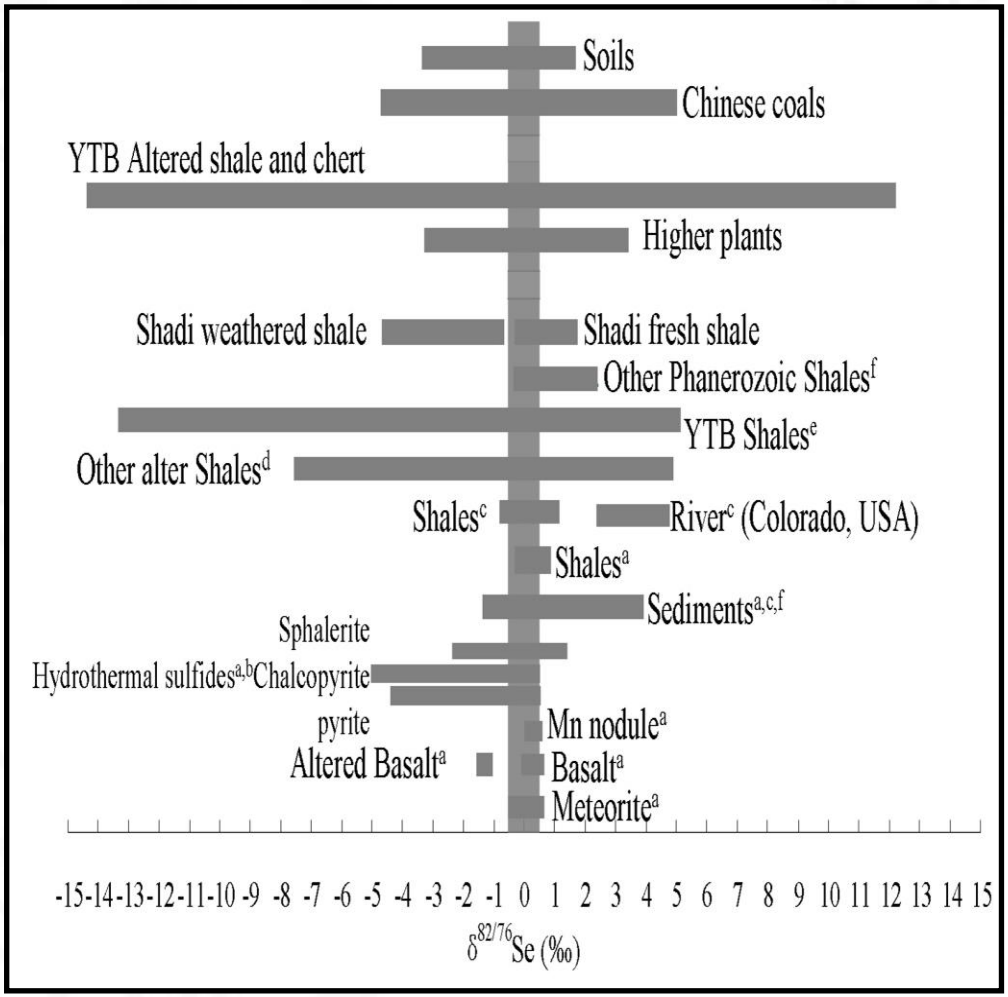

Zhu et al., unpublished

三、硒同位素理论分馏体系的构建

硒同位素分馏机理

同位素分馏理论： 平衡分馏与非平衡分馏(不包括非质量分馏)
(同位素交换) - (动力及瑞利分馏)

分馏机理：

化学过程：还原反应、氧化反应、沉淀溶解、**光化学反应**等

生物过程：异化还原、同化吸收、**细菌氧化**等

物理过程：吸附与解吸，**蒸发与冷凝**、物理/化学扩散等

三、硒同位素理论分馏体系的构建

3.1 硒的无机(非生物)还原过程

Table 7. Instantaneous isotopic fractionation ε caused by biogeochemical transformations.

Study	Transformation	Reacting agent	Measured ratio	ε, (‰)	ε ($\delta^{80/76}$Se)[a], (‰)	ε($\delta^{82/76}$Se)
(Rees and Thode, 1966)	Se^{6+} to Se^{4+}	HCl, 25°C	$^{82}Se/^{76}Se$	−18	−12	-18
This study	Se^{6+} to Se^{4+}	HCl, 70°C	$^{80}Se/^{76}Se$	−5.5	−5.5	-8.2
(Krouse and Thode, 1962)	Se^{4+} to Se^{0}	NH_2OH	$^{82}Se/^{76}Se$	−15	−10	-15
(Rees and Thode, 1966)	Se^{4+} to Se^{0}	Ascorbic acid	$^{82}Se/^{76}Se$	−19	−13	-19
(Webster, 1972)	Se^{4+} to Se^{0}	NH_2OH	$^{80}Se/^{74}Se$	−10	−7	-10.4
(Rashid and Krouse, 1985)	Se^{4+} to Se^{0}	NH_2OH	$^{82}Se/^{76}Se$	−11	−7	-10.4
(Rashid et al., 1978)	Se^{4+} to Se^{0}	Microbes	$^{82}Se/^{76}Se$	−5 to −40	−3 to −27	-5—40
This study	Soil–Se oxidation	Microbes?	$^{80}Se/^{76}Se$	<0.5	<0.5	0.75
This study	Se^{4+} adsorption	$Fe(OH)_3 \cdot nH_2O$	$^{80}Se/^{76}Se$	<0.5	<0.5	0.75
This study	Se volatilization	Algal culture	$^{80}Se/^{76}Se$	<1.1	<1.1	1.64
This study	Se volatilization	Soil (Microbes)	$^{80}Se/^{76}Se$	<0.6	<0.6	0.89

N-TIMS

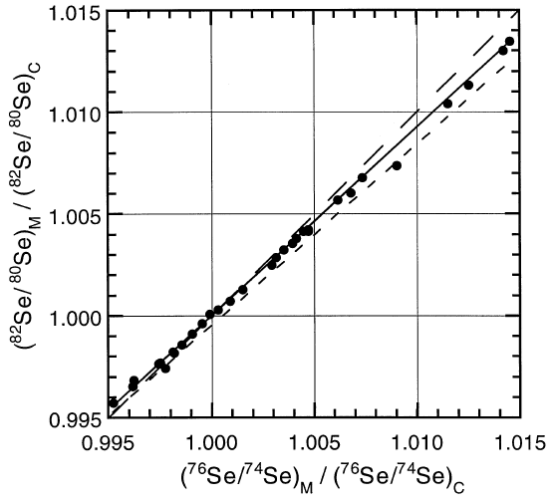

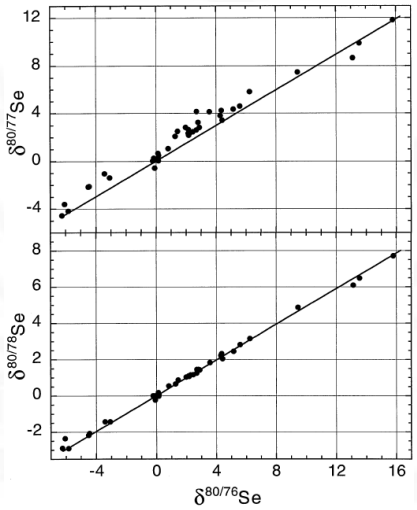

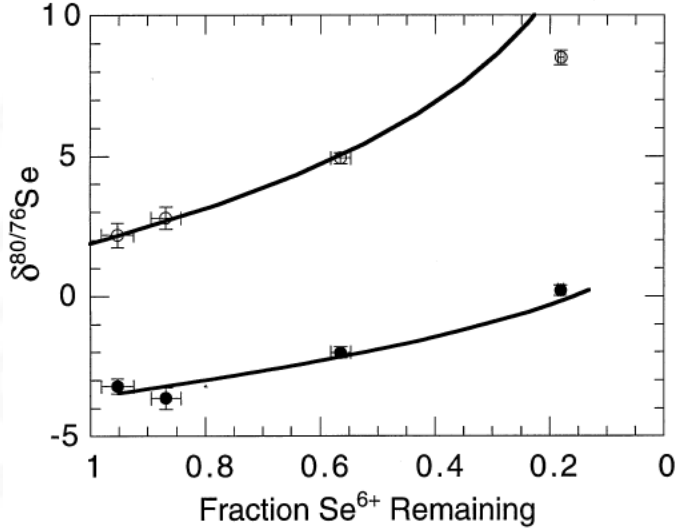

Johnson et al., 1999, GCA

三、硒同位素理论分馏体系的构建

Green rust 还原实验

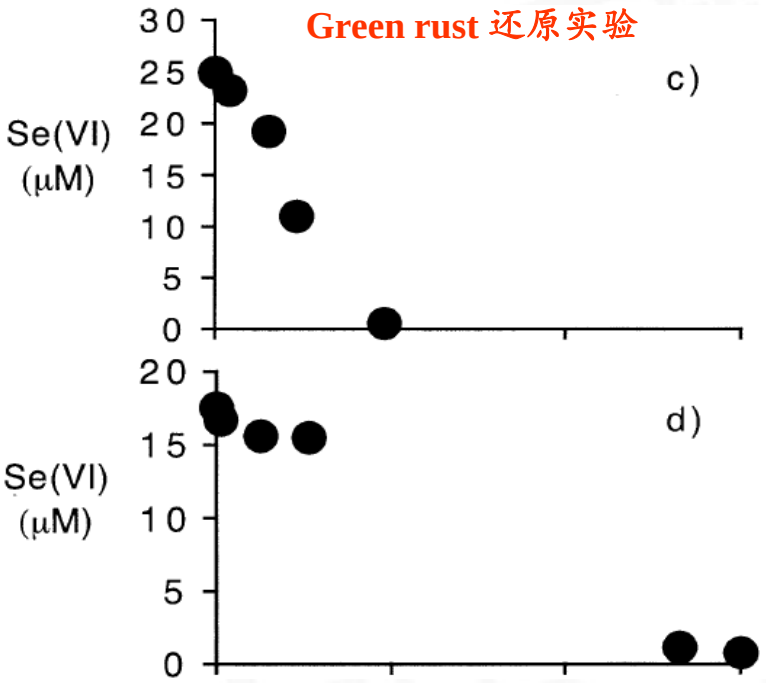

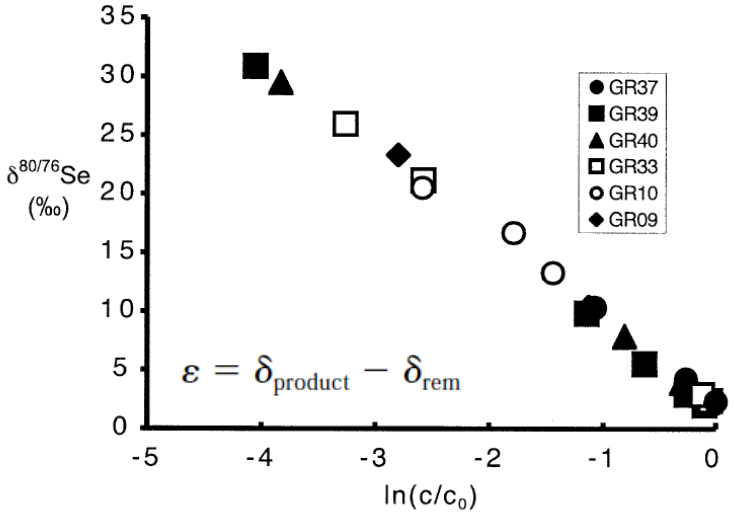

Fig. 4. Se isotope ratio data from all selenate reduction experiments plotted against $\ln(c/c_0)$, the natural logarithm of the fraction of unreduced Se remaining. The slope of the line gives ε. Uncertainty in $\ln(c/c_0)$ is approximately the width of the symbols. Uncertainty in $\delta^{80/76}$Se is ±0.2‰, much smaller than the symbols.

Table 1. Experimental conditions and results.

Experiment	Initial pH	Final pH	GR_{SO_4} (mM)	Fe(II) (mM)	SO_4^{2-} (mM)	Na^+ (mM)	Cl^- (mM)	Half-life[a] (h)	ε^b (‰)	n
GR37	7.0	6.0	0.41	0.50	3.7	6.5	0.0	20	−7.34 ± 0.4	3
GR39	7.0	5.9	0.41	0.16	1.1	1.8	0.0	2.9	−7.35 ± 0.2	5
GR40	6.9	5.9	0.41	0.24	2.0	3.4	0.0	4.3	−7.24 ± 0.2	4
GR33	6.8	6.8	0.80	1.20	7.2	13.0	0.0	11	−7.43 ± 0.3	4
GR10	7.3	7.3	0.67	0.17	2.1	6.8	2.12	15	−7.22 ± 0.4	4
GR09	6.2	6.3	0.48	0.28	1.6	3.7	0.99	7.9	−7.57 ± 0.4	3

[a] Selenate half-life was derived by fitting data to a first-order reaction model.

Johnson et al., 2003, GCA

三、硒同位素理论分馏体系的构建

零价Fe还原实验

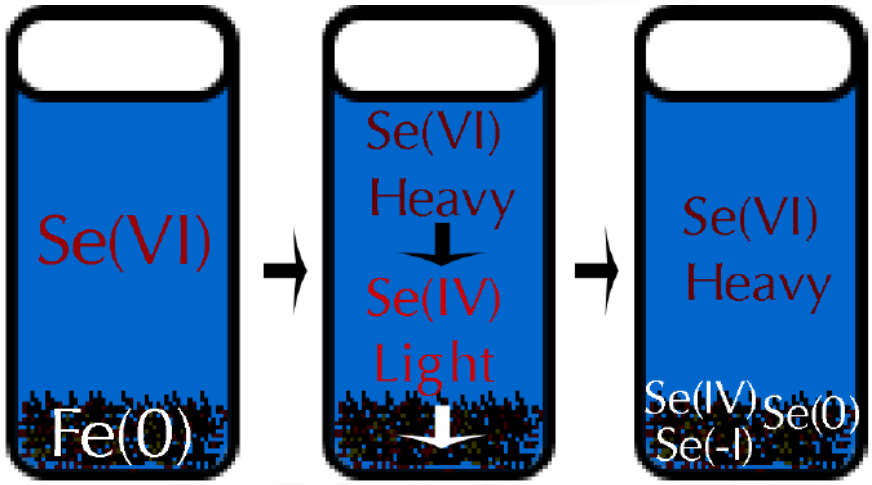

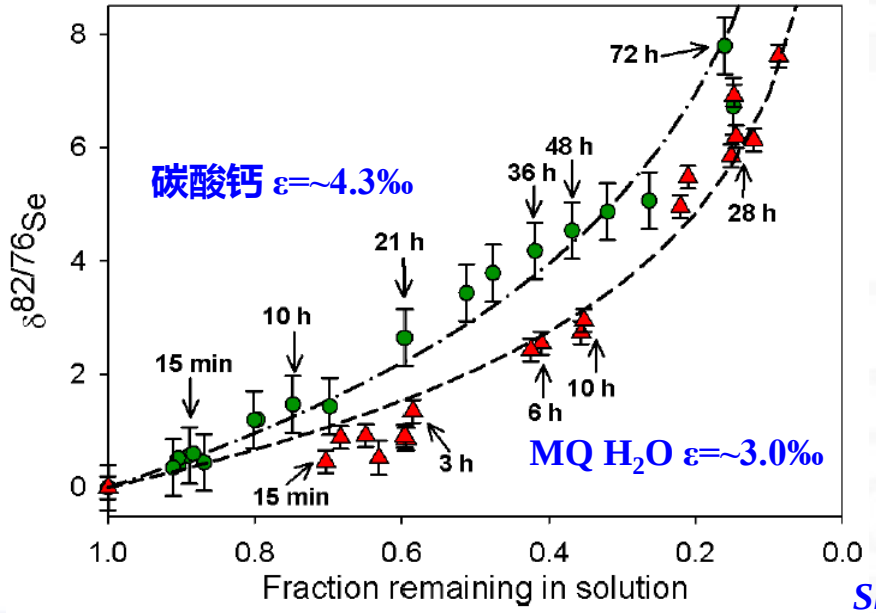

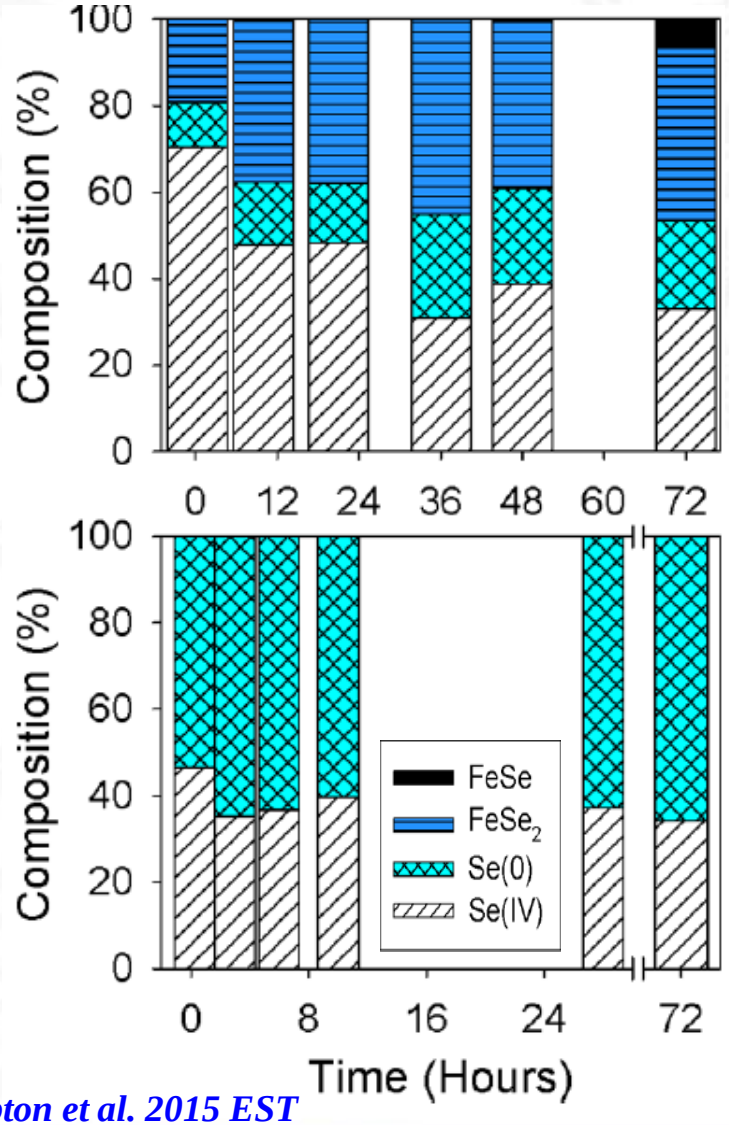

Shrimpton et al. 2015 EST

三、硒同位素理论分馏体系的构建

3.2 硒的生物还原过程

Fractionation of selenium isotopes during bacterial respiratory reduction of selenium oxyanions *Herbel et al., 2002, GCA*

Table 2. Maximum reduction rates and enrichment factors (ε) determined by fitting isotopic evolution models to the data from growing cultures.

Bacterium	Reduction couple	Maximum rate (10^{-15} mol · cell^{-1} · h^{-1})	ε (‰)
B. selenitireducens	Se(IV)–Se(0)	3.3	-8.0 ± 0.4
B. arsenicoselenatis	Se(VI)–Se(IV)	13.3	-5.0 ± 0.5
	Se(IV)–Se(0)	ND[a]	-6.0 ± 1.0
S. barnesii	Se(VI)–Se(IV)	1.5	-0.2 ± 0.2 to -4.0 ± 1.0[b]
	Se(IV)–Se(0)	0.067	-1.1 ± 0.4 to -8.4 ± 0.4[b]

Table 3. Maximum reduction rates and enrichment factors (ε) determined by fitting isotopic evolution models to the data from the *S. barnesii* washed cell suspension experiments.

Temp. (°C)	Electron acceptor	Reduction couple	Maximum reduction rate (1×10^{-15} moles Se · cell^{-1} · h^{-1})	ε (‰)
15	SeO_4^{2-}	Se(VI)–Se(IV)	0.41	-1.1 ± 0.3
		Se(IV)–Se(0)	0.47	-1.7 ± 0.4 to -9.1 ± 0.5[a]
30	SeO_4^{2-}	Se(VI)–Se(IV)	0.92	-1.1 ± 0.4
		Se(IV)–Se(0)	0.62	-8.3 ± 0.3
15	SeO_3^{2-}	Se(IV)–Se(0)	0.20	-7.9 ± 0.4
30	SeO_3^{2-}	Se(IV)–Se(0)	0.22	-8.0 ± 0.4

三、硒同位素理论分馏体系的构建

Table 1. $\delta^{82/76}$Se Values in Se(VI) and Se(IV) Standards, Media, Fungi, and Methylselenides of the Treatments with Se(VI) and Se(IV) at Each of the pH Values of 4 and 7

Schilling et al., 2012, EST; 2013,CG.

sample	Se species	day 3	day 4	day 5	day 11	day 12	day 13	day 14	day 15
standard	VI	−0.69 ± standard deviation 0.07‰ (n = 2)							
standard	IV	−0.20 ± 0.05‰ (n = 2)							
					pH 4				
medium	VI				−0.59	−0.59	−0.58	−0.58	−0.61
fungus	VI				−1.36	−1.17	−1.07	−0.71	−0.84
methylselenides	VI				−3.29	−3.42	−3.97	−3.67	−3.59
					pH 7				
medium	VI				−0.69	−0.76	−0.79	−0.76	−0.63
fungus	VI				−1.13	−1.09	not determined[a]	−0.96	−0.95
methylselenides	VI				−2.96	−3.66	−3.99	not determined[a]	−3.14
medium	IV	6.3	2.1	1.55					
fungus	IV	−2.07	−1.49	not determined[a]					
methylselenides	IV	−6.18	−5.81	−2.80					

[a] Yield of Se mass by the extract <100 ng which was not sufficient for isotope ratio analysis with our analytical equipment.

Table 3

Selenium isotopic composition ($\delta^{82/76}$ Se) of the unspiked soil and the components of the microcosms after 11 days of incubation.

Sample	Supplied Se	$\delta^{82/76}$Se values				
		Aqueous solution (medium)	Soil	Fungus	Methylselenide	Unspiked soil
		(‰)				
Stock	Se(IV)	−0.20 (n = 2)				
Stock	Se(VI)	−0.65 (n = 2)				
GA1	Se(IV)	1.7	0.35	−0.87	−3.56	0.16
GA1	Se(VI)	0.29	−0.81	−1.83	–	0.16
RS2	Se(IV)	1.11	−1.34	0.33	−4.67	0.45
RS2	Se(VI)	0.98	−0.61	−7.53	–	0.45
FO1	Se(IV)	0.51	0.33	–	–	−0.59
FO1	Se(VI)	−0.34	−0.3	–	–	−0.59

三、硒同位素理论分馏体系的构建

$^{82}Se/^{76}Se$ Fractionation: Reduction Reactions

Reductant	ε(‰)	Reference
Selenate reduction:		
Strong HCl	-18	Rees and Thode (1966)
Green Rust	-11	Johnson and Bullen (2003)
D. Viet, D. Co23	-9 , -12	**Schilling (2013)**
3 Microbes (high e^- donor)	-2 to -7	Herbel et al. (2000)
Dechloromonas sp. microcosms	-2	Kirk et al. (2009)
Pond/Estuarine Sediments	-4 to -5	Ellis et al. (2003)
Pond Sediments	-2	Clark and Johnson (2008)
Se(IV) reduction:		
NH2OH or ascorbic acid	-15 to -19	Krouse and Thode (1962), Rees and Thode (1966), Rashid and Krouse (1985)
3 Microbial strains (high e^- donor)	-9 to -14	Herbel et al. (2000)
4 Microbial strains	-6 to -8	Schilling (2013)
Pond/Estuarine Sediments	-8	Ellis et al. (2003)

Johnson et al. Poster

三、硒同位素理论分馏体系的构建

3.3 硒的无机氧化过程

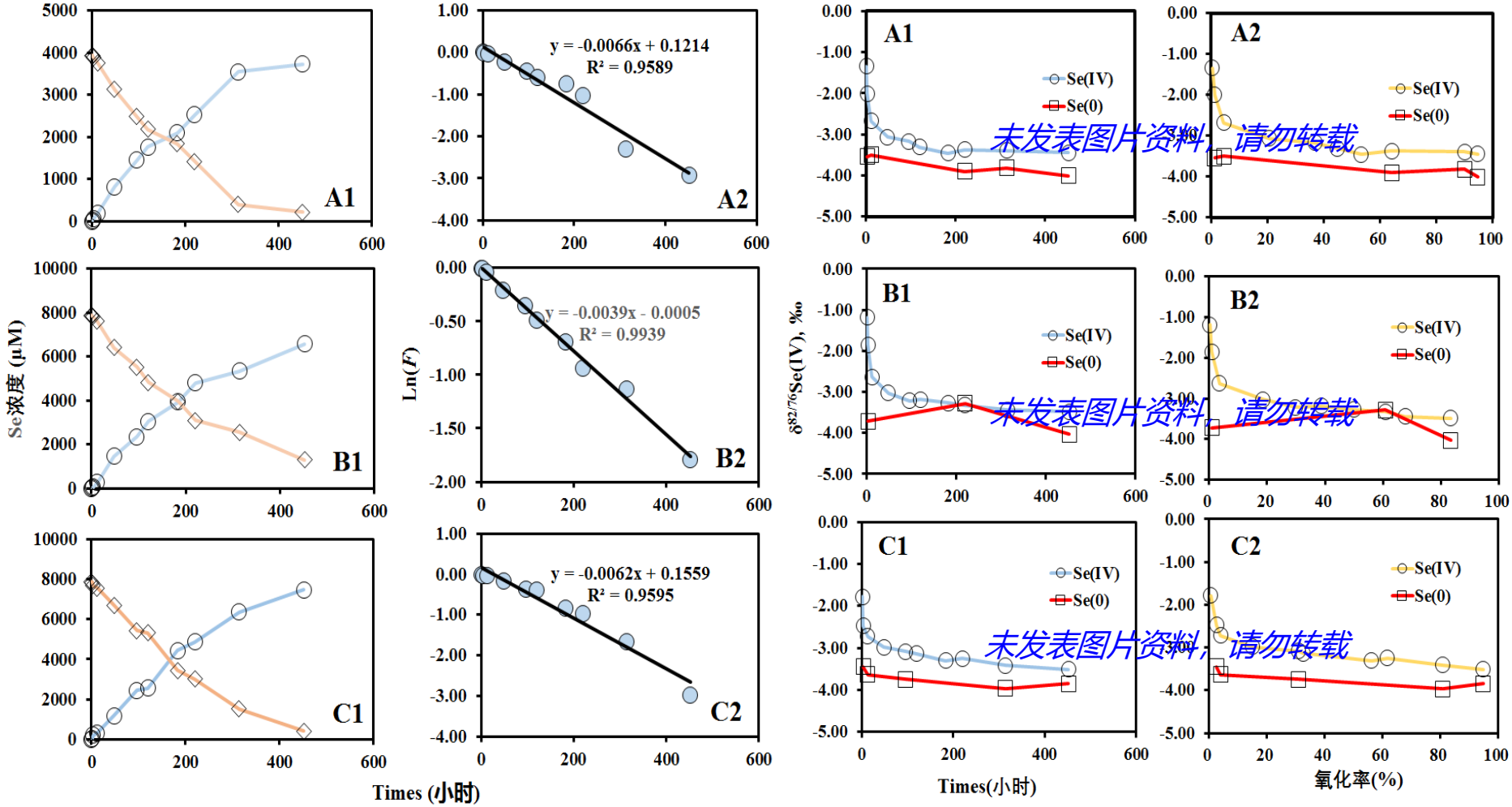

三、硒同位素理论分馏体系的构建

3.4 硒的吸附与解吸过程

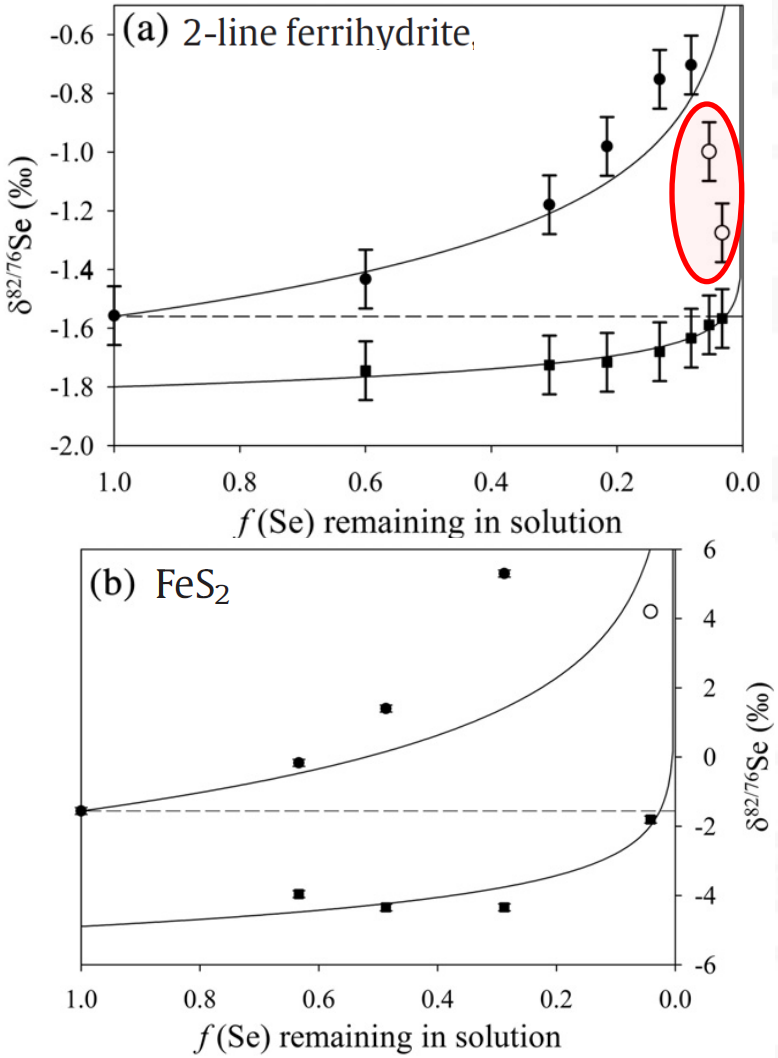

Table 3
Sorption experiments to iron oxide and iron sulfide minerals: Half-life for aqueous Se removal from solution, total % removal aqueous Se at end of experiment, and maximum fractionation observed during the course of the experiment. Y = yes; N = no.

Experiment	$t_{1/2}$ (min)	Total Se removed (%)	Reduction observed	ε_{max} (‰)	Relative error (‰)
Iron oxides					
Se(VI)					
Hematite		14	N		
Goethite		17	N		
2-line ferrihydrite	35	46	N	0.08	±1.2
Se(IV)					
Hematite	42	41	N	0.14	±2.4
Goethite	3.6	99	N	0.45	±0.6
2-line ferrihydrite	15	>99	N	0.93	±0.4
Iron sulfides					
Se(VI)					
Mackinawite (FeS)	60 h	20	Y	3.0	±0.2
Pyrite (FeS_2)	69 h	13	Y		
Se(IV)					
Mackinawite (FeS)	3.4	98	Y	3.7[a]	±0.3
Pyrite (FeS_2)	9 h	96	Y	9.7	±0.0

[a] Calculated using measured $\delta^{82/76}$Se of solid phase.

Mithcell et al., 2013,CG.

三、硒同位素理论分馏体系的构建

硒被铁、锰、铝氧化物吸附的过程

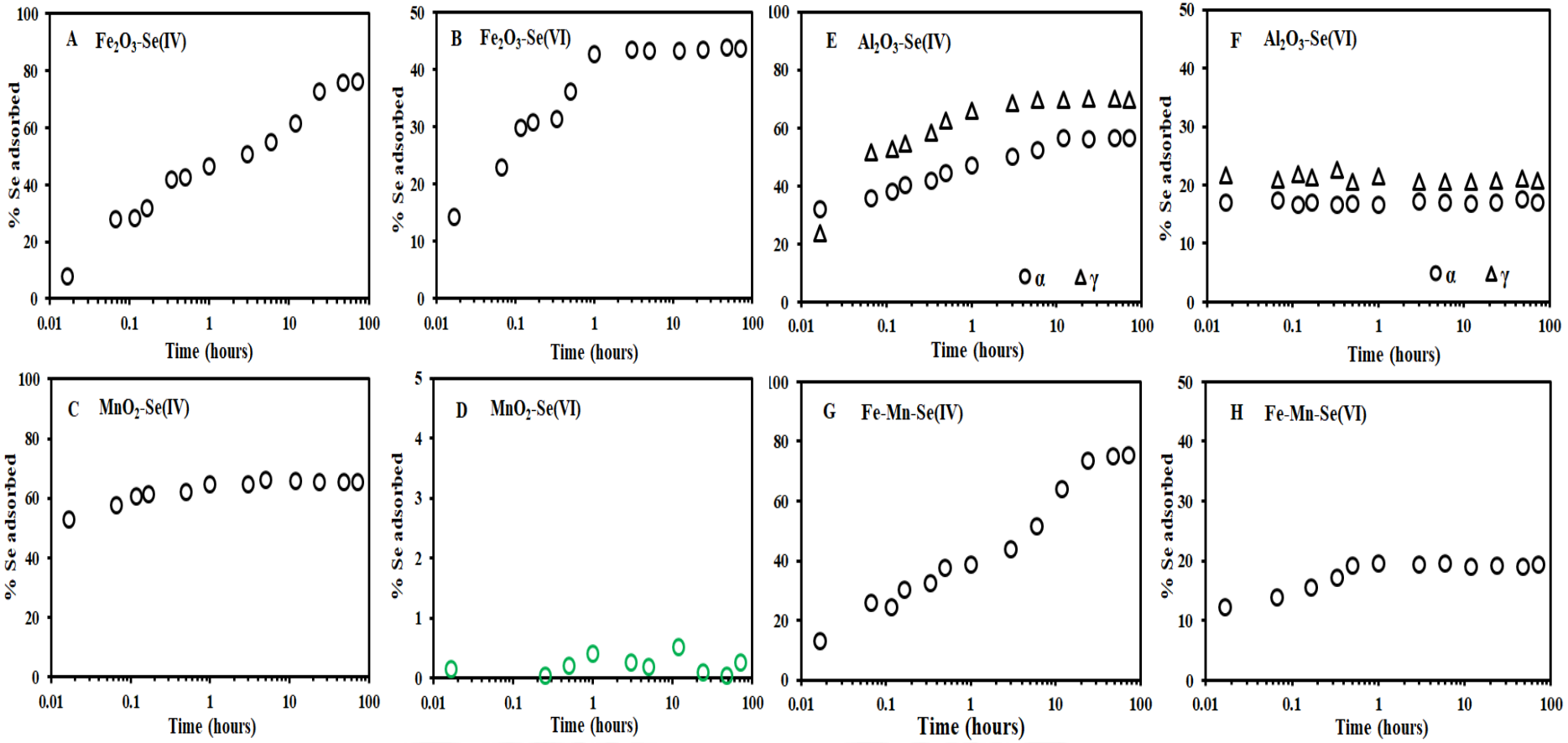

Xu et al., 2020,GCA.

三、硒同位素理论分馏体系的构建

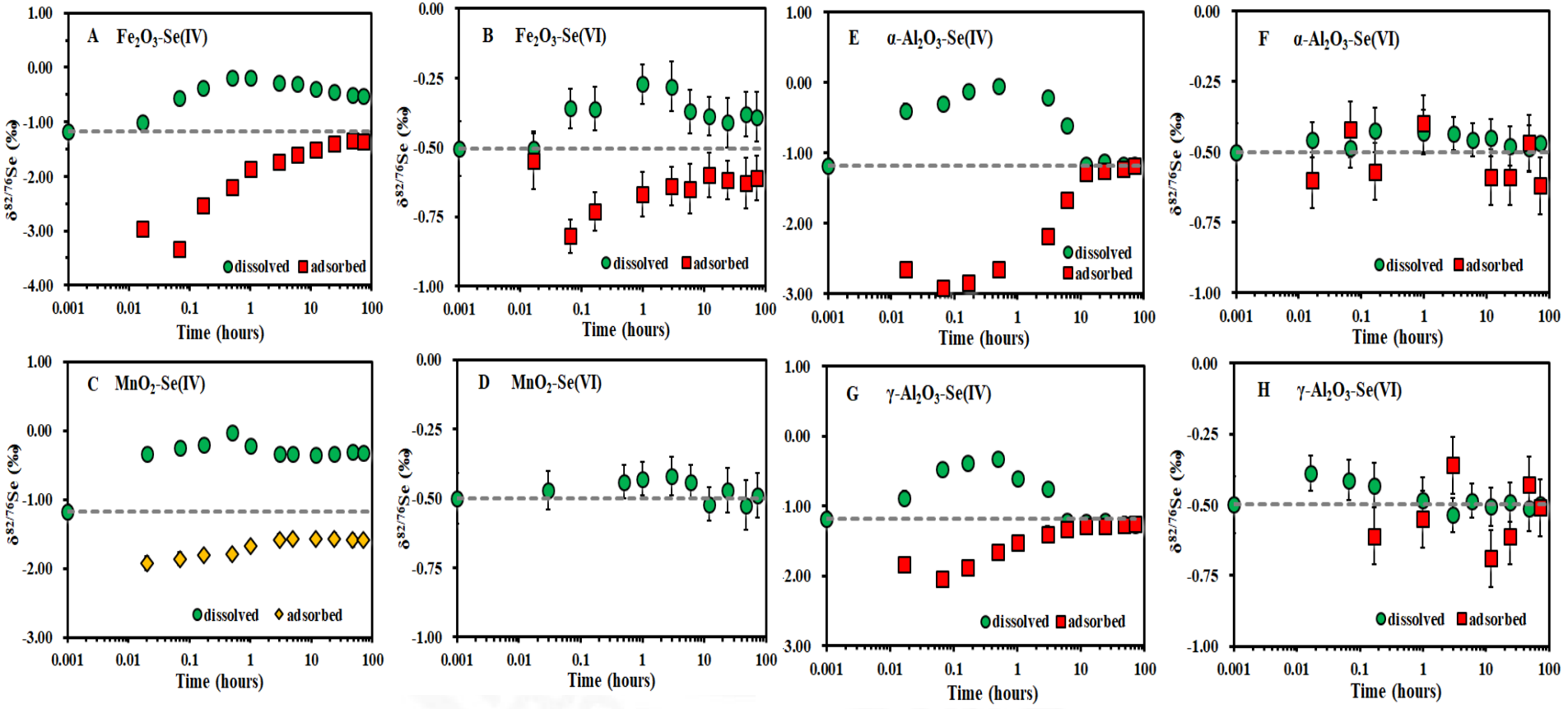

Xu et al., 2020,GCA.

三、硒同位素理论分馏体系的构建

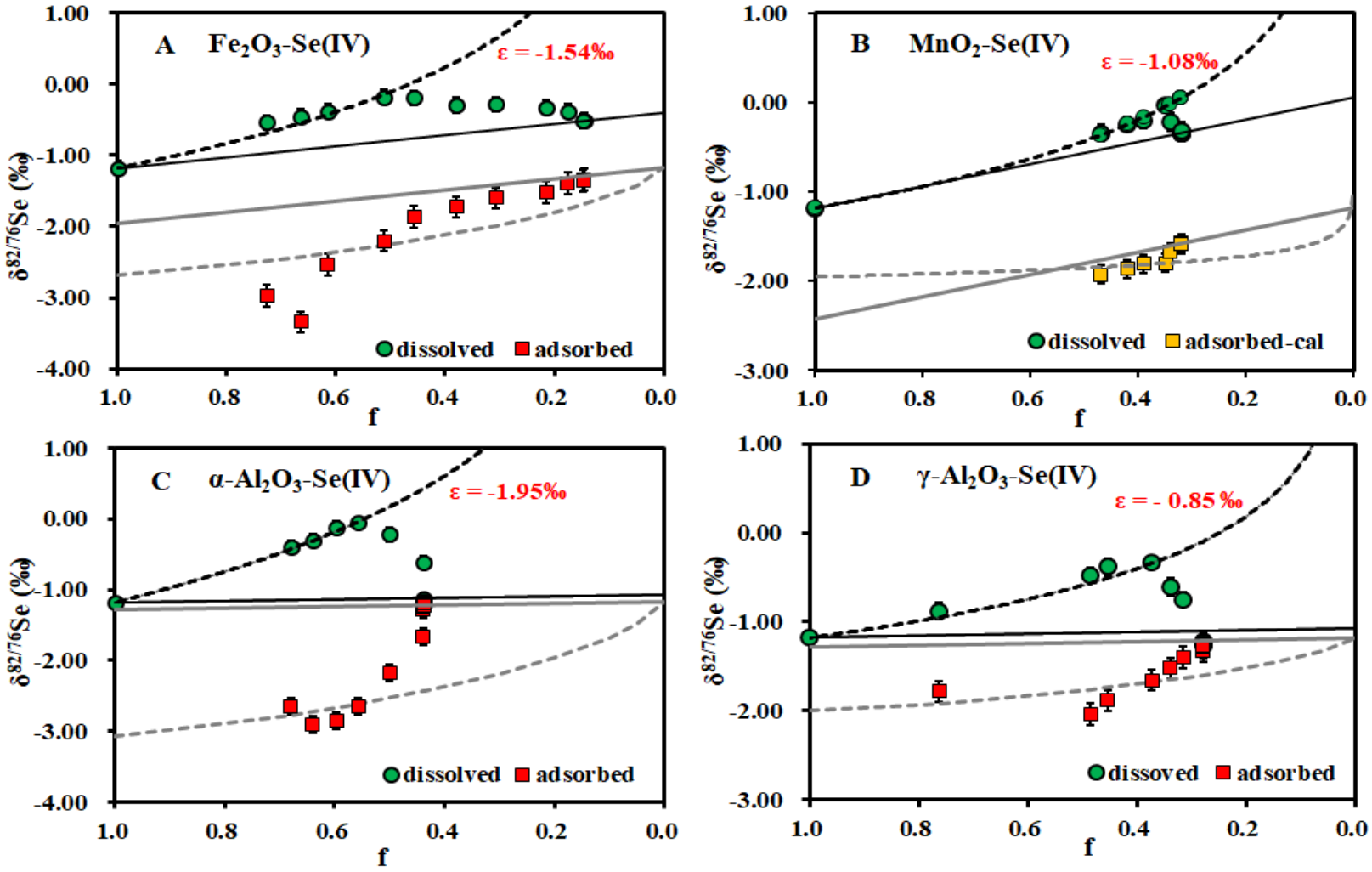

Xu et al., 2020,GCA.

三、硒同位素理论分馏体系的构建

硒被粘土矿物吸附的过程

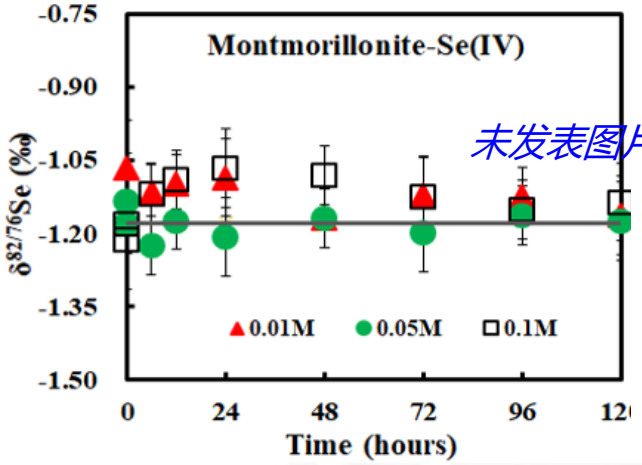

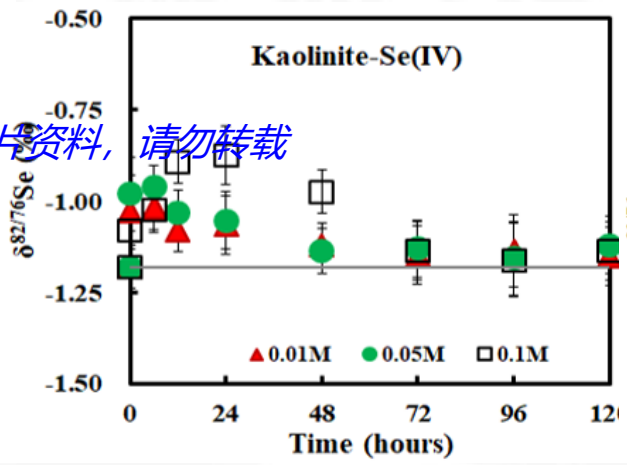

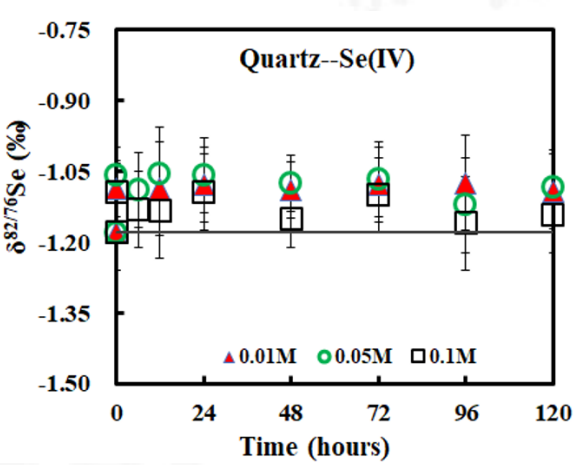

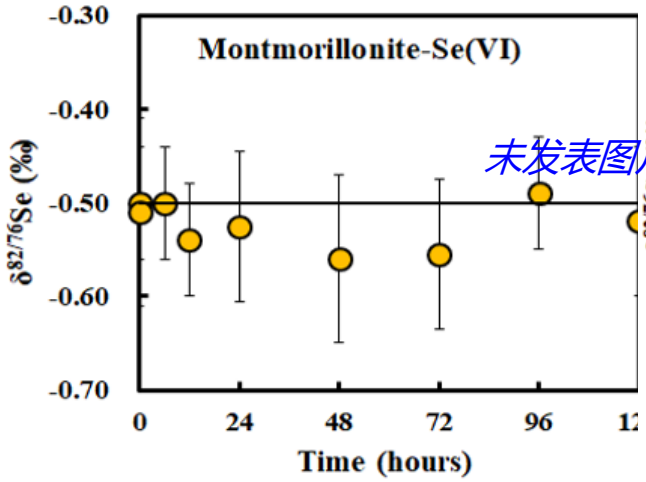

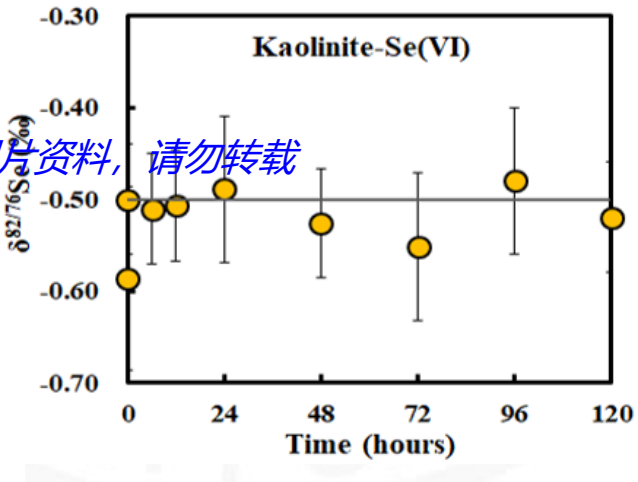

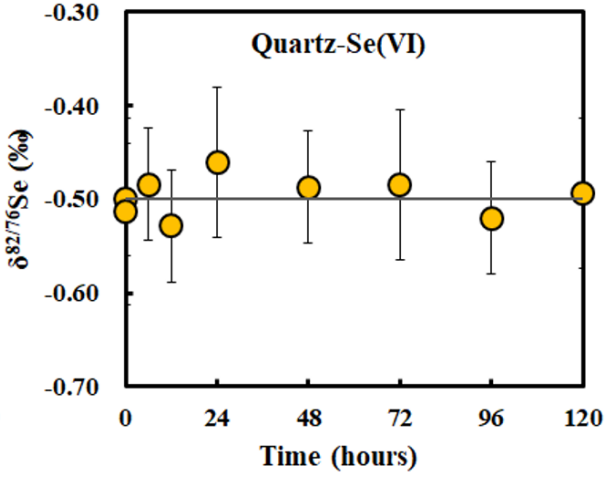

三、硒同位素理论分馏体系的构建

硒被有机质吸附的过程

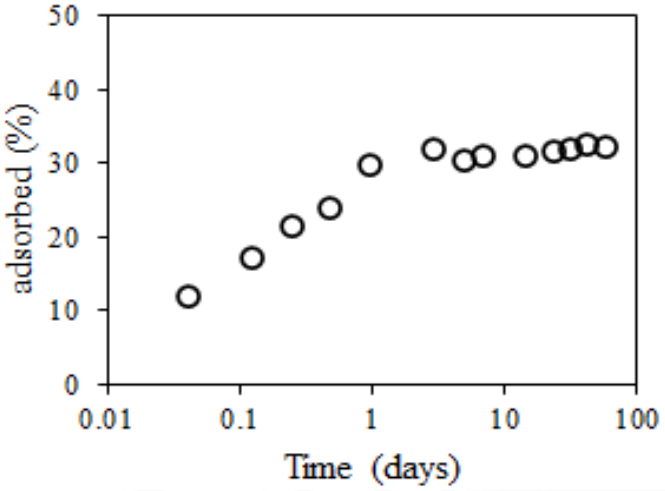

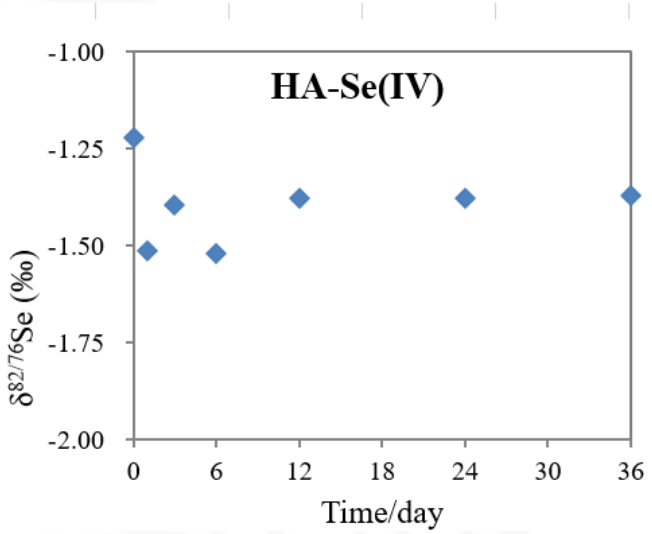

三、硒同位素理论分馏体系的构建

吸附小结

- Metal oxides
  - Fe oxides: hematite, HFO — $\Delta^{82/76}Se$ (IV)≤0.82 ‰; $\Delta^{82/76}Se$ (VI) ≤ 0.2 ‰
  - Manganese oxides: MnO_2 — $\Delta^{82/76}Se$ (IV)≤1. 2 ‰; $\Delta^{82/76}Se$ (VI) ≤ 0.1 ‰
  - Al oxides : γ-Al_2O_3 , α Al_2O_3 — $\Delta^{82/76}Se$ (IV)≤0.1 ‰; $\Delta^{82/76}Se$ (VI) ≤ 0.1 ‰
- Clay minerals
  - Montmorillonite
  - Illite
  - Kaolinite

  $\Delta^{82/76}Se$ (IV)≤0.1 ‰; $\Delta^{82/76}Se$ (VI) ≤ 0.1 ‰
- Organic matter
  - Humic acid- HA
  - Fulvic acid- FA

  $\Delta^{82/76}Se$ (IV)≤ ? ; $\Delta^{82/76}Se$ (VI) ≤ ?

三、硒同位素理论分馏体系的构建

3.5 不同形态硒的平衡交换

Table 4

Equilibrium Se isotope fractionation Δ_{A-B} between any two Se species in this paper at 25 °C.

Δ_{A-B}(‰) A \ B	SeO_2 1.02003	SeO 1.00843	Se_2 1.00562	H_2Se 1.00561	HSe^- 1.00438	DMSe 1.00999	DMDSe 1.00833	DMSeS 1.00872	SeO_4^{2-} 1.03777	SeO_3^{2-} 1.02407	$HSeO_3^-$ 1.02356	SeMet 1.01042	SeCyst 1.01030	Se(M)* 1.00601	Se(T)* 1.00595
SeO_2 1.02003	0.0	11.4	14.2	14.2	15.5	9.9	11.5	11.1	−17.2	−3.9	−3.5	9.5	9.6	13.8	13.9
SeO 1.00843		0.0	2.8	2.8	4.0	−1.5	0.1	−0.3	−28.7	−15.4	−14.9	−2.0	−1.9	2.4	2.5
Se_2 1.00562			0.0	0.0	1.2	−4.3	−2.7	−3.0	−31.5	−18.2	−17.7	−4.8	−4.7	−0.4	−0.3
H_2Se 1.00561				0.0	1.2	−4.3	−2.7	−3.1	−31.5	−18.2	−17.7	−4.8	−4.7	−0.4	−0.3
HSe^- 1.00438					0.0	−5.6	−3.9	−4.3	−32.7	−19.4	−18.9	−6.0	−5.9	−1.6	−1.6
DMSe 1.00999						0.0	1.6	1.3	−27.1	−13.8	−13.3	−0.4	−0.3	3.9	4.0
DMDSe 1.00833							0.0	−0.4	−28.8	−15.5	−15.0	−2.1	−2.0	2.3	2.4
DMSeS 1.00872								0.0	−28.4	−15.1	−14.6	−1.5	−1.4	2.7	2.8
SeO_4^{2-} 1.03777									0.0	13.3	13.8	26.7	26.8	31.1	31.3
SeO_3^{2-} 1.02407										0.0	0.5	13.4	13.5	17.8	17.8
$HSeO_3^-$ 1.02356											0.0	12.9	13.0	17.3	17.4
SeMet 1.01042												0.0	0.1	4.4	4.4
SeCyst 1.01030													0.0	4.3	4.3
Se(M)* 1.00601														0.0	0.0
Se(T)* 1.00595															0.0

*Se(M) denotes monoclinic structure; Se(T) denotes the trigonal one.

Li and Liu, 2011, EPSL

三、硒同位素理论分馏体系的构建

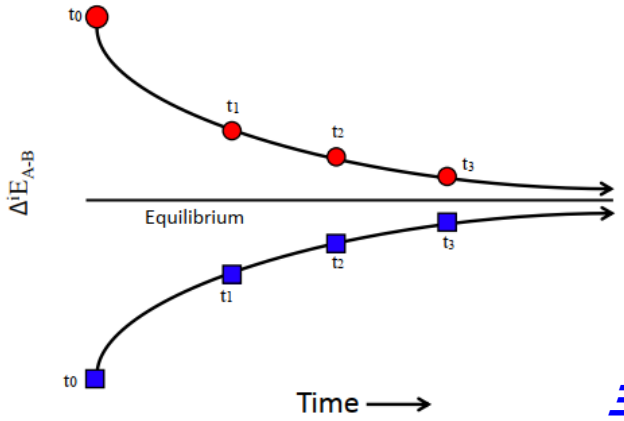

三同位素方法

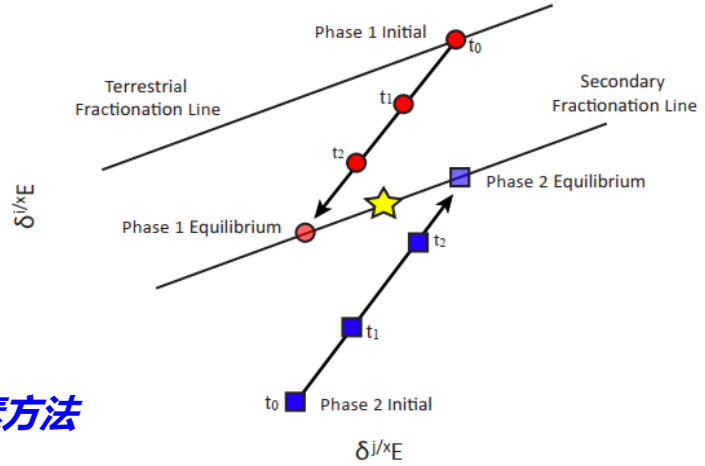

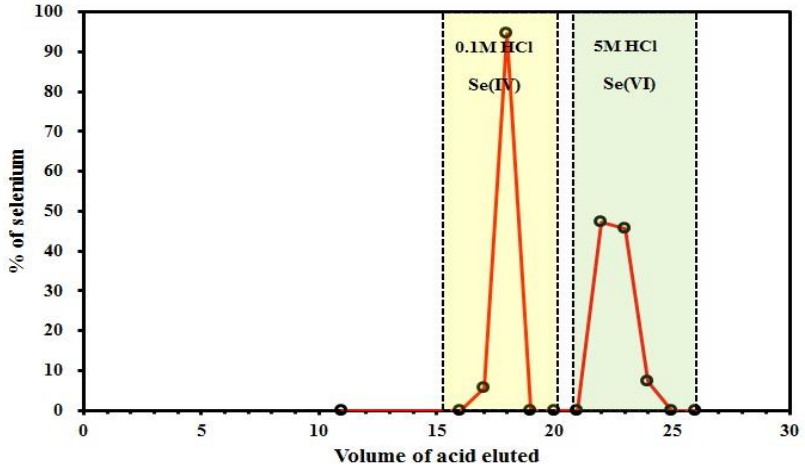

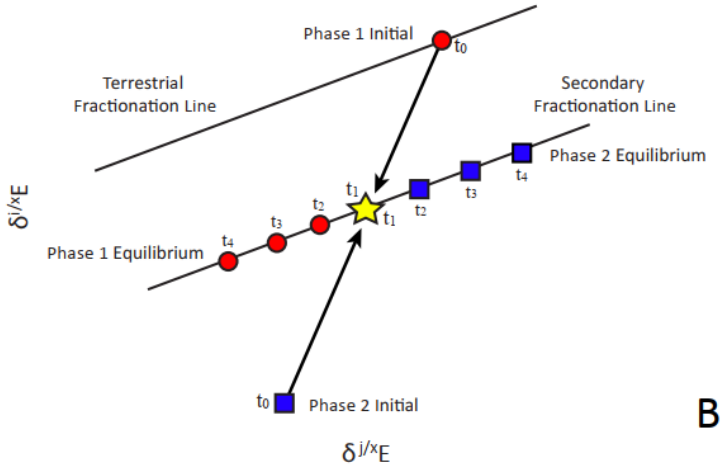

$$\delta^{82/76}\mathrm{Se(VI)}^{*} = \frac{\delta^{82/76}\mathrm{Se(VI)} - f \cdot \delta^{82/76}\mathrm{Se(IV)}}{1 - f}$$

Li et al., 2011; Shahar et al., 2008, 2017; Wang et al., 2015; Cao and Bao, 2017

三、硒同位素理论分馏体系的构建

Low-Se experiments：

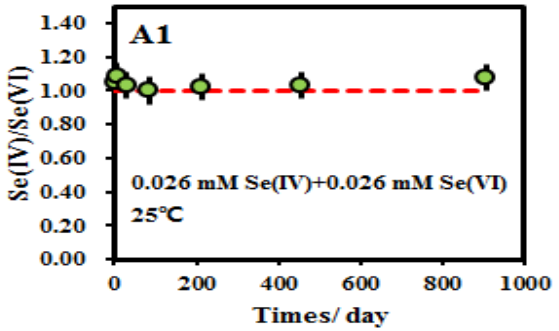

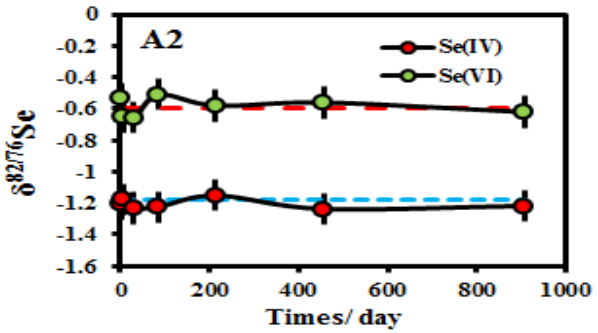

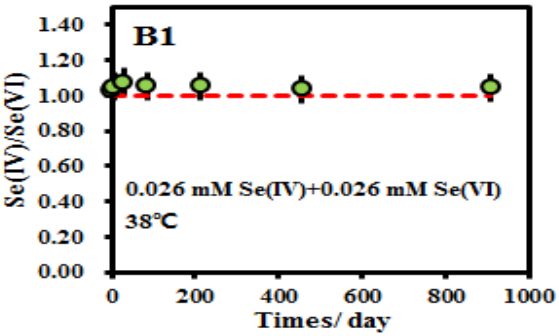

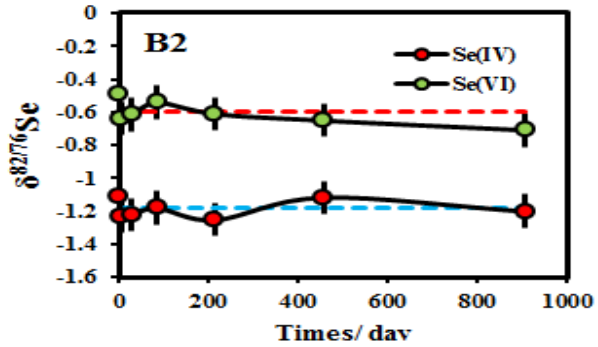

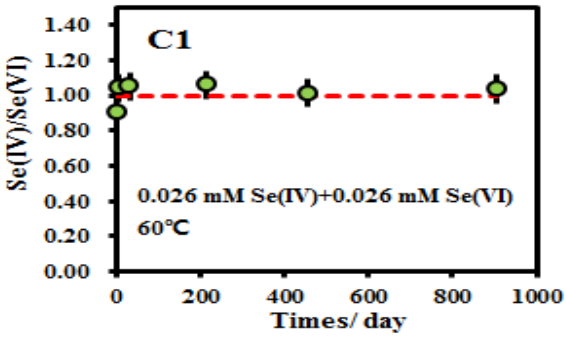

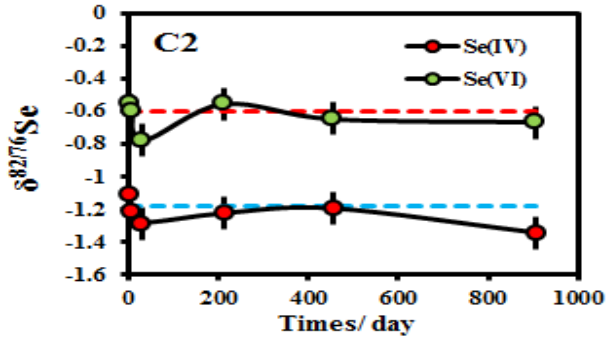

不同温度下，Se(IV)和Se(VI)的浓度(A1-C1)和同位素组成(A2-C2)随交换时间变化的趋势。

[Se(IV)]/[Se(VI)] ≈1

900 days交换后产生的交换率< 0.1%

Tan et al. 2020, GCA

三、硒同位素理论分馏体系的构建

High-Se experiments：

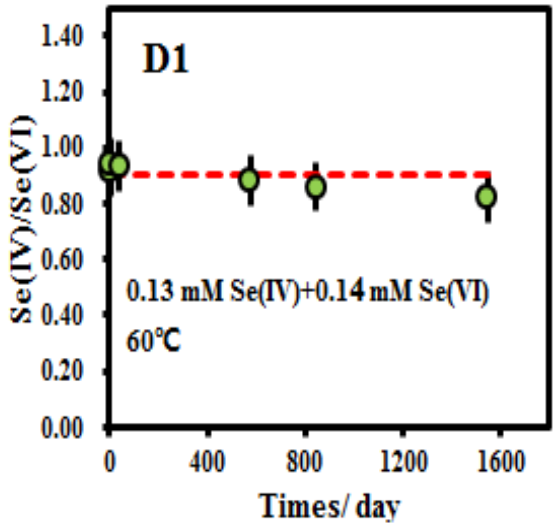

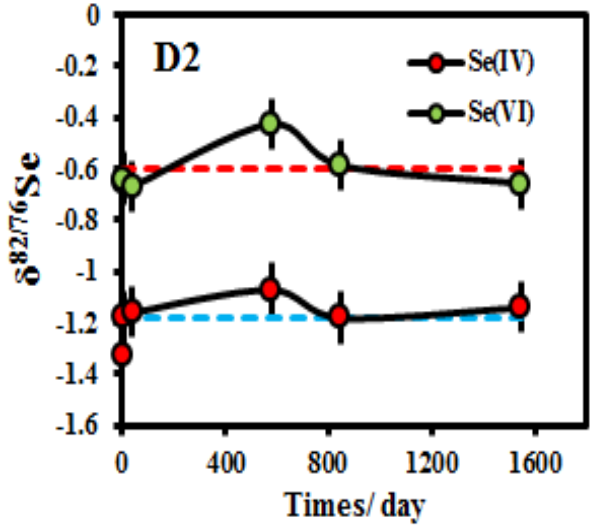

不同浓度下，Se(IV)和Se(VI)的浓度(D1-F1)和同位素组成(D2-F2)随交换时间变化的趋势。

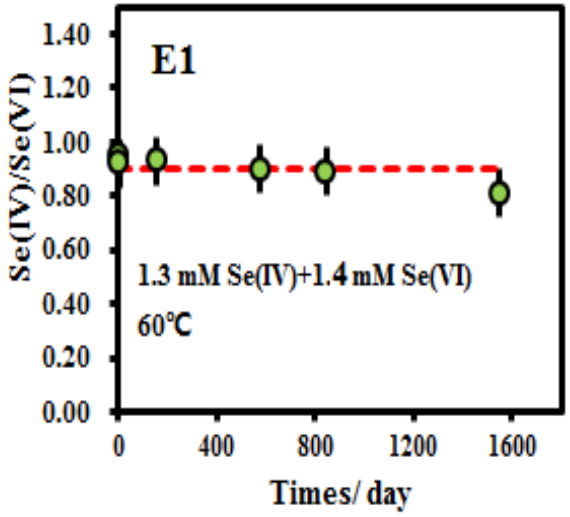

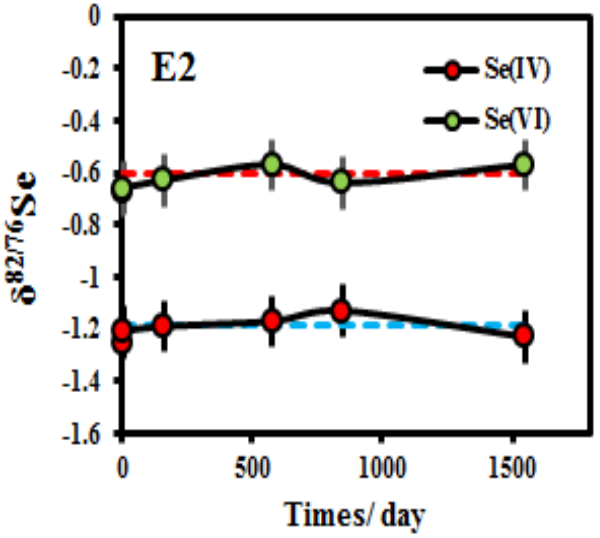

[Se(IV)]/[Se(VI)] ≈ 0.9

1457days交换后产生的交换率< 0.1%

Tan et al. 2020, GCA

三、硒同位素理论分馏体系的构建

Adding electron shuttle (AQDS)

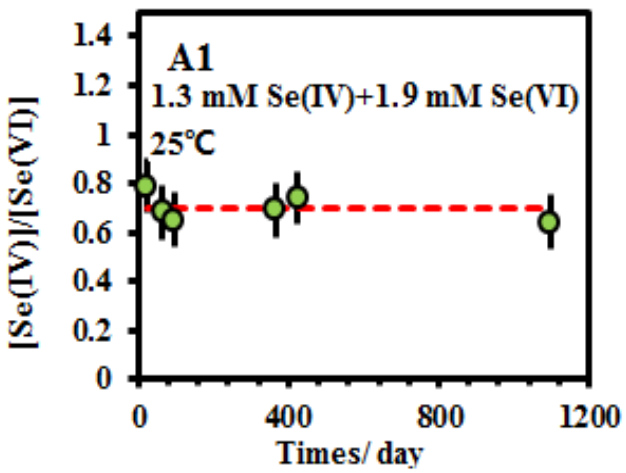

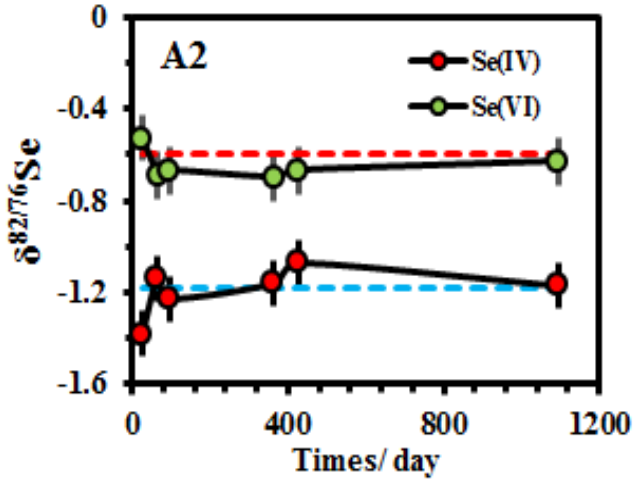

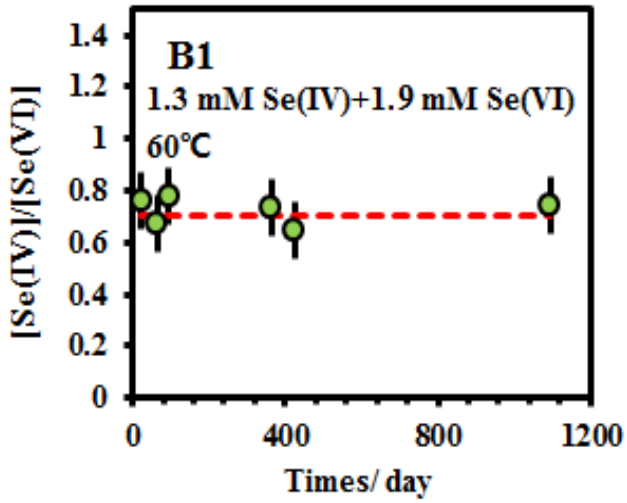

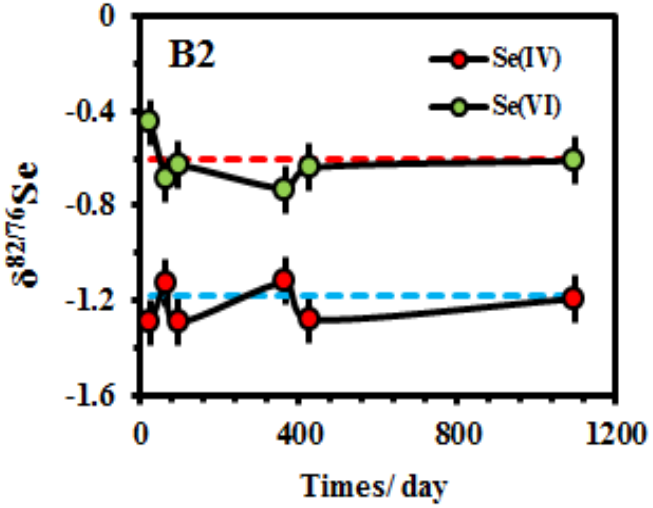

[Se(IV)]/[Se(VI)] ≈0.7，1059 days交换后产生的交换率< 0.1%。

Se(IV)和Se(VI)之间的同位素交换非常的缓慢，结果与前人研究的S(IV)-S(VI)体系类似。

Tan et al. 2020, GCA

三、硒同位素理论分馏体系的构建

^{82}Se-tracer experiments （$\delta^{82/76}$Se(IV)=1089‰）

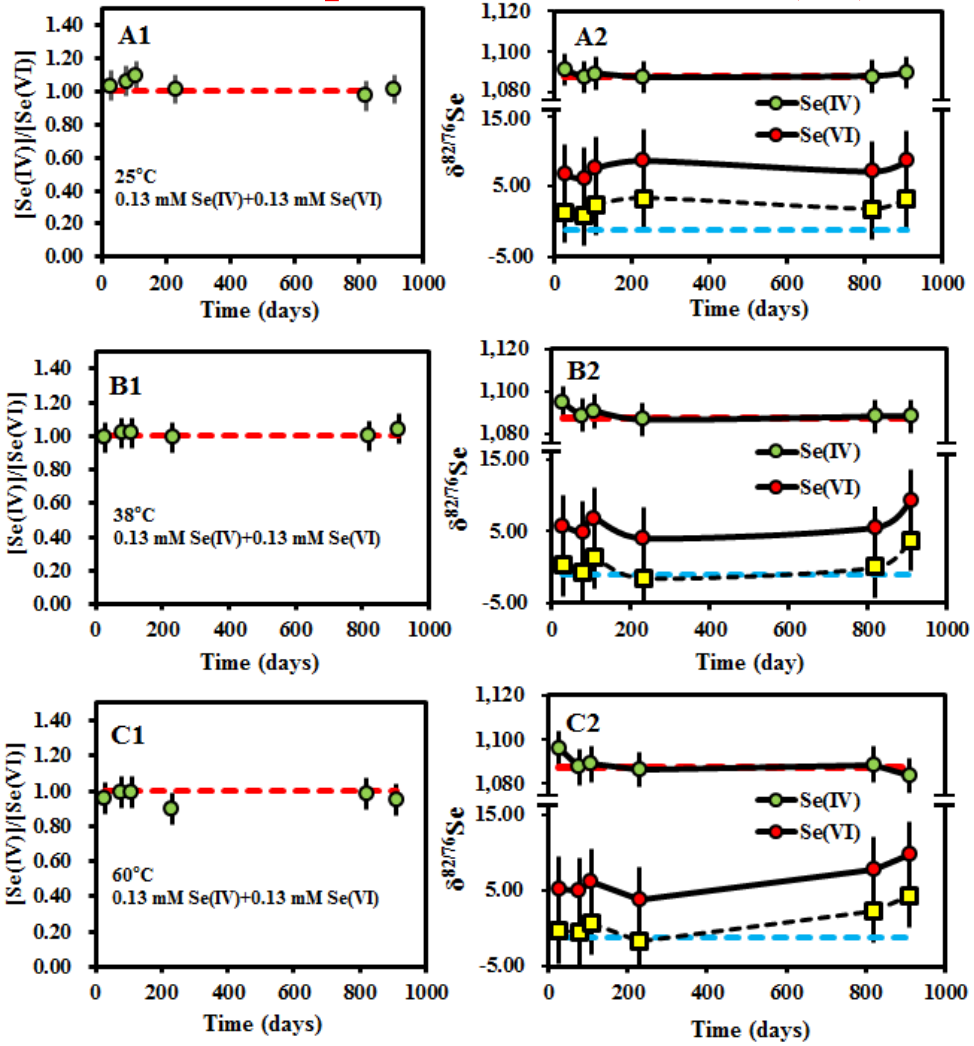

910天的反应后，$\delta^{82/76}$Se(VI)的值似乎存在一个系统性的增加的趋势。

Pearson线性相关检验表明，在0.05检验水平下仅60℃中$\delta^{82/76}$Se(IV)与时间呈现相关关系。

r = 0.85，p = 0.03

Tan et al. 2020, GCA

三、硒同位素理论分馏体系的构建

Se(IV)-Se(VI)同位素交换缓慢的原因

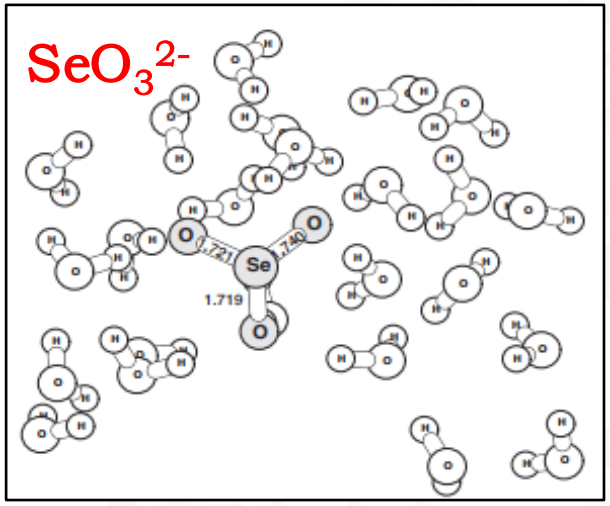

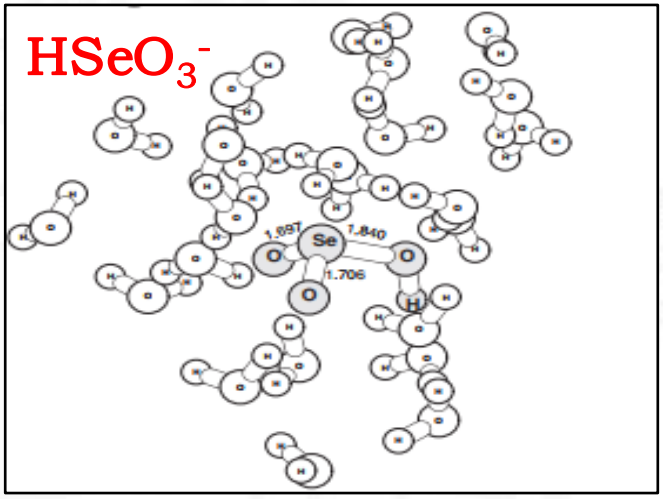

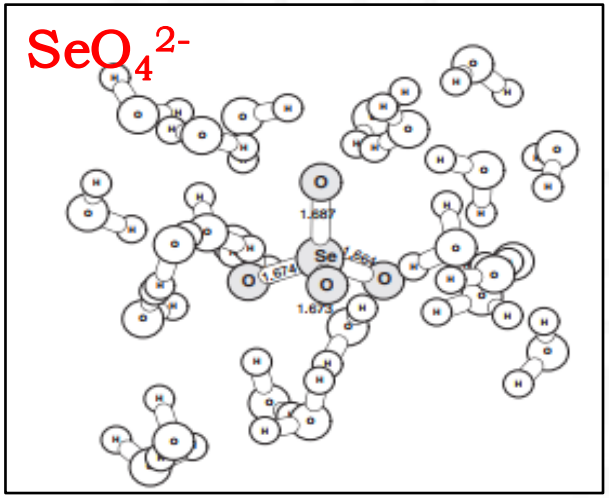

(1)结构上的差异,前人研究表明，含有相似结构的体系较含有不同结构的体系之间易发生同位素交换(Zink et al., 2010)。

(2)Se(IV)与Se(VI)之间的Se-O长差异较大。

3)周围的配位环境等。

三、硒同位素理论分馏体系的构建

Se(IV)-Se(VI)同位素交换可能的机制

每次碰撞仅转移1个电子：

$$^{82}Se(IV)+^{76}Se(VI) = ^{82}Se(V)+^{76}Se(V) \quad (3.1)$$

$$^{82}Se(IV)+^{76}Se(V)= ^{82}Se(V)+^{76}Se(IV) \quad (3.2)$$

$$^{82}Se(V)+^{76}Se(VI) = ^{82}Se(VI)+^{76}Se(V) \quad (3.3)$$

$$^{82}Se(IV)+^{76}Se(VI) = ^{82}Se(VI)+^{76}Se(V) \quad (3.4)$$

每次碰撞可转移2个电子：

$$^{82}Se(IV)+^{76}Se(VI) = ^{82}Se(VI)+^{76}Se(V) \quad (3.5)$$

鉴于前期的实验结果，Se(IV)-Se(VI)体系的同位素交换极为缓慢，使得我们更倾向于是多步反应。

三、硒同位素理论分馏体系的构建

同位素交换速率(R)的提取

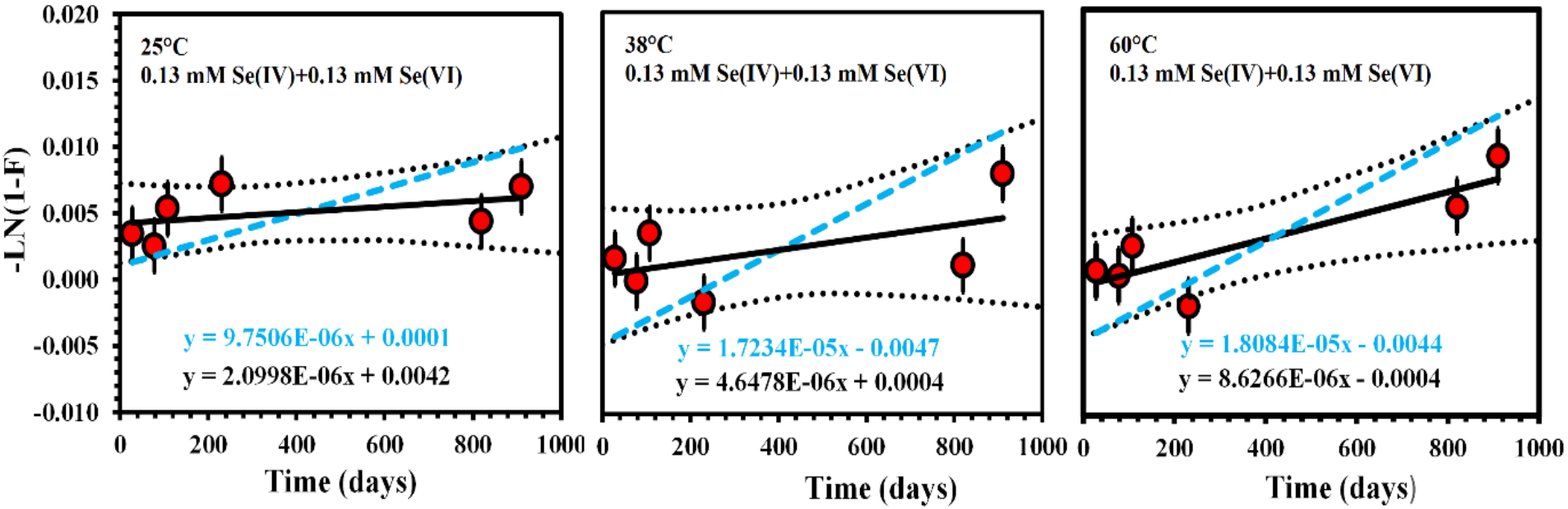

$\delta^{82/76}$Se(VI)值出现系统性的偏重（**910 days**）

R(25°C) = 1.81×10^{-10} M day^{-1} ($\leq 6.34\times10^{-10}$ M day^{-1}), Half-time=682年 ($\geq$ 160年)

R(38°C) = 3.03×10^{-10} M day^{-1} ($\leq 1.12\times10^{-09}$M day^{-1}), Half-time= 407年 ($\geq$ 111年)

R(60°C) = 5.63×10^{-10} M day^{-1} ($\leq 1.17\times10^{-09}$ M day^{-1}), Half-time= 219年($\geq$ 103年)

Tan et al. 2020, GCA

三、硒同位素理论分馏体系的构建

美国Colorado的Sweitzer Lake 和现代海水: t_{min} (出现可检测同位素交换的最小时间)和$t_{1/2}$(同位素交换到50%所需的时间)分别为: 1.8和44万年，0.27和0.51亿年。

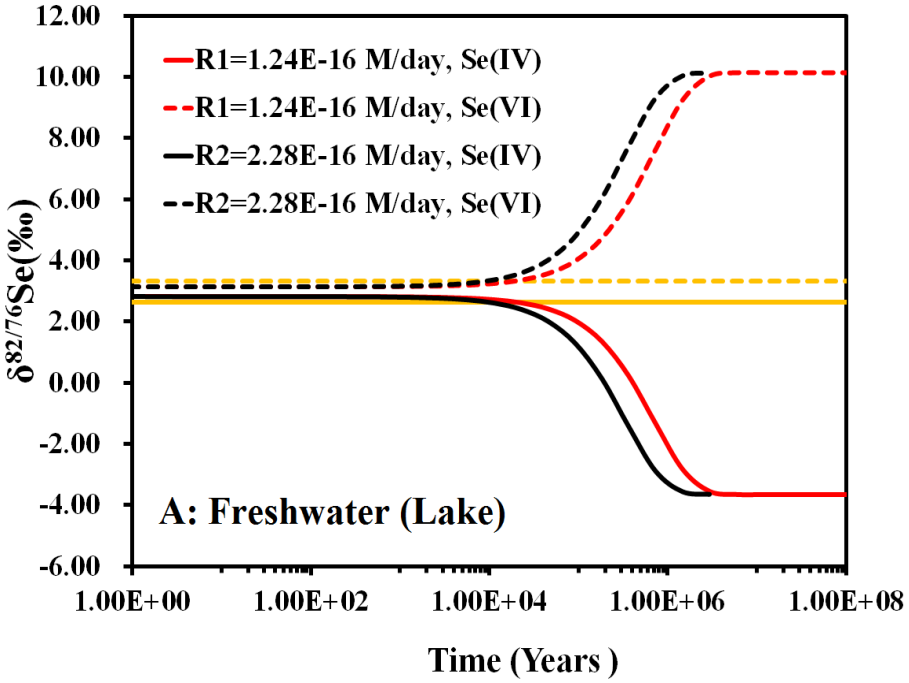

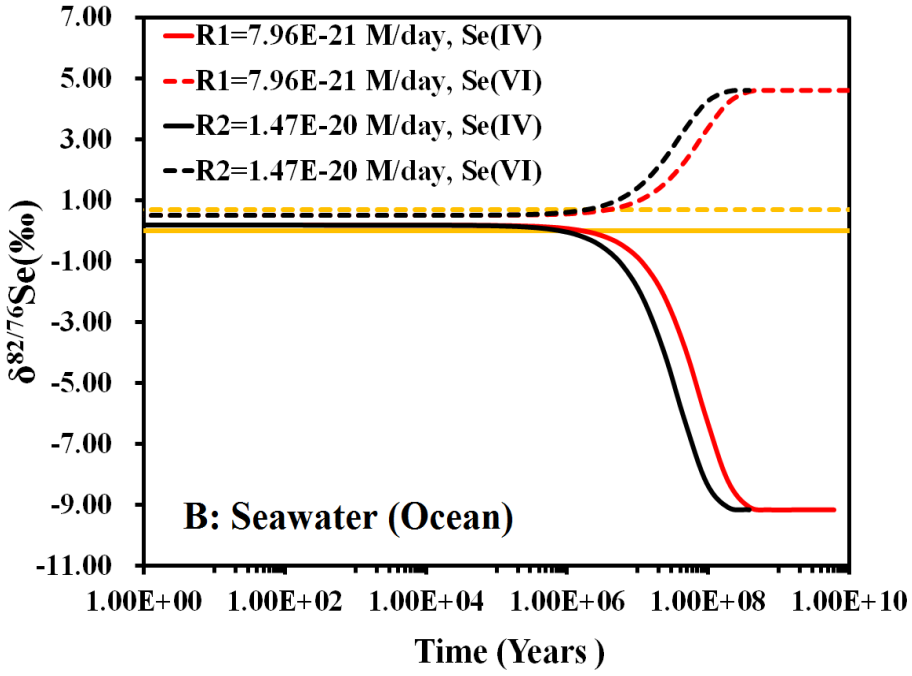

由于湖泊和现代海水中硒的居留时间分别为2.4年*(Clark and Johnson, 2010)*和2.6万年*(Large et al., 2015)*。使用Se同位素示踪湖泊和海洋的硒地球化学循环时，由同位素交换引起的分馏可以忽略不计。

Tan et al. 2020, GCA

三、硒同位素理论分馏体系的构建

小结

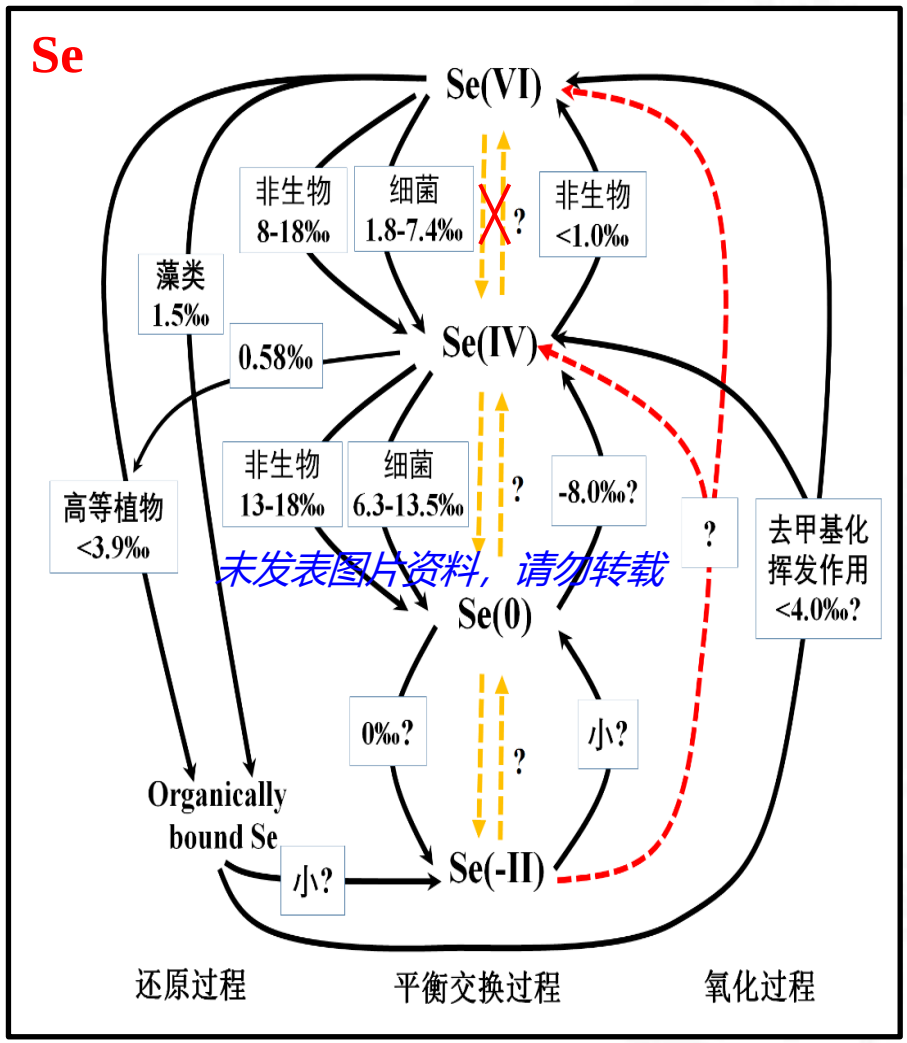

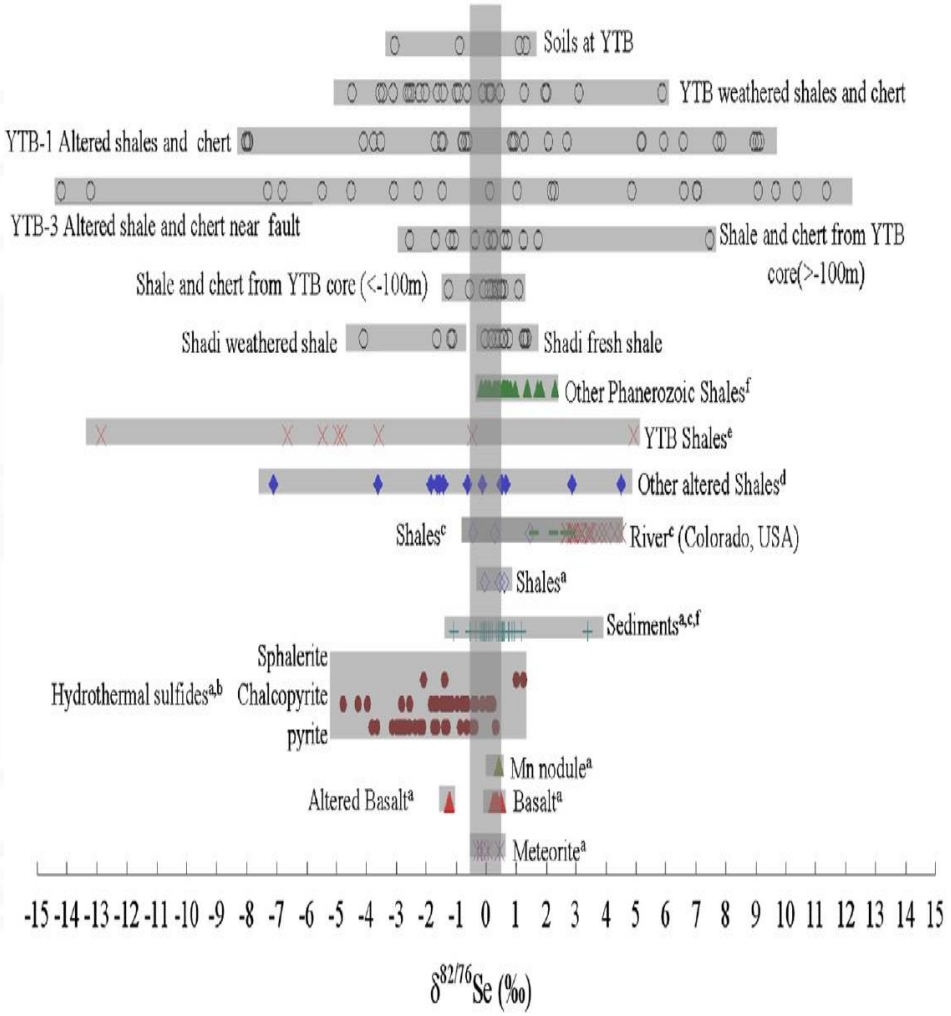

Zhu et al. 2014, GCA

四、硒同位素的应用

地表硒的生物地化循环

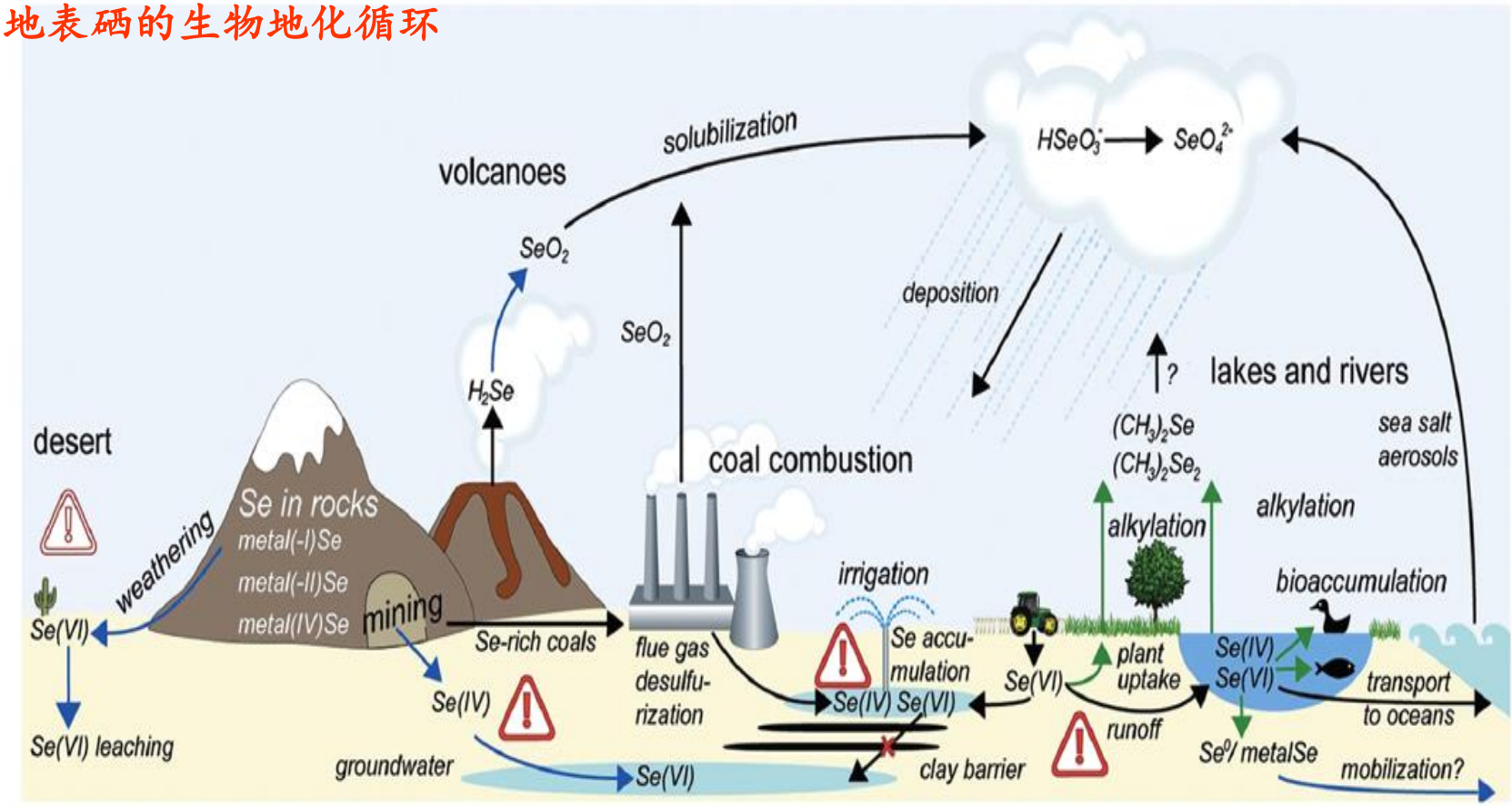

Figure 1. Schematic global cycle of Se with main focus on the terrestrial environment. Blue arrows indicate processes that involve oxidation of Se species and green arrows indicate processes that involve reduction of Se species. Warning symbols indicate specific environmental settings that are at risk of either developing Se deficiency (open warning symbol) or Se excess (shaded warning symbol).

Winkel, EST 2012

四、硒同位素的应用

4.1 现代环境

加州农业灌溉水处理系统中的硒同位素变化

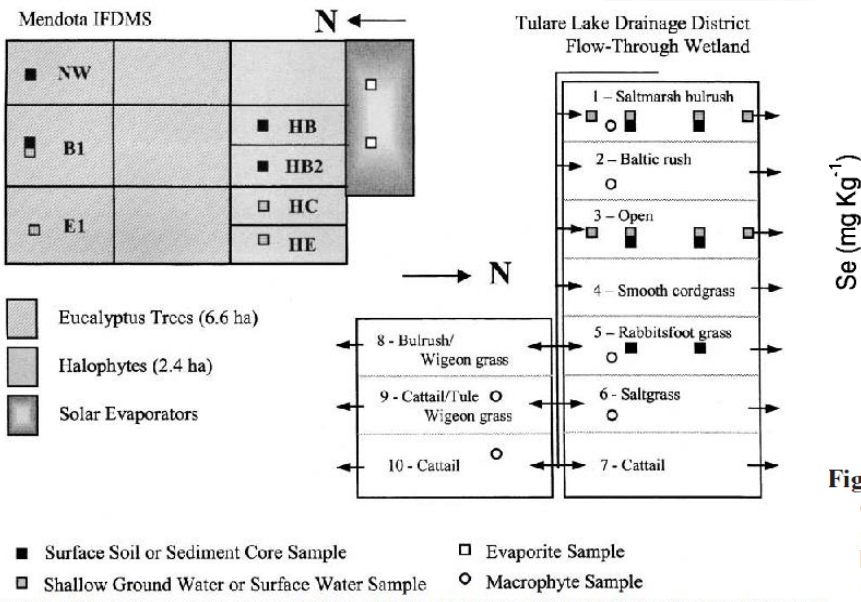

Fig. 2. Integrated on-farm drainage management system (IFDMS) and Tulare Lake Drainage District (TLDD) flow-through wetland generalized designs and sampling locations [after Tanji (1999) and Gao et al. (2000)].

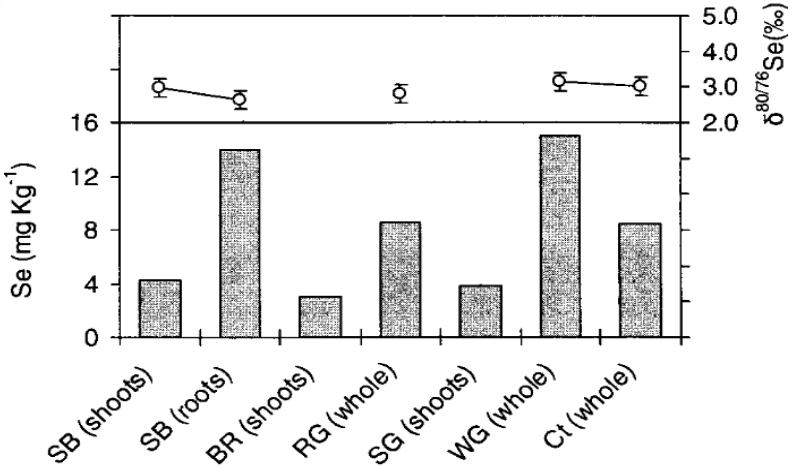

Fig. 3. Total Se concentrations and $\delta^{80/76}$Se values for macrophytes collected from various cells of the Tulare Lake Drainage District (TLDD) flow-through wetlands. Saltmarsh bulrush (SB, Cell 1), baltic rush (BR, Cell 2), rabbitsfoot grass (RG, Cell 5), saltgrass (SG, Cell 6), widgeon grass (WG, Cell 9), or cattails (Ct, Cell 10).

Table 1. Comparison of averaged $\delta^{80/76}$Se values (± standard deviation) for Tulare Lake Drainage District (TLDD) flow-through wetland sediment extracts, surface waters, and macrophytes.

Sediment depth	0.1 *M* K_2HPO_4 extract	*n*	0.1 *M* NaOH extract	*n*	1.0 *M* Na_2SO_3 extract	*n*
	‰		‰		‰	
0–5 cm	3.63 ± 0.30	3	3.01 ± 0.26	4	3.28 ± 0.24	4
5–10 cm	1.59 ± 1.40	2	5.25 ± 0.16	2	2.69 ± 0.32	4
Difference	−2.04		2.24		−0.59	

			Mean comparison (*P*)			
Water, macrophytes, or extract	$\delta^{80/76}$Se	*n*	0–5 cm (K_2HPO_4)	0–5 cm (NaOH)	0–5 cm (Na_2SO_3)	Macrophytes
	‰					
Se(VI) in water	3.65 ± 0.37	6	0.389	0.002**	0.024*	0.0003***
Se in macrophytes	2.91 ± 0.20	5	0.003**	0.276	0.360	
Na_2SO_3 (5–10 cm)					0.013*	

* Significant at the 0.05 probability level.
** Significant at the 0.01 probability level.
*** Significant at the 0.001 probability level.

$\delta^{80/76}Se_{MH495\text{-}3149}$=-2.30‰

Herbel et al., JME, 2002

四、硒同位素的应用

Table 2. Selenium speciation, concentrations, and $\delta^{80/76}$Se values for samples collected from the Mendota integrated on-farm drainage management system (IFDMS) site in 1996.

Sample	Se (total)	$\delta^{80/76}$Se ± standard error	Se(IV)	Se(VI)	Organic Se
	μg L^{-1}	‰	μg L^{-1}		
Shallow ground water					
M-WB1	1559.3	+3.65 ± 0.30	12.7	1457.7	88.9
M-WE1	2052.7		18.0	1859.7	185.0
M-WHC	728.8	+2.93 ± 0.60	56.3	640.0	32.5
M-WHE	589.5	+2.97 ± 0.50	68.4	494.8	26.3
	mg kg^{-1}		mg kg^{-1}		
Evaporites					
M-E10	5.61	+4.14 ± 0.25	0.52	5.01	0.08
M-E29	5.67	+4.13 ± 0.60	0.53	5.13	0.01

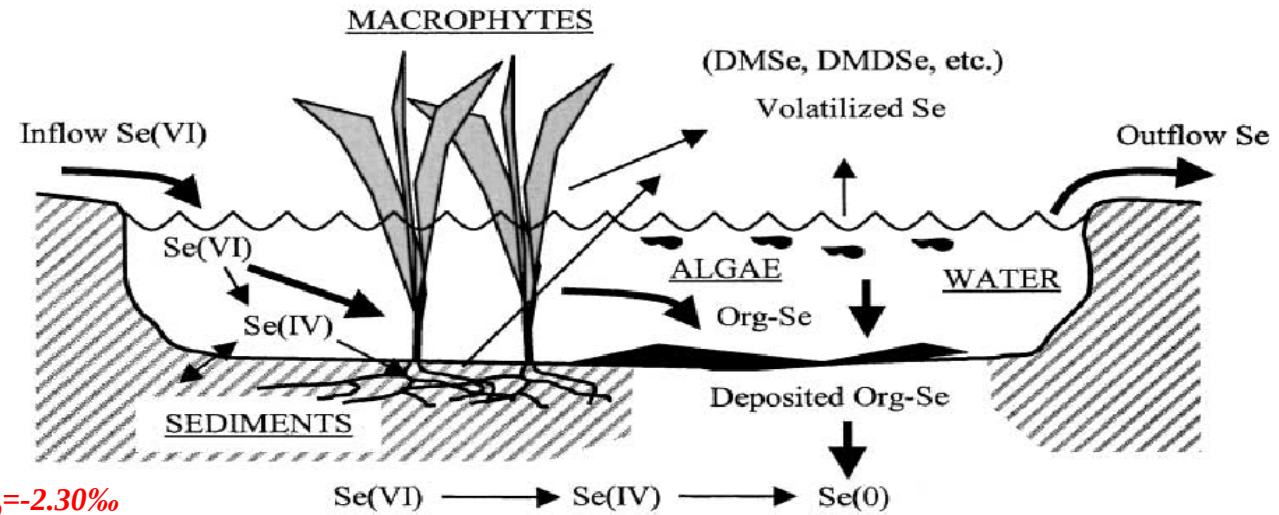

$\delta^{80/76}Se_{MH495\text{-}3149}$=-2.30‰

Fig. 7. Selenium cycling in the Tulare Lake Drainage District (TLDD) flow-through wetlands. Major loss pathways as suggested by comparison of $\delta^{80/76}$Se values are indicated by heavy arrows, while minor pathways are indicated by light arrows. DMSe, dimethylselenide; DMDSe, dimethyldiselenide; Org-Se, organic selenium.

四、硒同位素的应用

Selenium Stable Isotope Investigation into Selenium Biogeochemical Cycling in a Lacustrine Environment: Sweitzer Lake, Colorado

Clark and Johnson, 2010

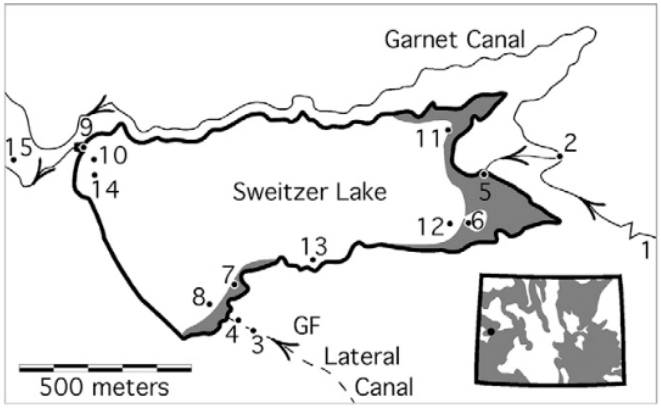

Fig. 1. Sampling locations at Sweitzer Lake. (1) Garnet Canal ≈8.35 km

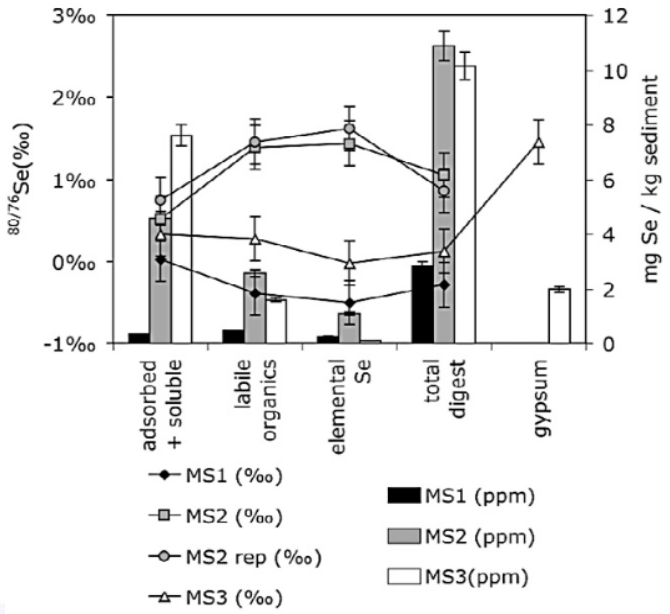

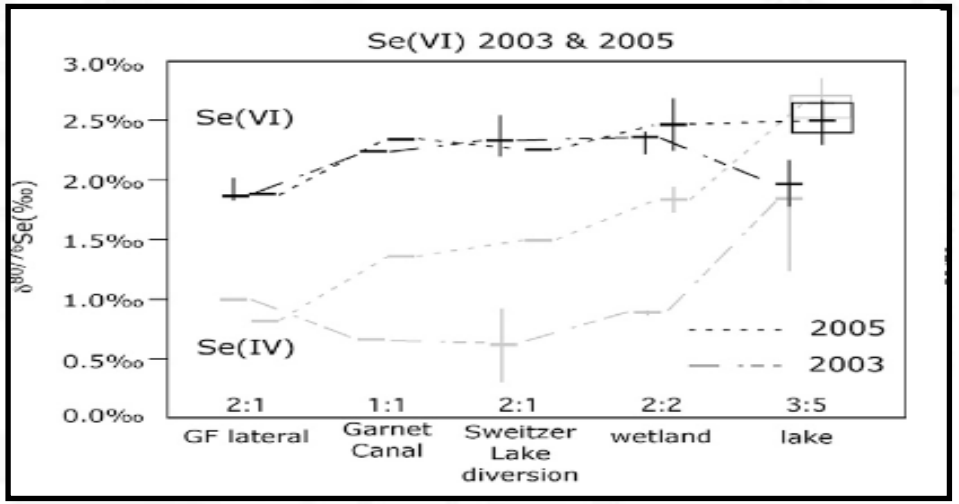

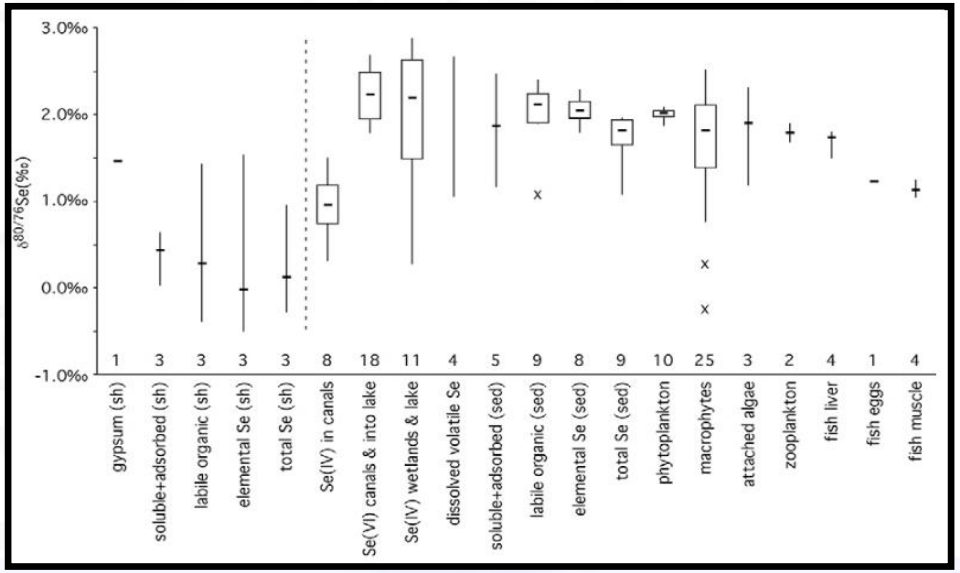

四、硒同位素的应用

Effective Isotopic Fractionation Factors for Solute Removal by Reactive Sediments: A Laboratory Microcosm and Slurry Study

SCOTT K. CLARK* AND
THOMAS M. JOHNSON
Department of Geology, University of Illinois at Urbana−Champaign, 245 Natural History Building, 1301 West Green Street, Urbana, Illinois 61801

Received June 30, 2008. Revised manuscript received September 08, 2008. Accepted September 16, 2008.

Wetlands remove many dissolved pollutants from surface waters by various mechanisms. Stable isotope ratio measurements may provide a means of detecting and possibly quantifying certain removal processes, such as reduction of SeO_4^{2-}, Cr(VI), NO_3^-, and $HClO_4^-$, that fractionate isotopes. However, the magnitude of the isotopic fractionation for a given reaction depends on the setting in which it occurs. We explore the case where isotope ratio shifts in surface waters are used to detect or quantify reactions occurring in pore waters of underlying sediments. A series of SeO_4^{2-} reduction experiments reveals that the effective isotopic fractionation, observed in the water column as a result of SeO_4^{2-} diffusion into underlying, Se-reducing sediments, is weaker than the intrinsic fractionation induced by the same reduction reactions in well-mixed systems in which reaction sites are not separated from measured SeO_4^{2-}. An intact sediment core yielded an effective ε ($\approx \delta_{react} - \delta_{instantaneous\ prod}$) of 0.20‰, whereas the intrinsic ε was 0.61‰. These results are consistent with previously published reactive transport models. Isotopic studies of sediment-hosted reactions in wetlands and other surface water systems should use the smaller effective fractionation values, which can be estimated using the models.

Clark and Johnson, 2008

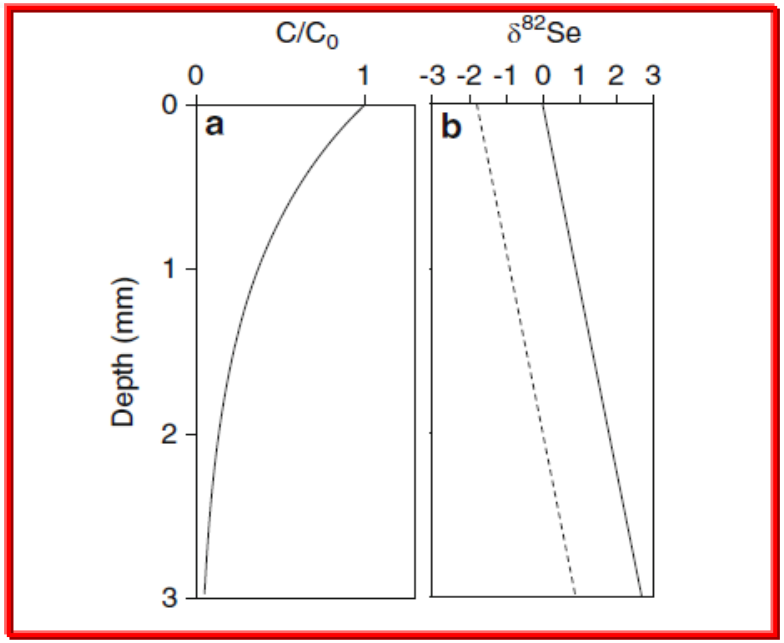

Fig. 9.6 Illustration of reservoir effects in a sediment-water system (Bender 1990; Clark and Johnson 2008). Concentration (**a**) and isotopic composition (**b**) of dissolved Se(VI) are given as a function of depth below the sediment/water interface. C_0 is the concentration in the overlying water. The *solid* and *dashed lines* in (**b**) give the isotopic compositions of Se(VI) in pore water and of reduced Se accumulating in the sediment, respectively. δ^{82}Se increases with increasing depth because isotopic fractionation enriches pore water Se(VI) in heavier isotopes. The magnitude of isotopic fractionation (ε) at any given point is 1.8‰. However, the average δ^{82}Se value of the accumulated reduced Se is offset from the overlying water by much less than 1.8‰, and thus the effective isotopic fractionation ($\varepsilon = 0.9$‰ for this particular model) is much smaller than the intrinsic fractionation

四、硒同位素的应用

风化过程是否产生同位素分馏(湖北恩施渔塘坝富硒碳质岩剖面)

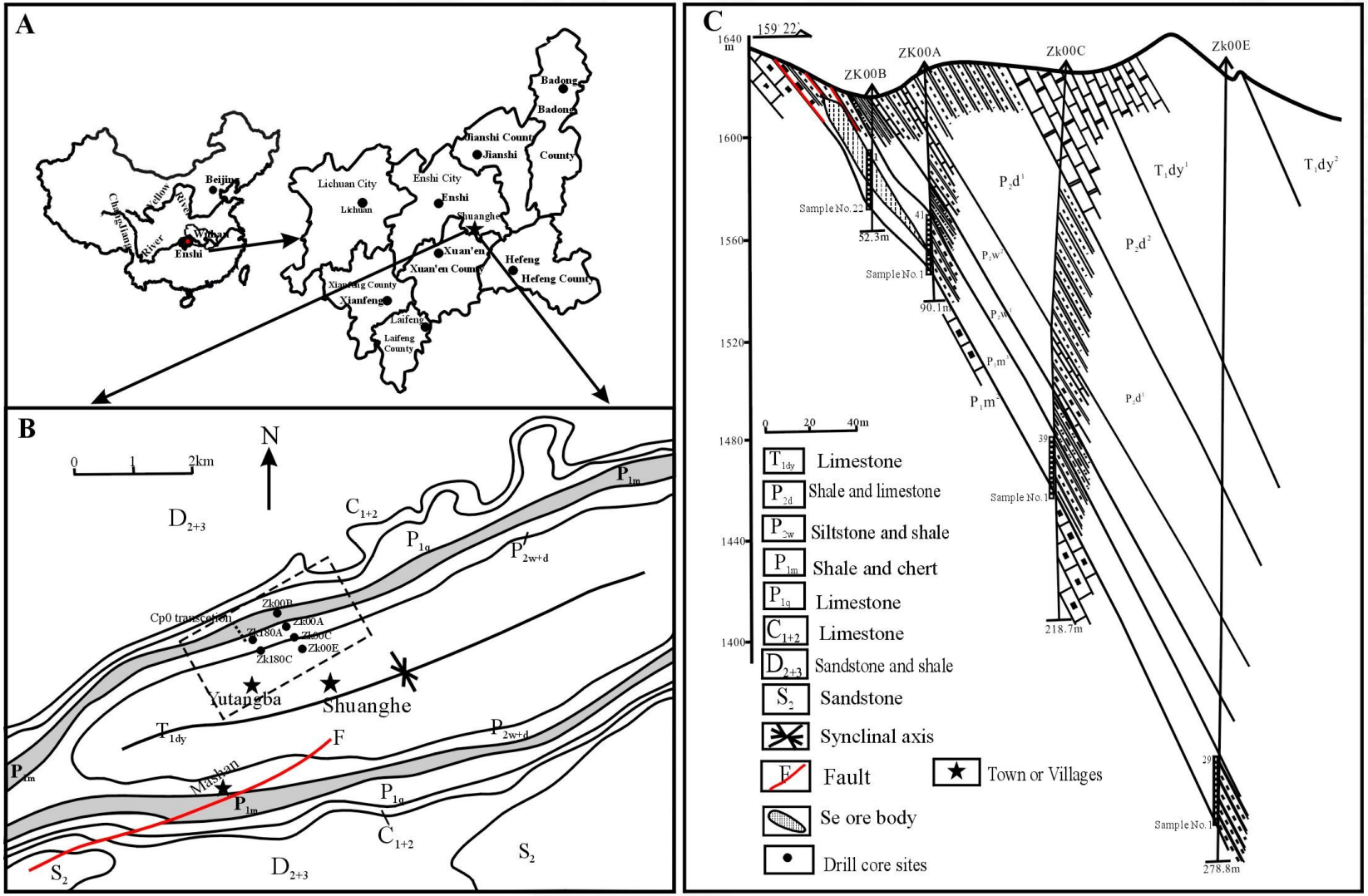

四、硒同位素的应用

恩施渔塘坝富硒碳质岩石风化剖面采样露头

四、硒同位素的应用

近地表至地表硒同位素的变化

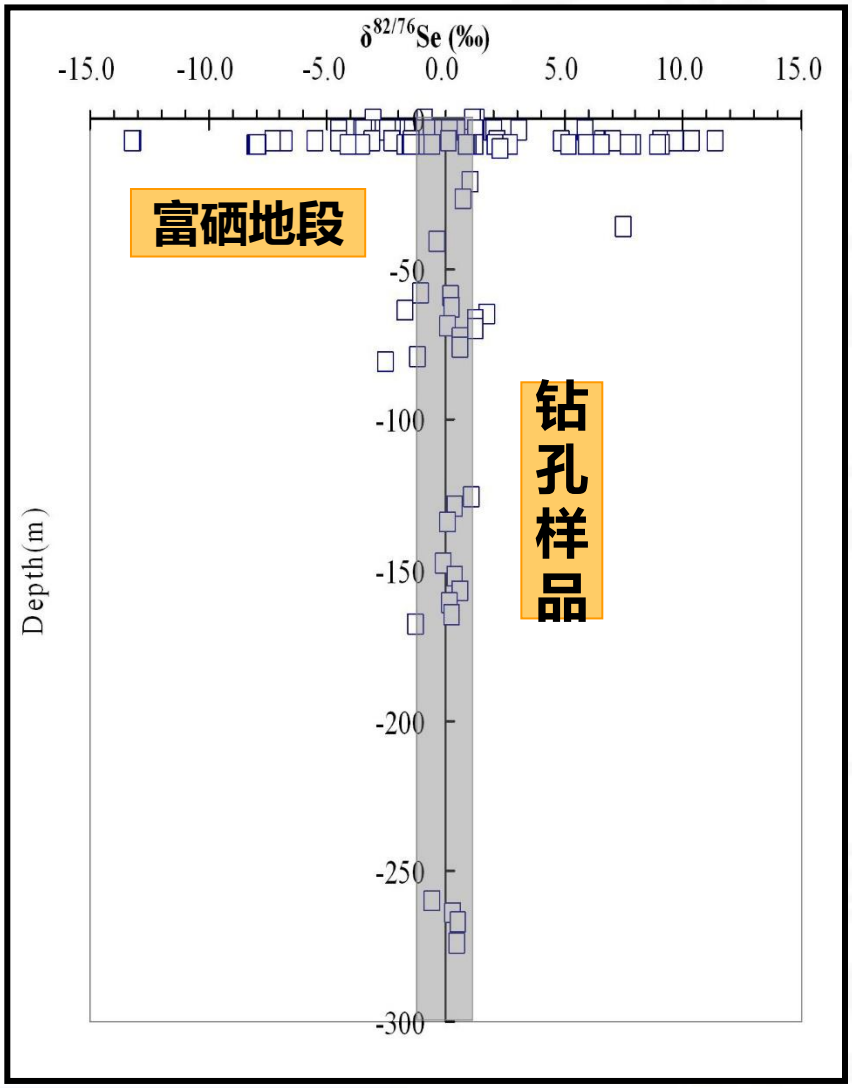

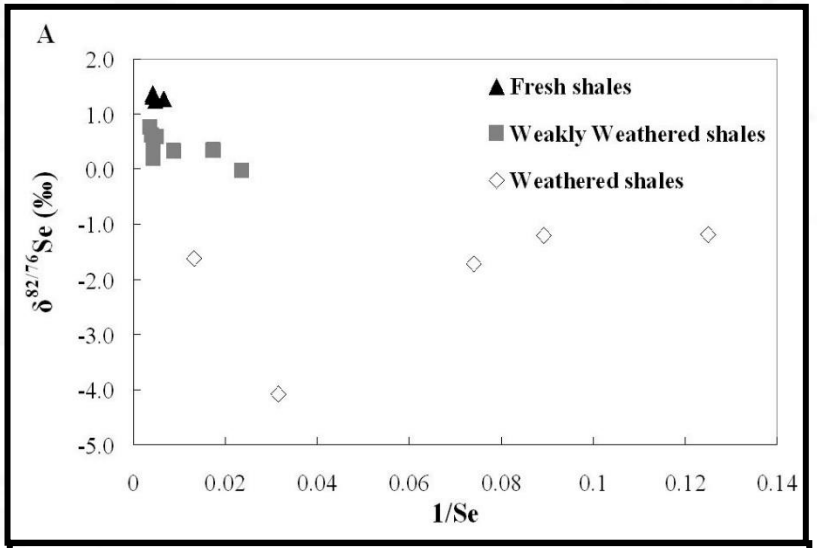

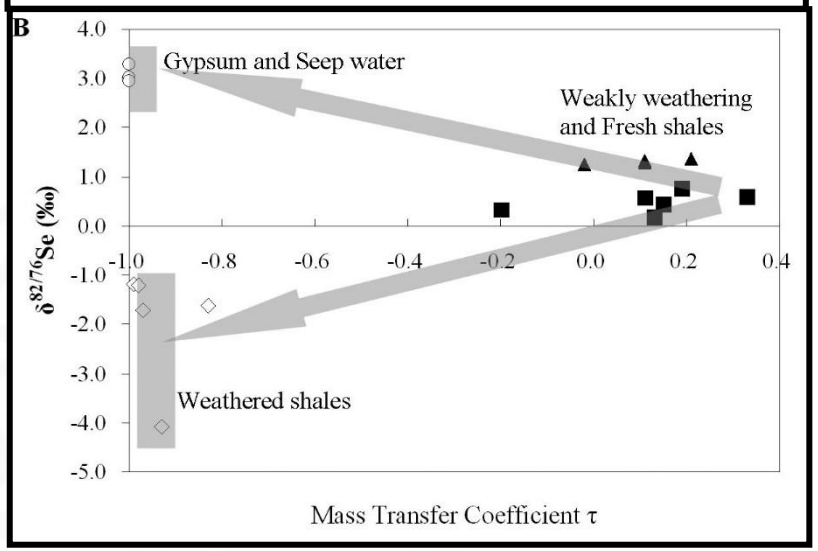

四、硒同位素的应用

The rise of oxygen in Earth's early ocean and atmosphere

Nature 2014

Timothy W. Lyons[1], Christopher T. Reinhard[1,2,3] & Noah J. Planavsky[1,4]

4.2 古环境：硒同位素能否指示氧化/还原事件？

The rapid increase of carbon dioxide concentration in Earth's modern atmosphere is a matter of major concern. But for the atmosphere of roughly two-and-half billion years ago, interest centres on a different gas: free oxygen (O_2) spawned by early biological production. The initial increase of O_2 in the atmosphere, its delayed build-up in the ocean, its increase to near-modern levels in the sea and air two billion years later, and its cause-and-effect relationship with life are among the most compelling stories in Earth's history.

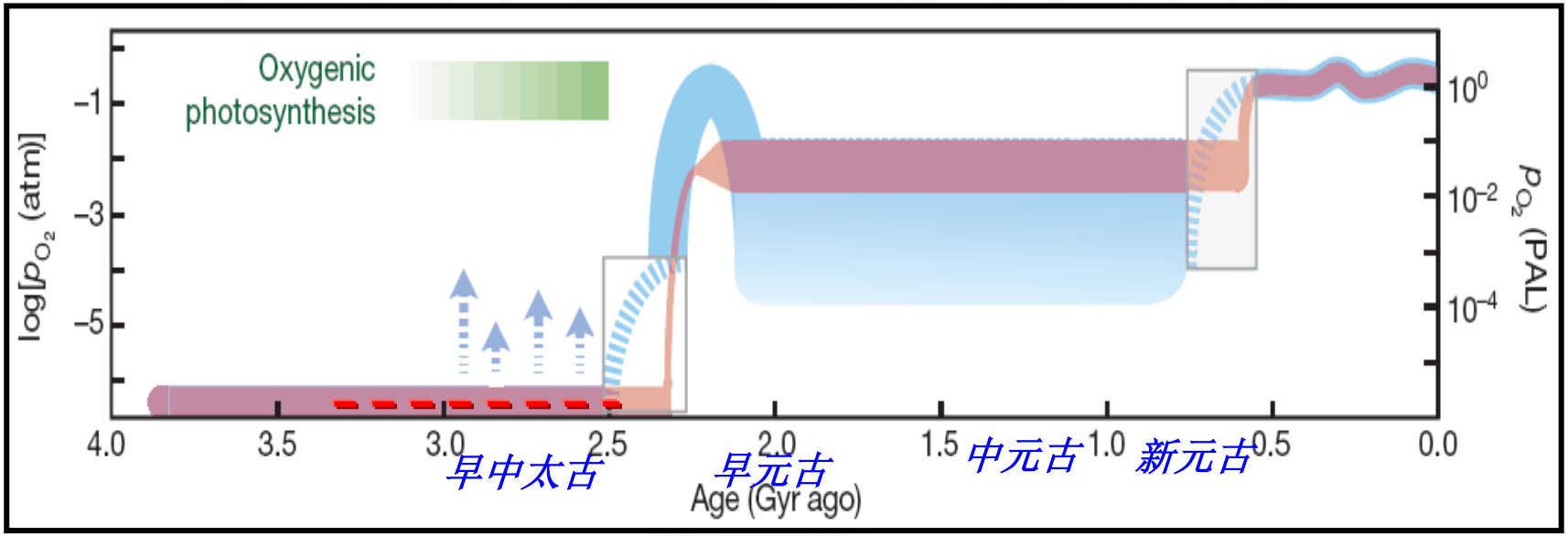

四、硒同位素的应用

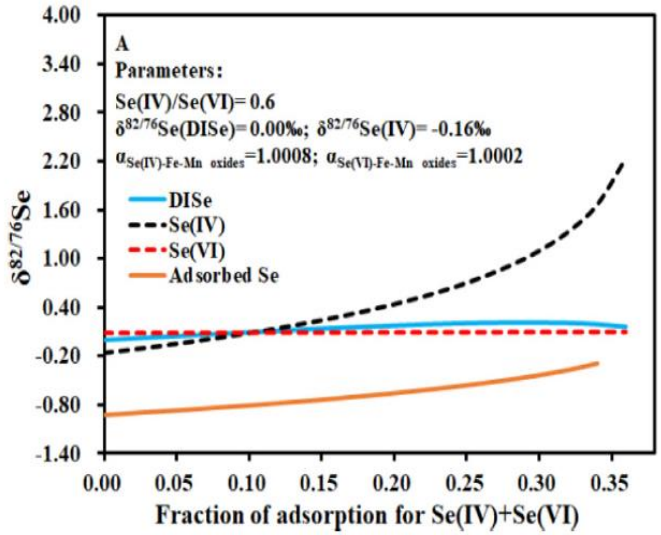

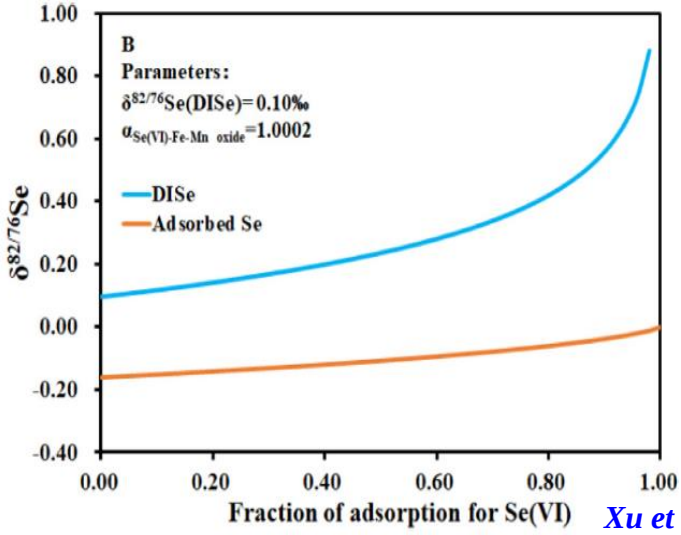

Xu et al. 2020, GCA

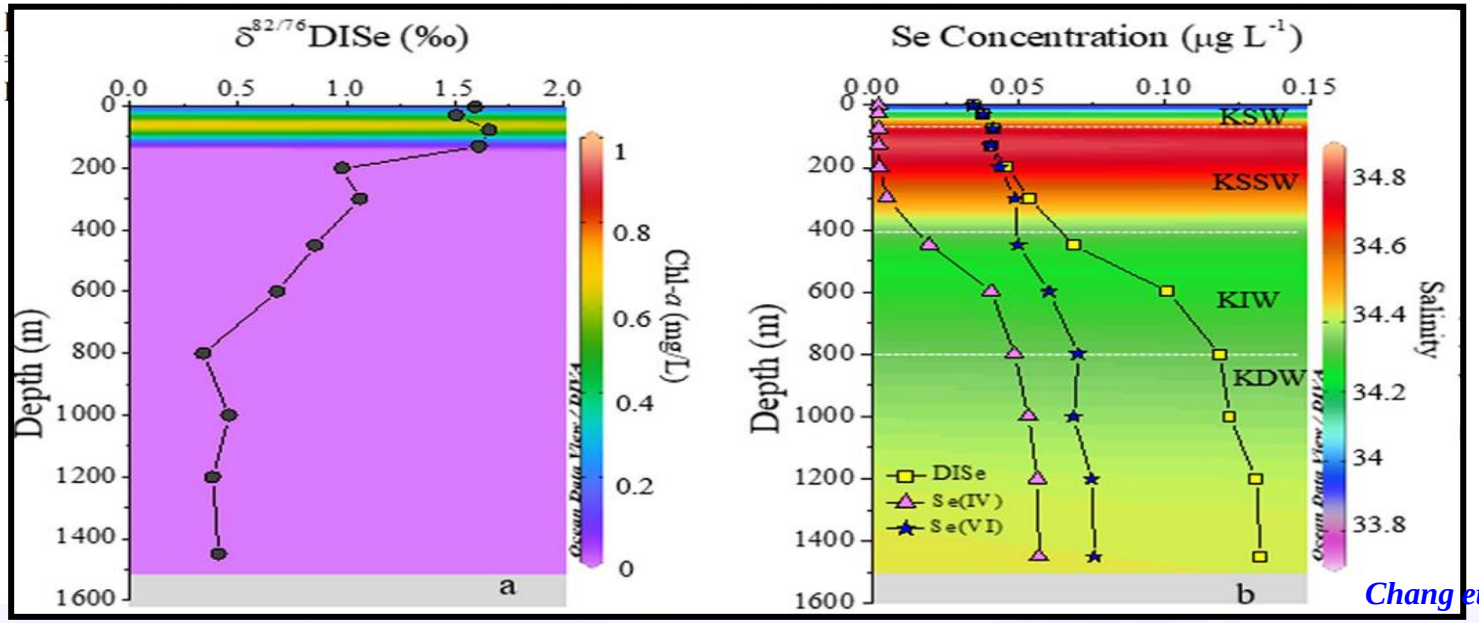

Chang et al. 2017, CG

四、硒同位素的应用

Selenium as paleo-oceanographic proxy: A first assessment

硒同位素能够作为古海洋环境(氧化/还原)的代用指标?

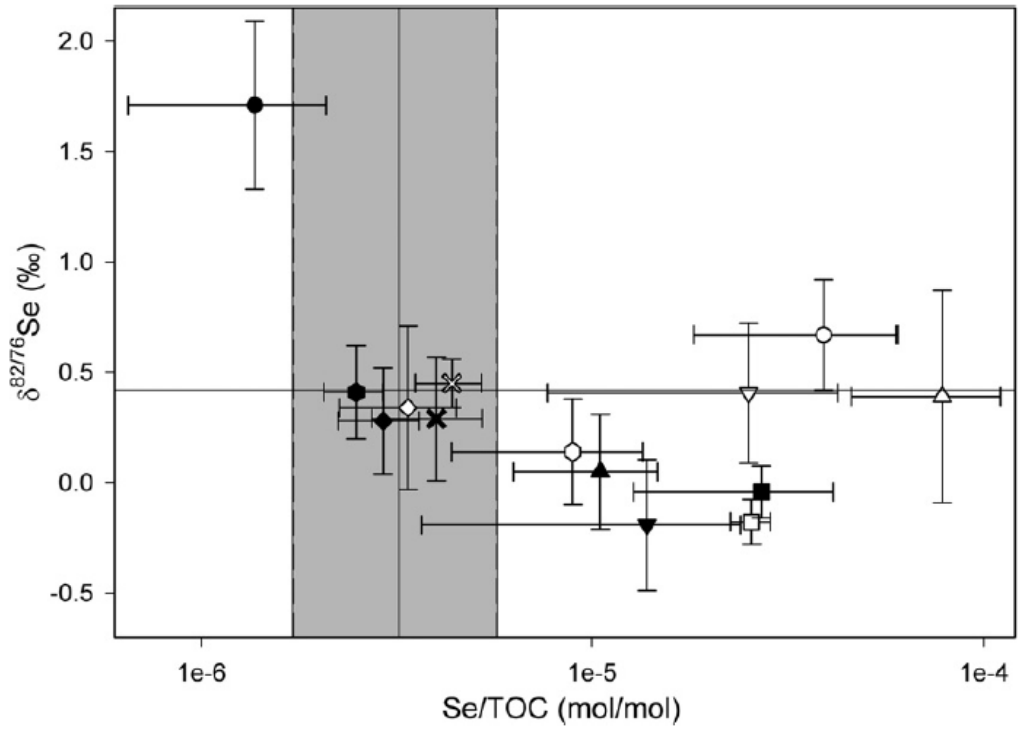

Fig. 3. Average Se/TOC ratios versus average $\delta^{82/76}$Se values. The solid vertical line indicates average Se/TOC of phytoplankton (Doblin et al., 2006). The shading encompasses the range of Se/TOC ratios observed in modern phytoplankton (upper limit, Doblin et al., 2006; lower limit, this study). The solid horizontal line indicates the average $\delta^{82/76}$Se of oligotrophic open Pacific Ocean plankton (this study). Symbols: X = Black Sea; circles = New Albany Shale; hexagon = Posidonia Shale; diamond = Alum Shale; square = Arabian Sea; triangle, down = Demerara Rise; triangle, up = Cape Verde Basin. Open and filled symbols correspond to the categories used in Fig. 2, with the exception of the OAE sequences where the before and after OAE data have been combined (see Section 4 in text for more details). Error bars indicate the standard deviations (1σ) of the average values Se/TOC and $\delta^{82/76}$Se values.

Mitchell et al., 2012, GCA

四、硒同位素的应用

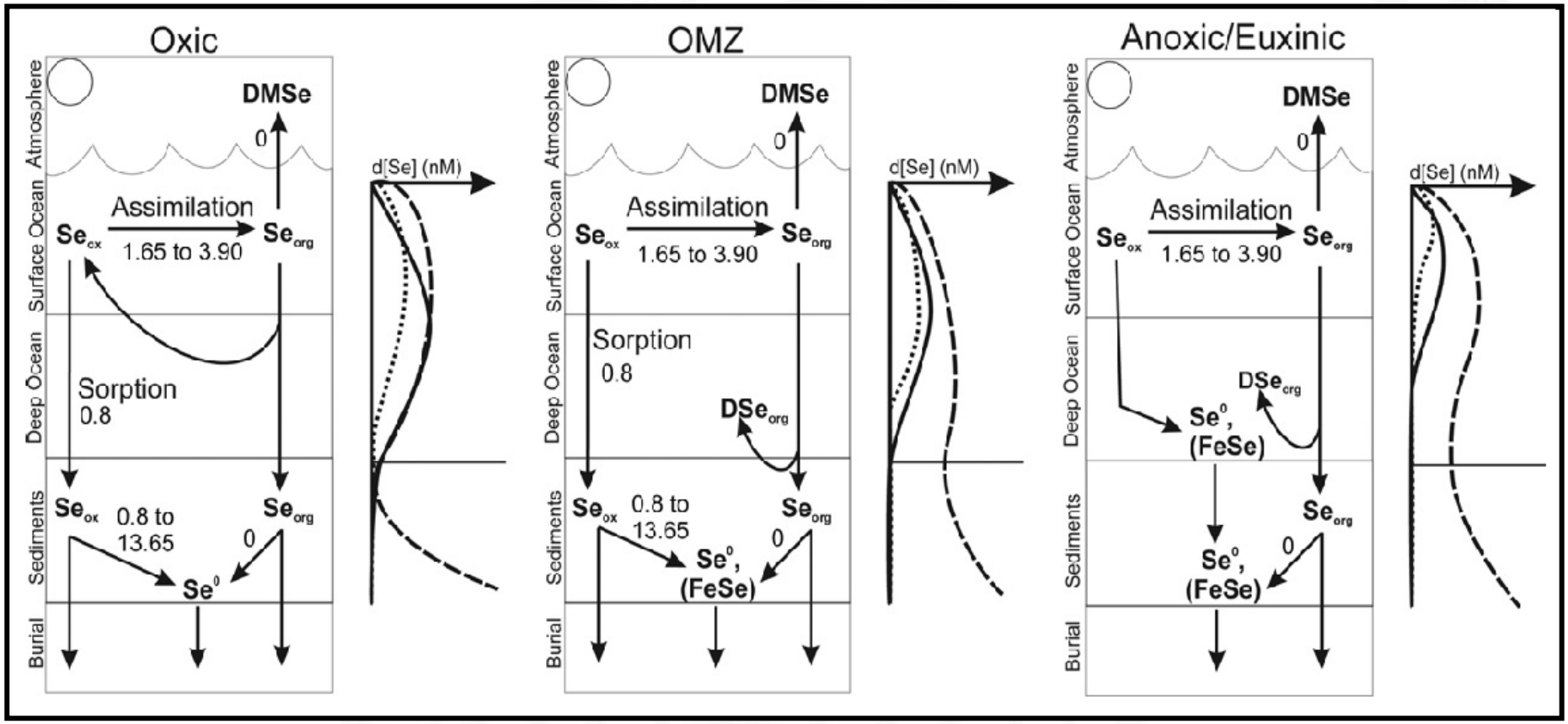

Albany Shale formation. Overall, our results indicate that to unlock the full proxy potential of marine sedimentary Se records, we need to gain a much more detailed understanding of the sources, chemical speciation, isotopic fractionations and cycling of Se in the marine environment.

Mitchell et al., 2012, GCA

四、硒同位素的应用

The evolution of the global selenium cycle: Secular trends in Se isotopes and abundances

Stueken et al., 2015,GCA

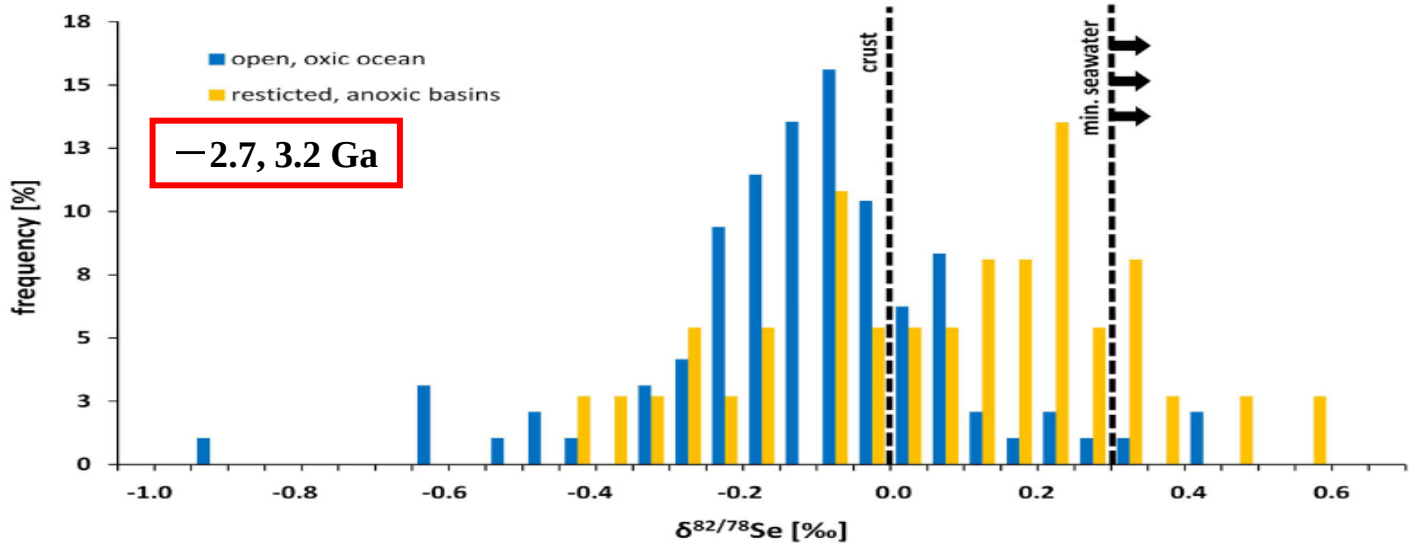

—2.7, 3.2 Ga

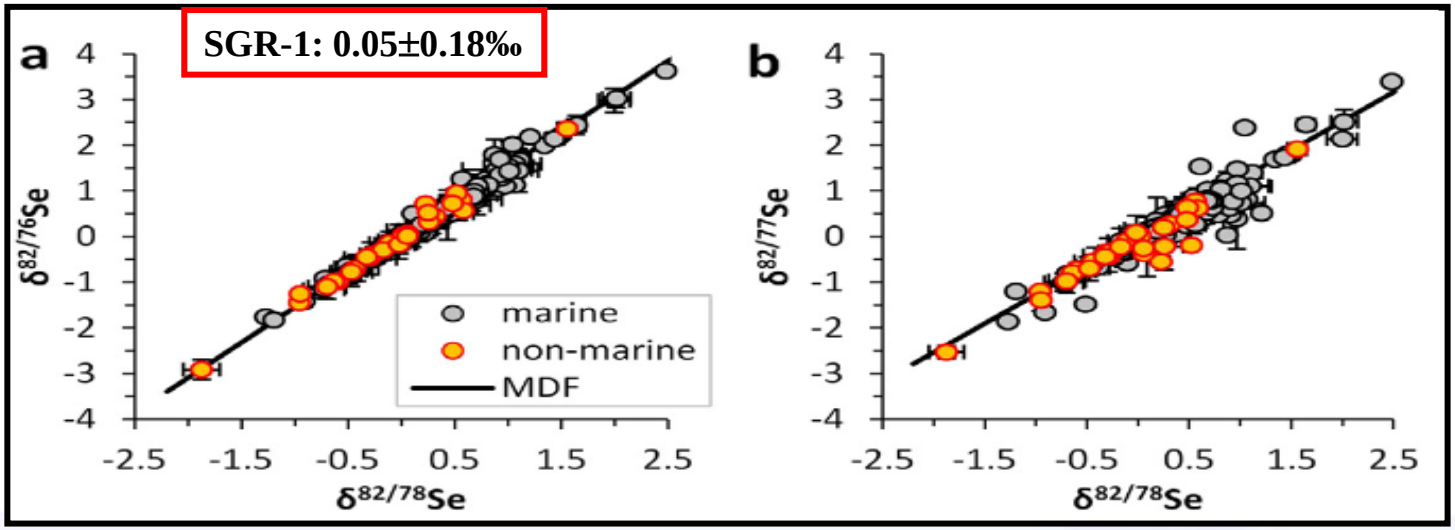

SGR-1: 0.05±0.18‰

四、硒同位素的应用

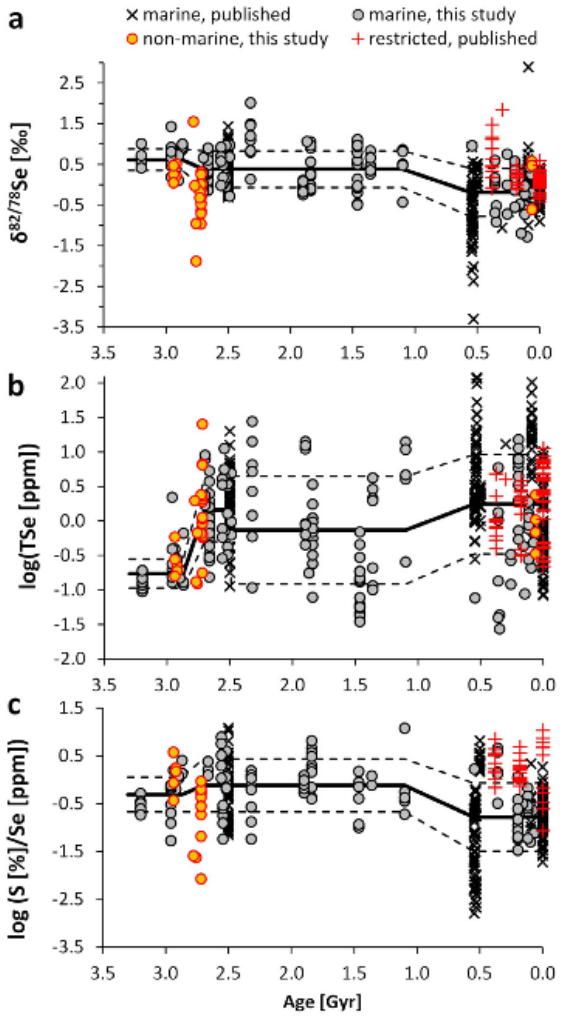

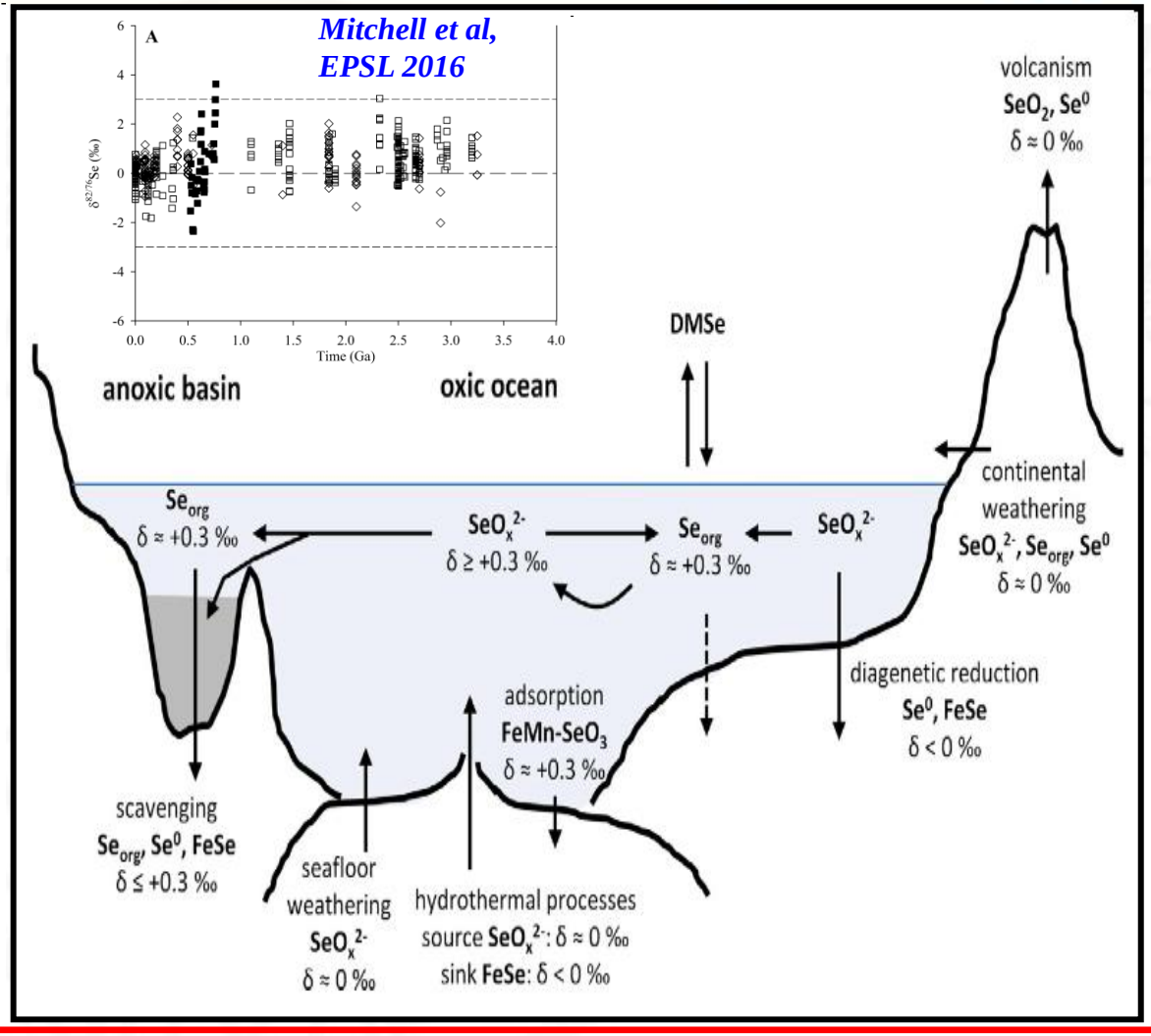

结论： 海洋沉积物(泥岩)中$\delta^{82/78}Se$比值不能明显反映大氧化事件；前寒武到显生宙的$\delta^{82/78}Se$值具有从0.42±0.45‰ 到 - 0.19±0.59‰变化的趋势性。

Stüeken et al. 2015,GCA

四、硒同位素的应用

Selenium isotopes support free O_2 in the latest Archean

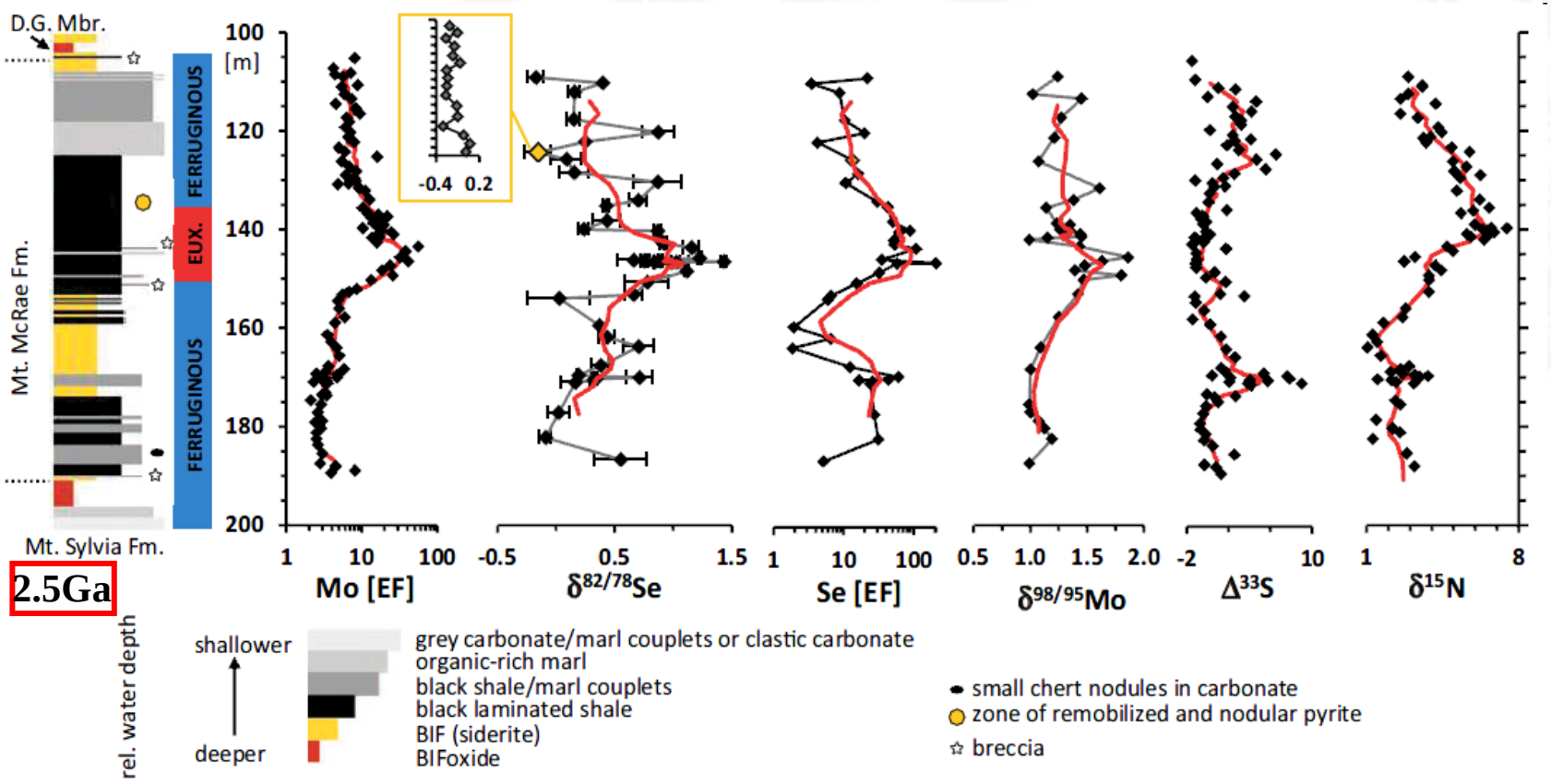

Figure 1. Stratigraphic section of core ABDP-9 in Mount McRae Shale (Hamersley Basin, Australia). Se data are plotted as averages ±1σ. EF is the enrichment factor in log scale. Red line represents five-point running mean. Inset shows $\delta^{82/78}$Se at high resolution over 16 cm from 124.06 m to 123.91 m (*y*-axis tick marks at 1 cm spacing, average = yellow data point). Water-column redox state inferred from iron speciation is indicated on left, where blue is ferruginous and red is euxinic. D.G.—Dale's Gorge; Mbr.—Member; Fm.—Formation; Mt.—Mount; BIF—banded iron formation; rel.—relative.

Stueken et al., 2015, Geology

应用案例：古环境氧化还原条件、大气氧逸度变化与环境污染等

四、硒同位素的应用

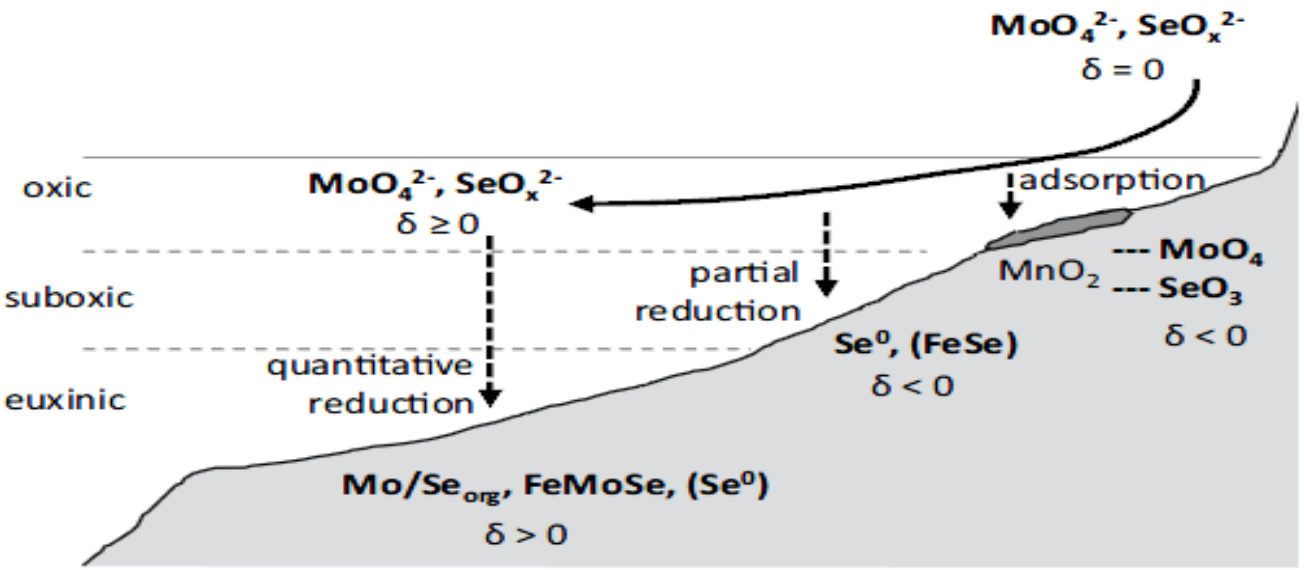

Figure 2. Proposed selenium cycle. Oxidative weathering produces molybdate (MoO_4^{2-}) and selenate (SeO_4^{2-}) or selenite (SeO_3^{2-}), here denoted as SeO_x^{2-}. Adsorbed Se in nearshore sediments will experience slight negative isotopic fractionation. Farther offshore, in suboxic conditions, partial reduction of Se oxyanions to pyrite-bound selenide (FeSe) or elemental Se (Se^0) in sediments should induce positive isotopic fractionation in residual SeO_x^{2-}. In euxinic waters, Se will be captured by sulfides during quantitative reduction as well as by organic selenide (Se_{org}). Euxinic sediments should thus record the isotopic composition of seawater Se oxyanions. δ stands for $\delta^{82/78}$Se and $\delta^{98/85}$Mo, respectively (values in ‰).

结论： $\delta^{82/78}$Se比值的异常变化是由局域或区域自由氧升高引起的，尽管全球氧逸度并未完全上升。

四、硒同位素的应用

Selenium isotope evidence for progressive oxidation of the Neoproterozoic biosphere

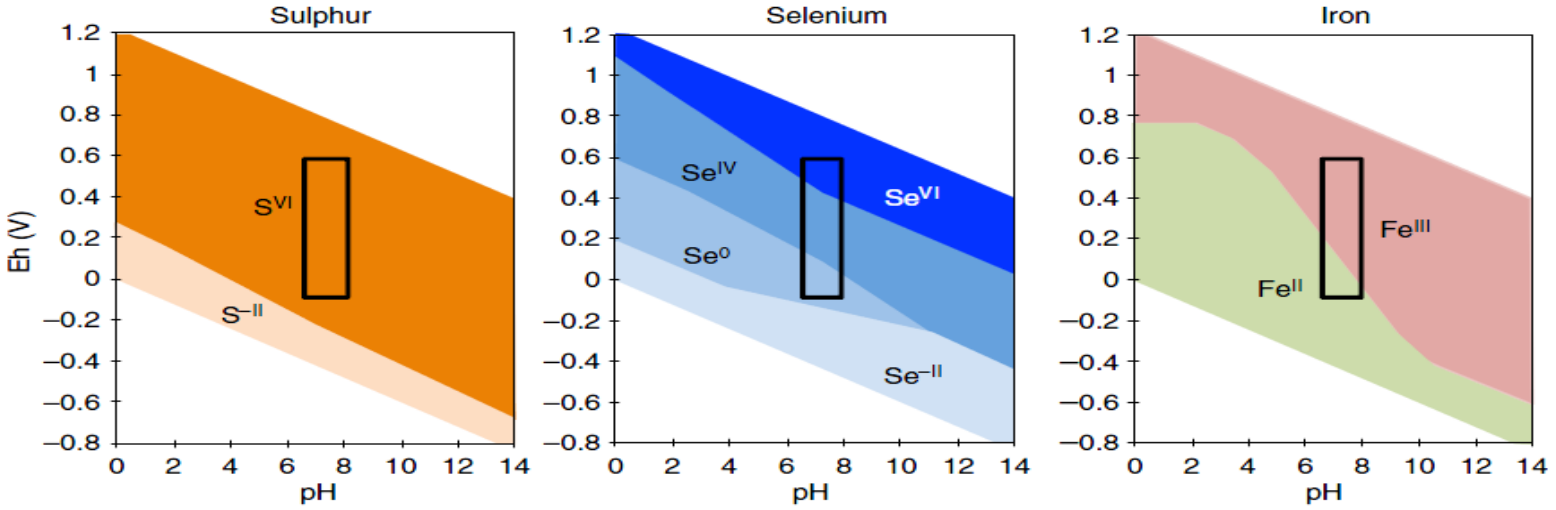

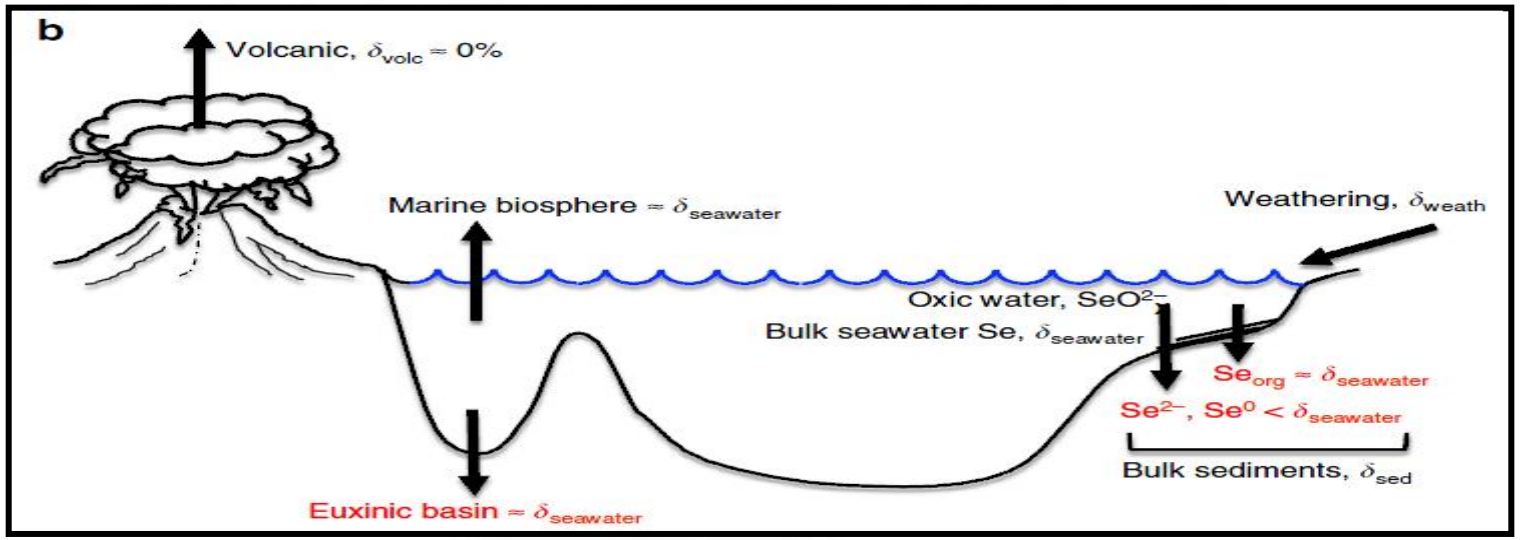

Standmann et al., 2015, NC

四、硒同位素的应用

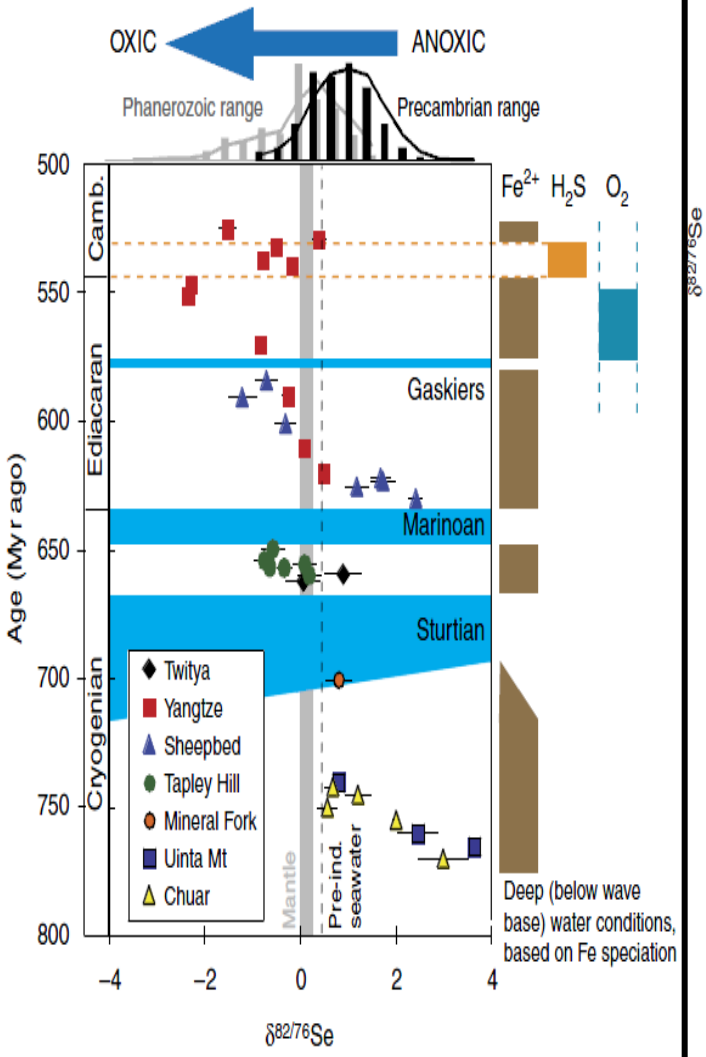

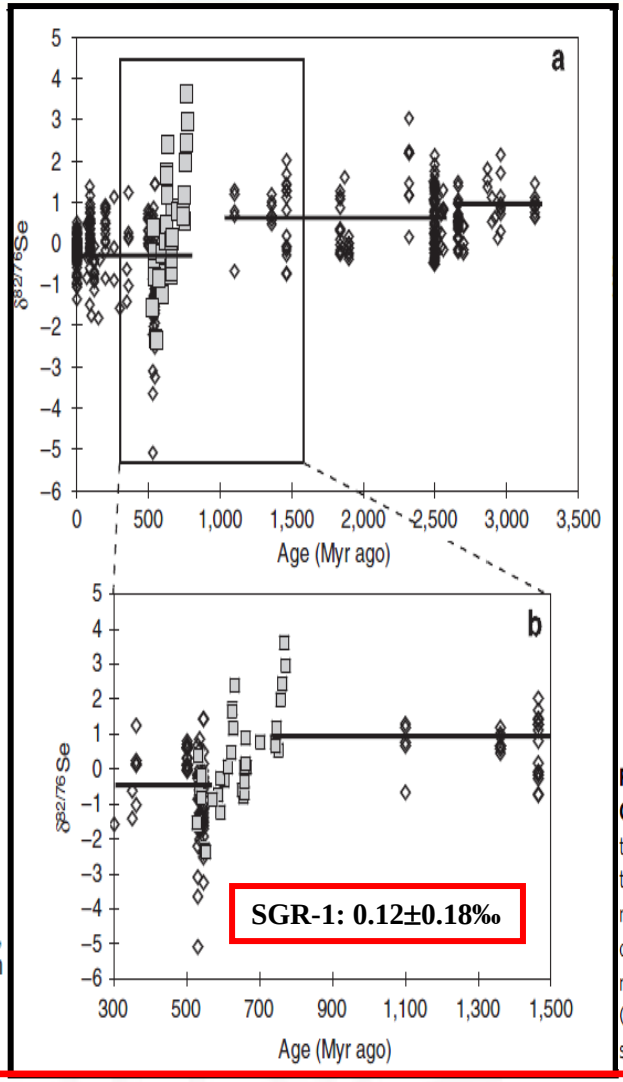

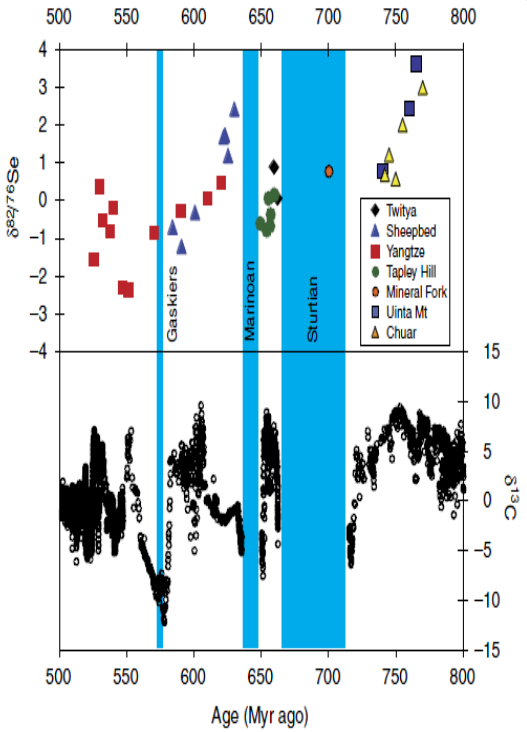

Figure 7 | Comparison of this study's Se isotope data with composite C isotope data. Se isotopes suggest that the oxidation of the oceans took at least 100 Myr ago. The lack of correlation with $\delta^{13}C$ suggests that the processes that control carbon (burial and oxidation of organic matter and carbonate dissolution/formation)[68] appear not to be controlling Se isotopes, meaning that Se is not controlled by organic matter. The timing of the Sturtian has been altered according to ref. 4 (Sturtian is not shown as diachronous, as opposed to Fig. 5, for simplicity's sake).

结论： 新元古1000—542 Myr年间大气与海洋中氧逸度是逐渐升高的， 大气与海洋中氧的升高至少应早于早期动物演化时期的100个百万年。

Standmann et al., 2015, NC

四、硒同位素的应用

Geological evolution of the marine selenium cycle: Insights from the bulk shale $\delta^{82/76}$Se record and isotope mass balance modeling *Mitchell et al., 2016, EPSL*

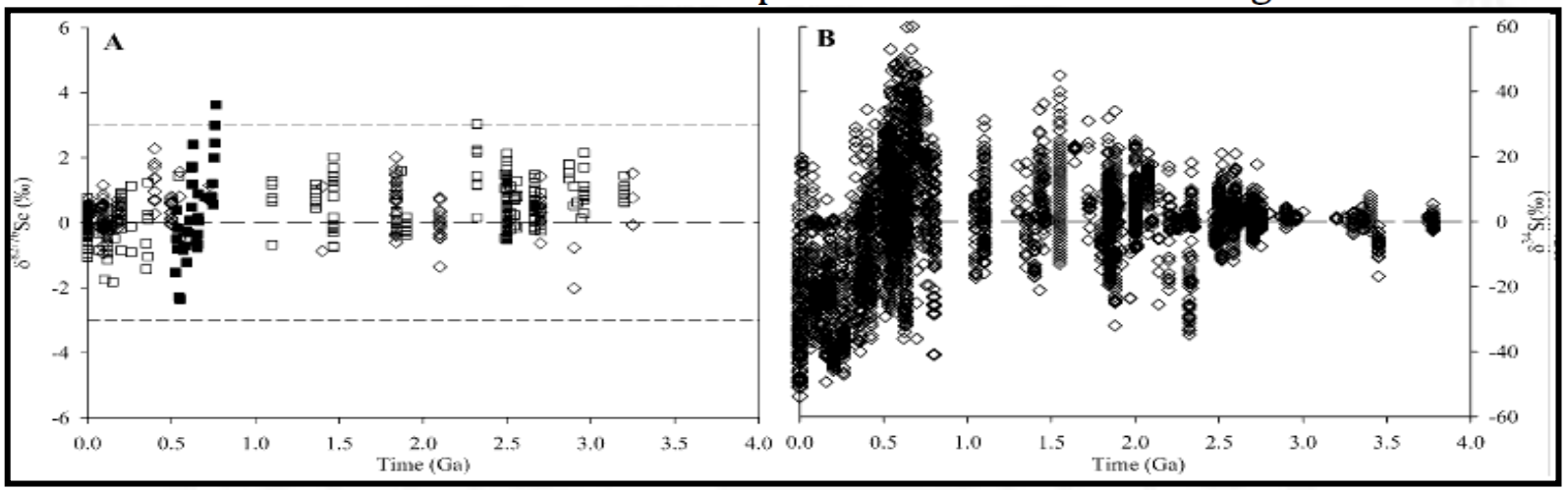

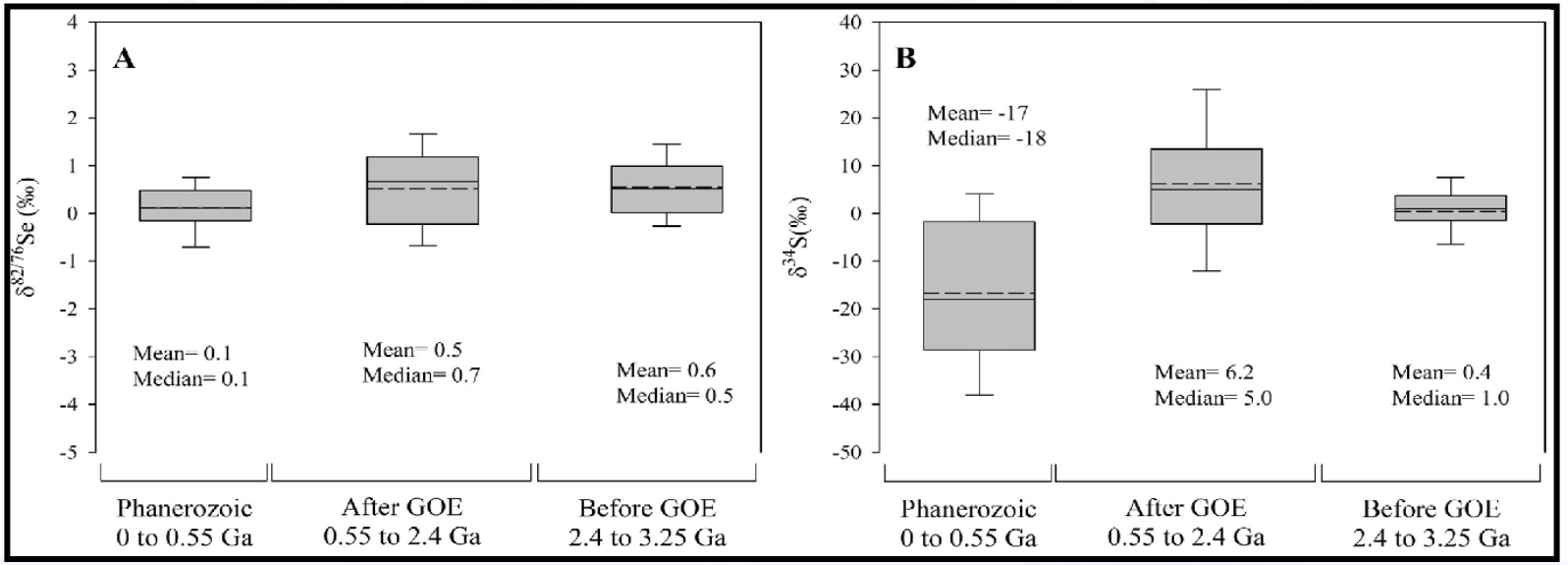

四、 硒同位素的应用

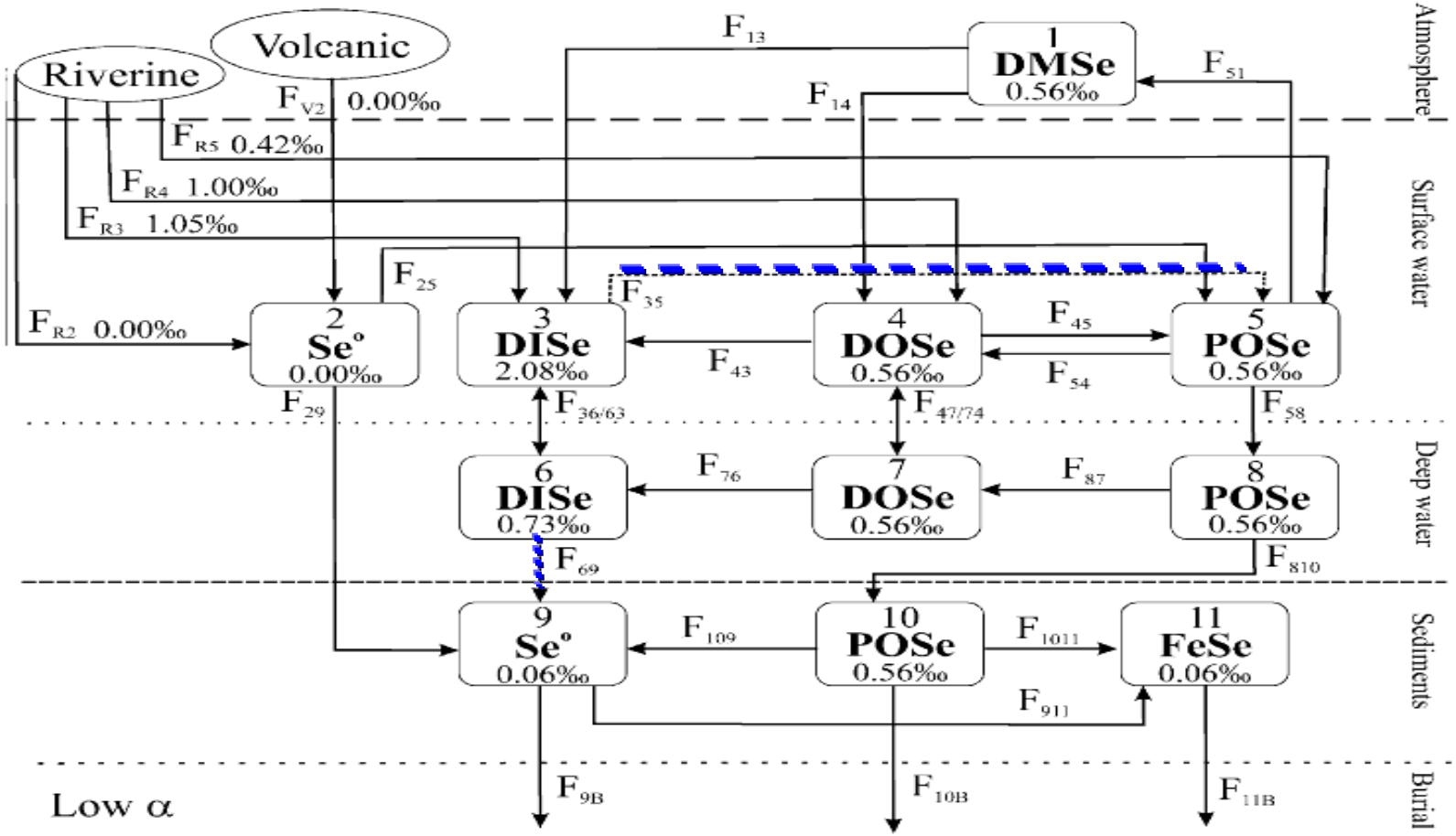

结论：太古代至现代，海洋页岩中$\delta^{82/76}$Se变化为-3至+3‰，小于实验中的“本质同位素分馏”，这与全球海洋的氧化还原条件变化并无直接关联。海洋中硒的循环由生物同化作用控制，仅能反映单独沉积硒库的古海洋地理信息。

Mitchell et al., 2016, EPSL

四、硒同位素的应用

Selenium isotopes record extensive marine suboxia during the Great Oxidation Event

Kipp et al., 2017, PNAS

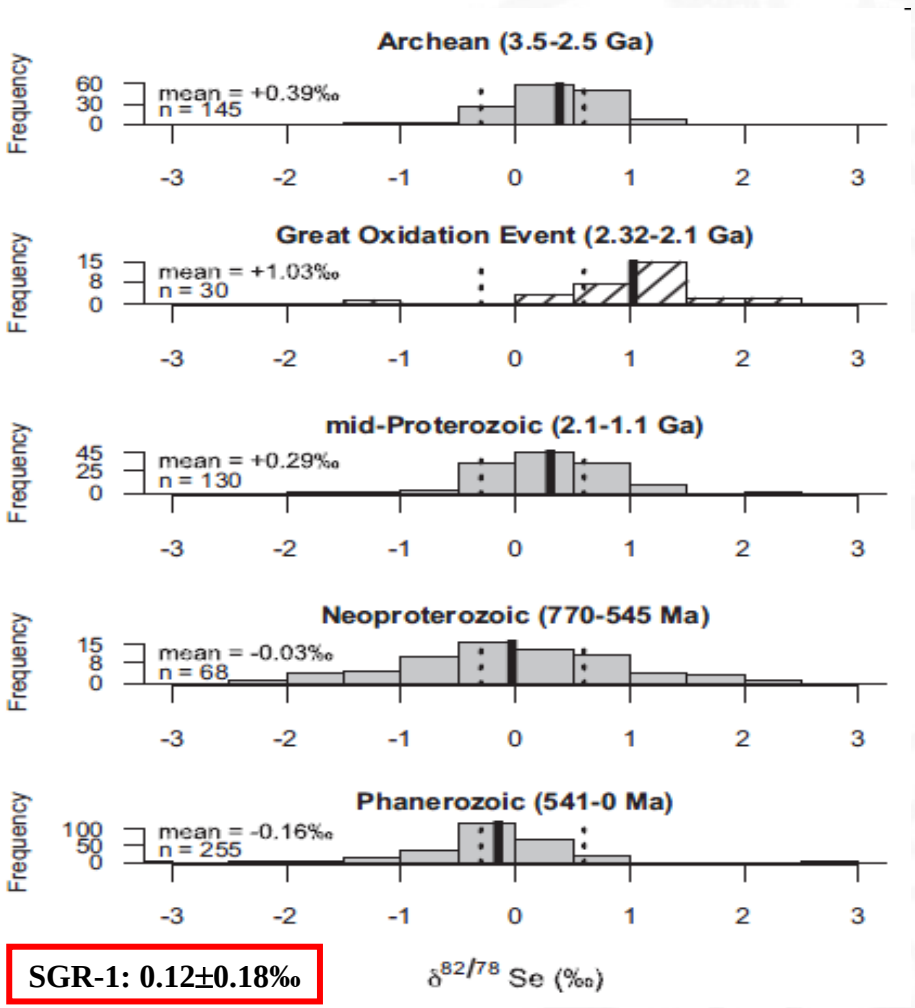

SGR-1: 0.12±0.18‰

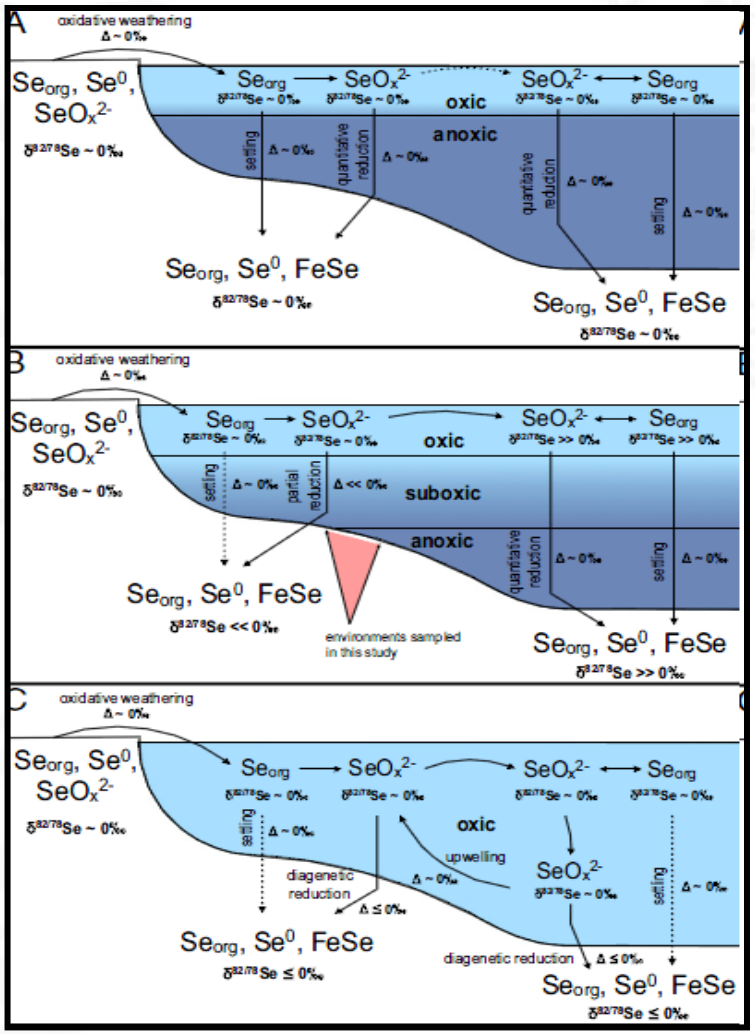

结论： 硒同位素能够记录大氧化期间海洋存在的广泛贫氧事件。

四、硒同位素的应用

4.3 硒的高温地球化学

Selenium isotope and S-Se-Te elemental systematics along the Pacific-Antarctic ridge: Role of mantle processes

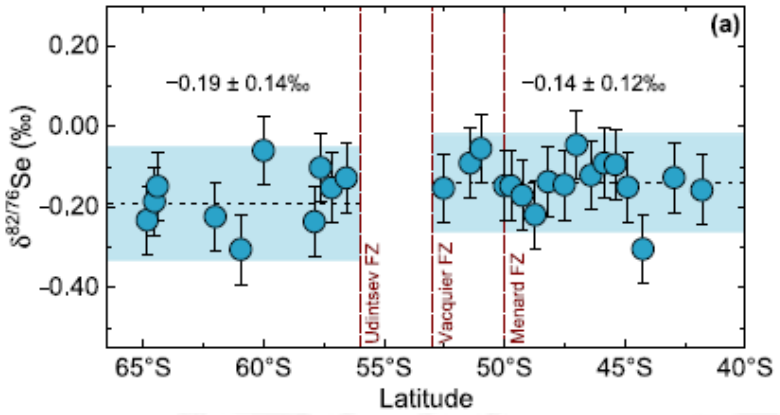

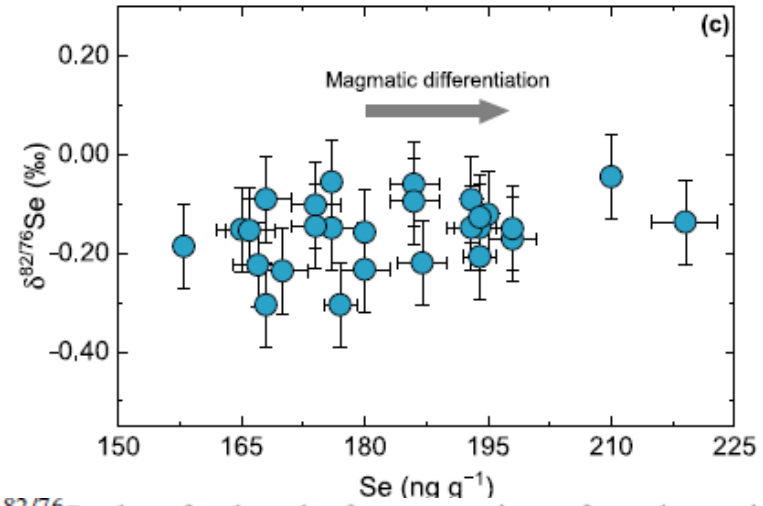

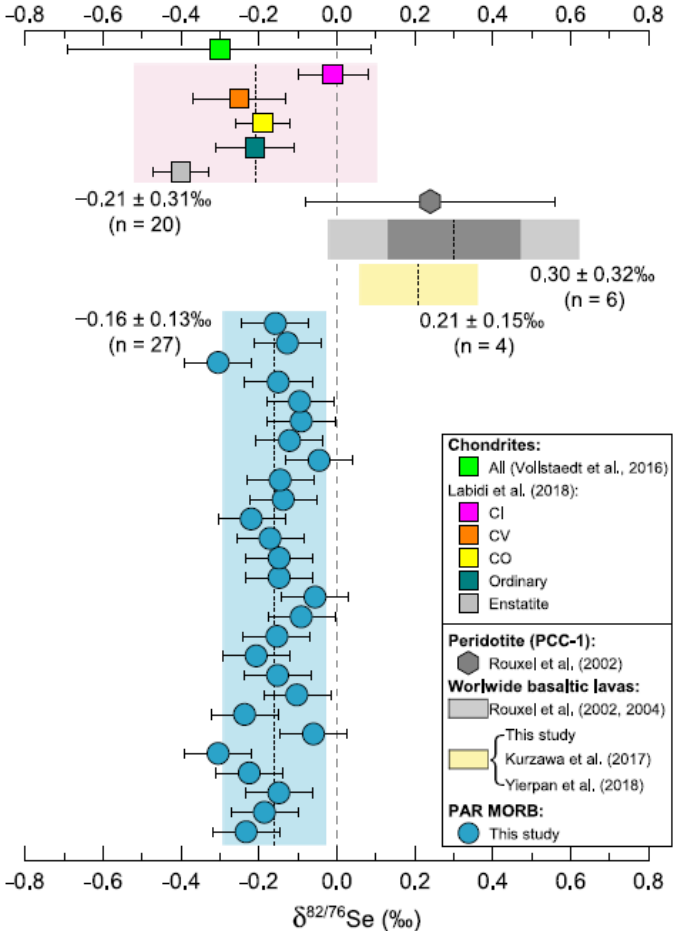

lished $\delta^{82/76}$Se data for basalts from a variety of geodynamic settings. The subtle but significant Se isotope variation observed within the investigated MORB suite (up to ~0.25‰) and between other mantle samples analyzed so far may reflect intrinsic source heterogeneity and potential isotopic differences across various mantle reservoirs.

Yierpan et al., 2019 GCA

四、硒同位素的应用

4.4天体化学中的应用

The isotope composition of selenium in chondrites constrains the depletion mechanism of volatile elements in solar system materials

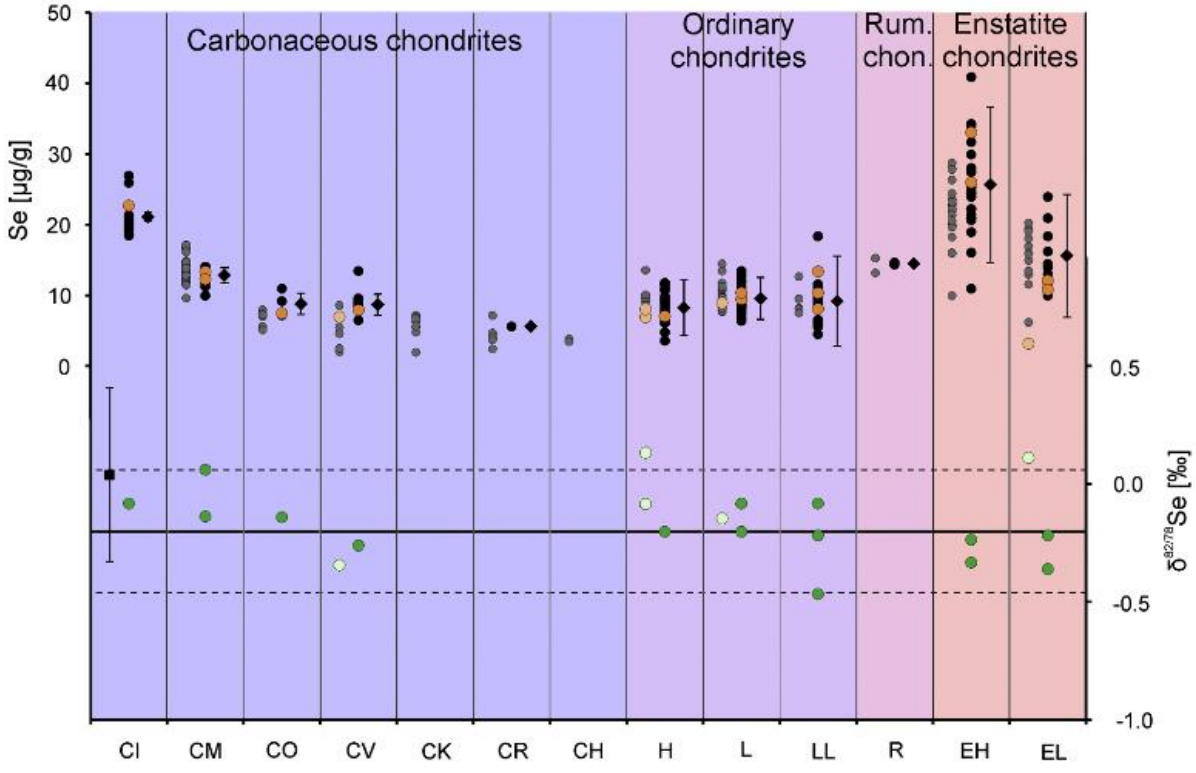

Meteorite group	Se (µg/g)	S/Se
Carbonaceous chondrites		
CI	21.2	2552
CM	12.8	2458
CO	8.8	2771
CV	8.7	2572
CK (finds)	5.6	255
CR	5.6	1963
CH (finds)	3.7	1166
Ordinary chondrites		
H	8.3	2456
L	9.6	2278
LL	9.2	2346
Rumuruti chondrites		
R	14.6	2795
Enstatite chondrites		
EH	25.7	1788
EL	15.7	

The long-term reproducibility of the shale standard SGR-1 of ±0.37‰ (2 s.d., $n = 8$; black square)

Vollstaedt,2016, EPSL

结论：硒作为中等挥发性元素，在陨石中的亏损与冷凝温度有关，极可能与母体中该元素的不完全冷凝有关；陨石中$\delta^{82/78}$Se均值为－0.2±0.26‰，反映了太阳星云中硒同位素的均一性以及高温冷凝过程的极微小分馏；硒的主要赋存相决定了全岩样品中的硒同位素组成。

四、硒同位素的应用

Selenium isotopes as tracers of a late volatile contribution to Earth from the outer Solar System

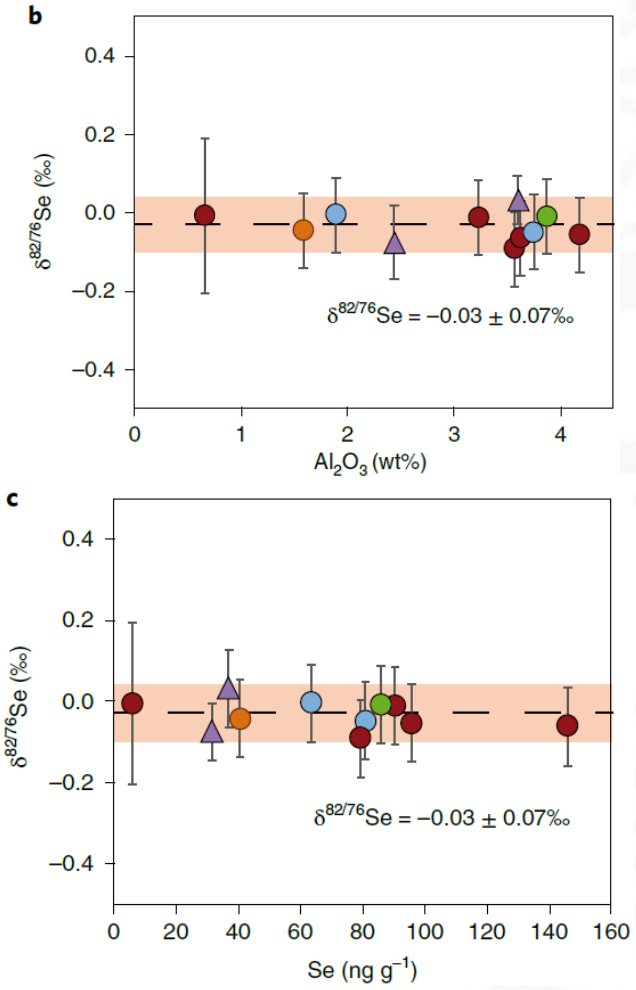

地幔橄榄岩的硒同位素组成

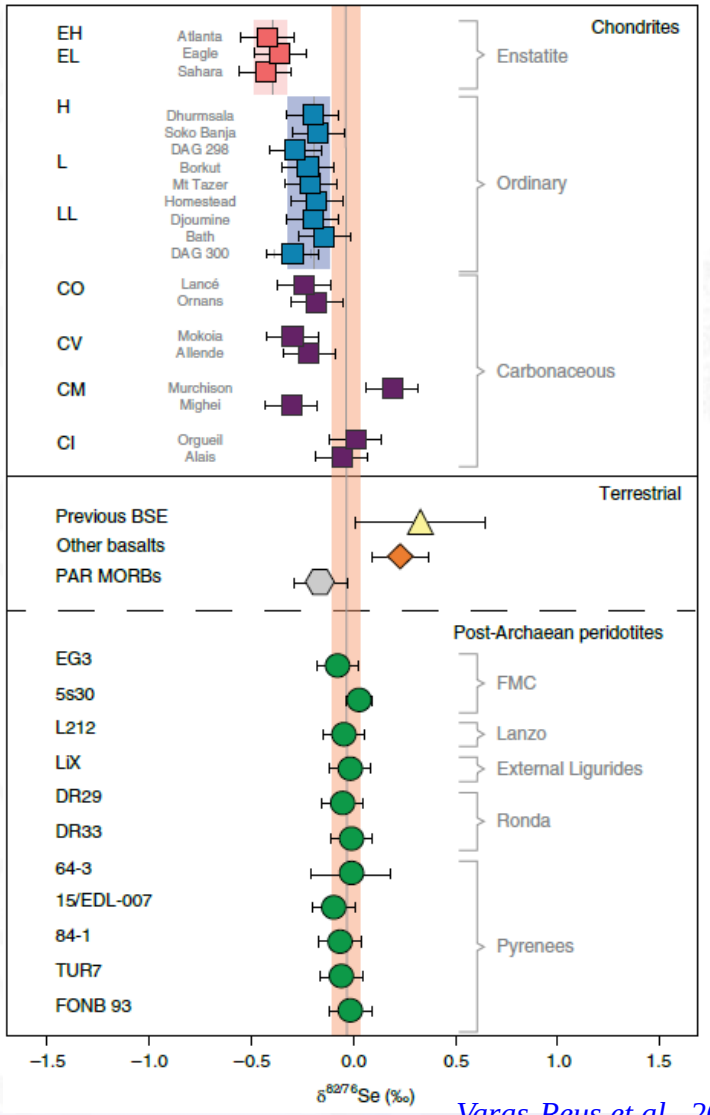

Varas-Reus et al., 2019, Nature Geoscience

致 谢

感谢国家自然科学基金委对本项研究的资助（U1612441,41673017，41473028）；

美国伊利诺伊大学地质系Johnson教授的无私指导和帮助；

中国科学院地质与地球物理所吴福元院士的长期鼓励和教诲；

中国地质科学院地质所同位素实验室朱祥坤研究员及其团队人员的长期帮助；

中国地质大学(北京)李曙光院士研究团队各位同事的鼎力协助；

感谢广州地化所张兆峰、中科大黄方、中科院地化所刘耘研究员课题组和南京大学鲍惠铭教授等的无私交流，以及西北大学袁洪林、黄康俊教授的邀请。

王静

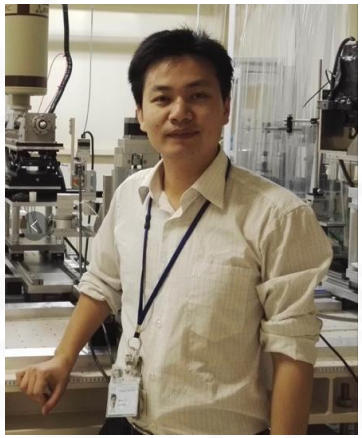

秦海波

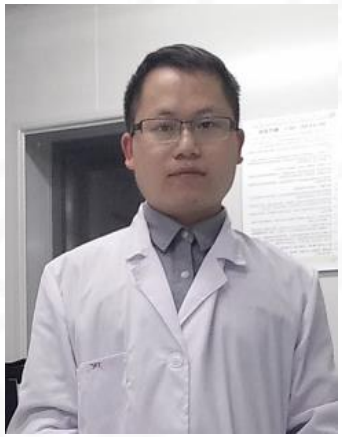

谭德灿

徐文坡

感谢大家的关注和批评指正